Unusual Matter Models in Cosmology

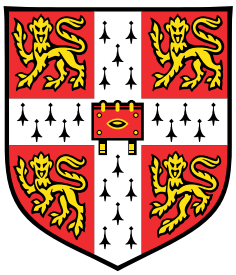

Charles Board

Supervisor: Prof. J. D. Barrow

Department of Applied Mathematics and Theoretical Physics
University of Cambridge

This dissertation is submitted for the degree of
Doctor of Philosophy

Trinity Hall

September 2019

In Memoriam

Professor John David Barrow

Declaration

This thesis is the result of my own work and includes nothing which is the outcome of work done in collaboration except as declared in the Preface and specified in the text. It is not substantially the same as any that I have submitted, or, is being concurrently submitted for a degree or diploma or other qualification at the University of Cambridge or any other University or similar institution except as declared in the Preface and specified in the text. I further state that no substantial part of my dissertation has already been submitted, or, is being concurrently submitted for any such degree, diploma or other qualification at the University of Cambridge or any other University or similar institution except as declared in the Preface and specified in the text.

Charles Board
September 2019

Acknowledgements

First and foremost, I would like to thank my supervisor, Prof. John Barrow for his advice, support, and guidance with my research projects and throughout my time as a PhD student. Without him this thesis would not exist, and I wish to express my deep gratitude for the opportunity he has given me.

I would also like to thank Özgür Akarsu, N. Merve Uzan and J. Alberto Vasquez for our fruitful and enjoyable collaboration during the last two years.

I would like to thank my examiners, Tessa Baker and Paul Shellard for their helpful comments and suggestions for this thesis.

My PhD was funded by a studentship from the Science and Technology Facilities Council, and I would like to thank them for enabling me to conduct this research. I would also like to thank the Department of Applied Mathematics and Theoretical Physics, and Trinity Hall, Cambridge for their support during this time.

I have been very fortunate during my time in DAMTP to have enjoyed the company and friendship of my fellow students, for which I am grateful to Antoni, Jack, Johnathan, Nathan, Alec, Ben, Chandrima, Chris, Alex, Chris, James, Miren and Owain, and especially to my office-mates, Roxana and Toby. I would also like to thank my friends from Trinity Hall; Will, Ben, Greg, Jay, Josh, Juliet, Marianne, Sam, and Will.

I would like to thank my parents, Wendy and John, and my sister, Sarah, for their love and support. Most of all, my thanks go to Julija.

Abstract

This thesis is divided into three sections.

In the first section, we discuss Singular Inflation, in which a scalar field exhibits a weak singularity, originally illustrated by the non-integer powerlaw potentials. We expand the class of potentials that result in this phenomenon, by providing constraints on the derivatives of the functions.

In the second section, we study the cosmological effects of adding terms of the form $f(T_{\mu\nu}T^{\mu\nu}) = \eta(T_{\mu\nu}T^{\mu\nu})^n$ to the matter Lagrangian of general relativity. The resulting cosmological theories give rise to field equations of similar form to several particular theories with different fundamental bases, including bulk viscous cosmology, loop quantum gravity, k-essence, and brane-world cosmologies. We find a range of exact solutions for isotropic universes, discuss their behaviours with reference to the early- and late-time evolution, accelerated expansion, and the occurrence or avoidance of singularities. We briefly discuss extensions to anisotropic cosmologies and delineate the situations where the higher-order matter terms will dominate over anisotropies on approach to cosmological singularities.

Finally, in the third section, we study a related model, called Energy-Momentum Log Gravity (EMLG), constructed by the addition of the term $f(T_{\mu\nu}T^{\mu\nu}) = \alpha \ln(\lambda\, T_{\mu\nu}T^{\mu\nu})$ to the Einstein-Hilbert action with cosmological constant Λ. This choice of model results in constant effective inertial mass density and has an explicit exact solution of the matter energy density in terms of redshift. We look for viable cosmologies, in particular, an extension of the standard ΛCDM model. EMLG provides an effective dynamical dark energy passing below zero at large redshifts, accommodating a mechanism for screening Λ in this region, in line with suggestions for alleviating some of the tensions that arise between observational data sets within the standard ΛCDM model. We present a detailed theoretical investigation of the model and then constrain the free

parameter α', a normalisation of α, using the latest observational data. The data do not rule out the ΛCDM limit of our model ($\alpha' = 0$), but prefers slightly negative values of the EMLG model parameter ($\alpha' = -0.032 \pm 0.043$), which leads to the screening of Λ. We also discuss how EMLG relaxes the persistent tension that appears in the measurements of H_0 within the standard ΛCDM model.

Table of contents

List of figures

List of tables

Chapter 1

Introduction

The field of Cosmology is the study of the history and evolution of the universe, a subject that has provoked thought and investigation throughout the ages. Since the earliest days of human history, mankind has looked up to the stars and attempted to craft descriptions of the universe. At first these descriptions took the form of stories and myths, particularly creation myths in which the behaviours and actions of various divinities and forces which shaped the universe, whether that be the Babylonian *'Enûma Eliš'* in which Tiamat and Apsu are the primordial water-gods from which all else springs, or the Greek tale of Gaia stepping forth from chaos to create Ouranos and then the other titans.

As the tools of science and mathematics became more developed, it started to become possible to describe models precisely and to conduct calculations and experiments to test them. By the third century BCE, several attempts to calculate the size of the universe had occurred, including Archimedes in his work *'The Sand Reckoner'*, [2] in which he calculated the diameter of the universe as 10^{14} stadia, or $1 - 2$ light years in modern units. This was done in order to estimate the number of grains of sand that would fill the universe, and required a combination of experiments, new mathematical concepts and previous heliocentric models, in order to create what may be one of the earliest scientific research papers.

Over subsequent millenia, many advances were made in both mathematics and astronomy, and in 1687 Isaac Newton published *'Philosophiæ Naturalis Principia Mathematica'* [3], in which he laid out a series of fundamental ideas in modern physics and mathematics. This included the theory of calculus, of mechanics, and of significant

cosmological relevance, the theory of gravitation that still bears his name. These tools and theories allowed him to calculate the motion of celestial objects, including providing mathematical proofs of laws discovered observationally by Kepler. In later work, he considered the cosmological question of the extent of the universe, concluding that the universe must necessarily be of infinite extent and filled uniformly with stars, lest it collapse under the gravitational force [4], a hypothesis that bears resemblance to the assumptions of homogeneity and isotropy in modern cosmology. In the years after this, attention and analysis began to turn to some cosmological problems, not least Olbers' paradox - the question of why, if there are infinitely many stars such that every line of sight should reach one, the night sky is not as bright as day. This sort of consideration marked a further step forward in the development of cosmology, but it was not until the early twentieth century that the modern study of cosmology can truly be said to have begun.

In 1915, Albert Einstein published his theory of General Relativity, providing for the first time a unified description of gravitation arising from a geometric description of space and time. This coherent mathematical framework for gravitation allowed the development of a truly mathematical theory of cosmology, and in 1917 Einstein produced a paper in which he argued for a static cosmological model in which a precise positive cosmological constant allowed a universe without end or beginning. Following this, other solutions were found, including de Sitter's discovery of a solution for an exponentially expanding universe later the same year. In 1922 the expanding spacetime which forms the basis for the standard model of cosmology, ΛCDM was first discovered, by Alexander Friedmann [5, 6]. The spacetime was rediscovered, independently, by Georges Lemaître [7], and during the 1930s Howard Robertson and Arthur Walker further developed the model, proving that this was the most general description of an expanding, isotropic and homogeneous universe. Today the spacetime is known by various combinations of the names of these four, but typically is referred to as the Friedmann-Lemaître-Robertson-Walker metric, or FLRW for short. The development of this model built on the work of Edwin Hubble, who measured the distance and redshift of various galaxies, and determined the famous relationship, now known as Hubble's law, that more distant galaxies are receding faster than nearer ones, thus providing evidence for an expanding universe. The initial calculations had very large errors, and the Hubble constant which codified the relationship was calculated as orders of magnitude larger than modern measurements suggest.

During the late 1940s and 1950s, there were two major paradigms in Cosmology. The first, proposed by Bondi, Gold and Hoyle was the Steady State model [8, 9], which proposed that the universe was an eternal de Sitter, expanding forever with neither beginning nor end. This was in accordance with the so-called 'perfect cosmological principle', which asserted that a universe would be homogeneous in both space and time. This would then require that matter be continuously created in order to prevent the energy content of the universe from being diluted by the expansion. The alternative to this model was the Big Bang theory, initially proposed by Lemaître [10], and refined by George Gamow, in which the universe began from an initial point singularity at some finite past time, before expanding and cooling into its current state. This was initially disfavoured by most cosmologists who preferred the steady state universe, but gradually evidence grew in support of the big bang, culminating in the detection in 1965 of the Cosmic Microwave Background by Penzias and Wilson [11]. The CMB is relic radiation which was produced in the early universe, and is still detectable in the present era. The CMB was predicted by the big bang model, but not by the steady state, thus cementing the big bang as the favoured description of our universe, a status it enjoys to the present day.

After many theoretical and observational refinements, the current formulation of the big bang model as the standard model of cosmology is known as ΛCDM. This consists of an FLRW universe with no curvature, and with the addition of two 'dark sector' components. The first of these is dark matter, which is a form of matter hypothesised to make up the large majority of the matter component of the universe, implied by various observation which are inconsistent with the only matter being the readily visible baryonic matter, such as the galaxy rotation curves, and many others. The second is the reintroduction of the cosmological constant, Λ, originally proposed and then later withdrawn by Einstein. A non-zero cosmological constant is used to explain the modern evidence, drawn from observations of the CMB, Baryon acoustic oscillation measurements, and galaxy lensing effects, that the universe is not simply expanding, but is undergoing an accelerated expansion. The history of the universe then consists of an initial singularity, now believed to have occurred approximately 13.7 billion years ago, followed by an era in which radiation dominated the energy content of the universe. The radiation era was followed by an era in which non-relativistic matter, 'dust', dominated, before entering a phase of accelerated expansion dominated by a positive cosmological constant. Over all this time, the ΛCDM model has remained in very good accordance with observational data, from a wide array of land based and

space based experiments. Even the most recent measurements of the CMB from the Planck satellite have been extremely well fit by the standard ΛCDM model [12].

However, ΛCDM is not without its problems. An example of these is the horizon problem, which suggests that although the CMB is very uniform now, the universe is not old enough for us to expect it to be so uniform. One proposed resolution to this has been the theory of inflation [13], which suggests a period of early acceleration, and this has been a popular area of study since its first introduction in the 1980s. Other serious problems include explanations of both dark sector components. Although the existence dark matter has been hypothesised for a long time, there is still no satisfactory explanation for its exact form, and although the idea that it is some sort of weakly interacting massive particle, known as WIMPs, is popular there is still no direct detection of such a particle. The cosmological constant also has theoretical issues, despite accurate observational measurements, the predictions of its size from quantum calculations are many tens of orders of magnitude larger. This suggests a requirement for some mechanism to protect Λ from being washed out by quantum fluctuations, or more radically, a modification to the theory of General Relativity itself in order to cause the observed value to arise naturally.

1.1 Outline

In this thesis we consider three different models of cosmology which arise due to unusual behaviour of matter. These unusual contributions result in new cosmological features, which may help explain some of the seemingly problematic aspects of the standard cosmological model.

This thesis is structured as follows. In the remainder of this chapter we provide a brief summary of General Relativity in order to establish the fundamental theory underlying modern cosmology. After that, we discuss the modern theory of cosmology, particularly focussing on aspects that will be of importance to the rest of the thesis.

In the second chapter we discuss Singular Inflation, in which a scalar field exhibits a particular kind of weak singularity in a finite amount of future time. This has been originally discussed in the context of a scalar field acting in a power-law potential, where the exponent was not an integer. We expand the class of potentials that result in

this phenomenon, by providing sufficient conditions on the derivatives of the function to ensure that a finite-time singularity of the appropriate time occurs.

In the third chapter, we consider a particular theory of modified gravity in which the energy-momentum tensor contributes directly to the action. This is an extension of the $F(R)$ theory of modified gravity to allow the action to further depend upon the square of the energy-momentum tensor, known as $F(R, T^{\mu\nu}T_{\mu\nu})$ gravity. We study the cosmological effects of this model when the modification takes the form of adding $f(T_{\mu\nu}T^{\mu\nu}) = \eta(T_{\mu\nu}T^{\mu\nu})^n$ to the matter Lagrangian of general relativity. The resulting cosmological theories give rise to field equations of similar form to several particular theories with different fundamental bases, including bulk viscous cosmology, loop quantum gravity, k-essence, and brane-world cosmologies. We find a range of exact solutions for isotropic universes, discuss their behaviours with reference to the early- and late-time evolution, accelerated expansion, and the occurrence or avoidance of singularities. We briefly discuss extensions to anisotropic cosmologies and delineate the situations where the higher-order matter terms will dominate over anisotropies on approach to cosmological singularities.

Finally, in the fourth chapter, we study another model of $f(R, T^{\mu\nu}T_{\mu\nu})$ gravity, which we call Energy-Momentum Log Gravity (EMLG), constructed by the addition of the term $f(T_{\mu\nu}T^{\mu\nu}) = \alpha \ln(\lambda\, T_{\mu\nu}T^{\mu\nu})$ to the Einstein-Hilbert action with cosmological constant Λ. This choice of model results in constant effective inertial mass density and has an explicit exact solution of the matter energy density in terms of redshift. We look for viable cosmologies, in particular, an extension of the standard ΛCDM model. EMLG provides an effective dynamical dark energy passing below zero at large redshifts, accommodating a mechanism for screening Λ in this region, in line with suggestions for alleviating some of the tensions that arise between observational data sets within the standard ΛCDM model. We present a detailed theoretical investigation of the model and then constrain the free parameter α', a normalisation of α, using the latest observational data. The data do not rule out the ΛCDM limit of our model ($\alpha' = 0$), but prefers slightly negative values of the EMLG model parameter ($\alpha' = -0.032 \pm 0.043$), which leads to the screening of Λ. We also discuss how EMLG relaxes the persistent tension that appears in the measurements of H_0 within the standard ΛCDM model.

1.2 General Relativity

In this section we now provide a brief summary of the basic theory of General Relativity, in order to establish the background required for the study of modern Cosmology. What follows is only a brief overview of the field, and for a more detailed treatment of the subject, there are many thorough textbooks, for example [14–17]

The theory of General Relativity is a metric theory of gravitation, in which we define a space-time as a pair $(\mathcal{M}, g)$, where $\mathcal{M}$ is a Lorentzian manifold and g is a metric. We then provide some description of the matter content of the universe, and link the two through appropriate field equations. This provides us with a geometric description of our universe, in which gravitational forces arise due to curvature of space-time.

1.2.1 Notations and convention

We use the sign convention $(-,+,+,+)$ for our metric throughout this thesis.

We use Latin indices $a, b, c, ...$ to denote spacetime indices, whilst $i, j, k...$ indicate spatial indices only.

We use the Einstein summation convention throughout, in which paired indices in an expression should be summed over all values of the index, but the explicit summation symbols are ommitted, e.g.

$$T^{ab}S_{bc} \equiv \sum_{b=0}^{d-1} T^{ab}S_{bc} \ , \tag{1.1}$$

where d is the number of dimenstions. Throughout this thesis we will work in $d = 4$ dimensions.

We use $,a$ to denote partial differentiation with respect to the coordinate a

$$X^b_{,a} \equiv \frac{\partial X^b}{\partial x^a} \equiv \partial_a X^b \ . \tag{1.2}$$

We use $;a$ to denote covariant differentiation with respect to the coordinate a

$$X^b_{;a} \equiv \nabla_a X^b \ . \tag{1.3}$$

1.2.2 Definitions of Differential Geometry

We begin by discussing some basic concepts of differential geometry, which are fundamental to understanding General Relativity.

A **Manifold** is a space which looks locally like Euclidean (flat) space. Importantly, however, it need not be globally flat.

A **Tensor** is an object defined on a manifold. An (n, m) tensor is a multi-linear map from the product of n copies of the cotangent space and m copies of the tangent space to the real numbers. In General Relativity we typically consider **tensor fields** in which the components are functions of the points on the manifold, but still refer to these simply as tensors. An (n,m) tensor can be written as $T^{a_1\ldots a_n}_{b_1\ldots b_m}$ where the n superscript indices are known as the contravariant components, and the m subscript indices are the covariant components.

Tensors transform in a particularly simple way under change of variables. The tensor transformation law for a transformation from coordinates (x^μ) to $(\tilde{x}^\alpha)$ is given by

$$\tilde{T}^{\alpha_1\ldots\alpha_n}_{\beta_1\ldots\beta_m} = \frac{\partial\tilde{x}^{\alpha_1}}{\partial x^{\mu_1}}\ldots\frac{\partial\tilde{x}^{\alpha_n}}{\partial x^{\mu_n}}\frac{\partial\tilde{x}^{\nu_1}}{\partial x^{\beta_1}}\ldots\frac{\partial\tilde{x}^{\nu_m}}{\partial x^{\beta_m}}T^{\mu_1\ldots\mu_n}_{\nu_1\ldots\nu_m} \ . \tag{1.4}$$

Because of this, equations consisting solely of tensorial expressions will hold regardless of the choice of co-ordinate system. This allows us to perform calculations without reference to a specific set of co-ordinates.

A **metric tensor** is a symmetric $(0, 2)$ tensor, g_{ab}, defined on the manifold. The metric tensor, commonly referred to simply as the 'metric', can be understood as the distance measure on a manifold.

A convenient way of writing down a metric in a particular coordinate system is the **line element**, ds^2, which is the length of an infinitesimal displacement and is related to the metric by

$$ds^2 = g_{ab}dx^a dx^b z, \tag{1.5}$$

where x^a are our chosen coordinates. ds^2 is an important invariant quantity, and it is worth noting that although it is not strictly the same as the metric, one can be uniquely recovered from the other and they are often referred to somewhat interchangeably.

A **Lorentzian metric** of dimension 4 a metric with signature ± 2, that is that the elements after diagonalisation have either $(-,+,+,+)$ or $(+,-,-,-)$, which are the same up to choice of sign. This can be seen as a generalisation of the nature of the Minkowski metric used in special relativity taking the form $\pm\text{diag}(-1,1,1,1)$, and as identifying a time coordinate which, although part of our manifold, has somehow different behaviour to the spacelike ones.

In order to perform tensorial calculations, we wish to be able to differentiate tensors on our manifold. However, the partial derivative is not itself tensorial, and so we define the **covariant derivative** of an (n,m) tensor as

$$\nabla_a T^{b_1\ldots b_n}_{c_1\ldots c_n} = \partial_a T^{b_1\ldots b_n}_{c_1\ldots c_n} + \Gamma^{b_1}_{ad} T^{d\ldots b_n}_{c_1\ldots c_n} + \ldots + \Gamma^{b_n}_{ad} T^{b_1\ldots d}_{c_1\ldots c_n} - \Gamma^{d}_{ab_1} T^{b_1\ldots b_n}_{d\ldots c_n} - \ldots - \Gamma^{d}_{ab_n} T^{b_1\ldots b_n}_{c_1\ldots d} \ , \quad (1.6)$$

where Γ^a_{bc} are the **connection components**. The connection components, in principle, are not fixed by our choice of manifold and metric. However, in general relativity, we typically choose our connection to have two properties which together uniquely define a specific choice of connection, known as the **Levi-Civita connection**. Firstly, we ask that the connection be 'Torsion-free', $\Gamma^a_{bc} = \Gamma^a_{cb}$. Secondly, we ask that the connection be 'metric-compatible', such that $\nabla_a g_{bc} = 0$. The connection components are then determined by the metric as:

$$\Gamma^a_{bc} = \frac{1}{2} g^{ad}(g_{dc,b} + g_{bd,c} - g_{bc,d}) \ . \quad (1.7)$$

This means that, in general relativity, the geometric structure on the manifold is defined solely by the metric.

1.2.3 Postulates of General Relativity

General Relativity begins with four postulates.

1. There exists a **spacetime**, which consists of a four-dimensional manifold, $\mathcal{M}$, equipped with a Lorentzian metric, g_{ab}.

2. Free particles travel on timelike, or null, geodesics.

3. Energy, momentum and stress are described by a symmetric tensor, T_{ab}, such that $\nabla_a T^{ab} = 0$.

4. The metric satisfies the Einstein field equations.

The first of these postulates is explained using the definitions in 1.2.2, and we will discuss the remaining postulates in the following subsections. We should also note that, strictly speaking, these postulates are not all independent.

1.2.4 Geodesics in General Relativity

A **geodesic** is a curve between two points in spacetime which extremises the proper time, τ along that curve. This means extremising

$$\tau = \int \sqrt{-g_{ab}\dot{x}^a\dot{x}^b}d\lambda \ , \tag{1.8}$$

where $\dot{x}^a$ represents differentiation with respect to some affine parameter λ, and is the 4-velocity, which we may also write as $u^a \equiv \dot{x}^a$.

By varying this action, we can calculate the Euler-Lagrange equations for these curves

$$\ddot{x}^a + \Gamma^a_{bc}\dot{x}^b\dot{x}^c = 0 \ , \tag{1.9}$$

where Γ^a_{bc} are the **Christoffel Symbols**. In the case of the Levi-Civita connection, they conveniently coincide with the connection components, although for a general connection they would be different. This equation is also known as the **geodesic equation**. The geodesic equation may alternatively be written in the compact form

$$u^a\nabla_a u^b = 0 \ . \tag{1.10}$$

Geodesics may then be classified into three types, by considering the value of $g_{ab}\dot{x}^a\dot{x}^b$, which must take a constant value for a specified curve (implied by the geodesic equation)

$$\text{A geodesic is} \begin{cases} \text{timelike} \\ \text{null} \\ \text{spacelike} \end{cases} \quad \text{if} \quad g_{ab}\dot{x}^a\dot{x}^b \begin{cases} < 0 \\ = 0 \\ > 0 \end{cases} . \tag{1.11}$$

Massive and massless particles moving freely then travel on timelike and null geodesics respectively, in accordance with postulate 2. Often it will be convenient to rescale the lagrangian so that timelike curves have $g_{ab}\dot{x}^a\dot{x}^b = -1$ and spacelike have $g_{ab}\dot{x}^a\dot{x}^b = 1$.

1.2.5 Forms of matter

In general relativity, the matter content of the universe is described by the **Energy-momentum tensor**, T_{ab}, which is a symmetric $(0, 2)$ tensor. This means that all information about the matter source under consideration is encoded by the tensor's ten independent components. From the third postulate above, we know that the energy-momentum tensor must also satisfy $T^{ab}{}_{;b} = 0$, which is to say that it is **conserved**

In this thesis we consider primarily three different forms of matter. The first, and simplest, form is **vacuum**, given by $T^{ab} = 0$. This is the case in which there is no matter content in the universe and so the evolution of the universe is determined entirely by the metric. This results in significantly simplified equations of motion.

A relativistic **perfect fluid** is a type of fluid, which has no viscosity and does not conduct heat. This results in the energy-momentum tensor depending only on two functions, ρ, the energy density, and p, the pressure in the comoving frame of the fluid. The form of the energy-momentum tensor is then given by

$$T_{ab} = (\rho + p)u_a u_b + p g_{ab} \ . \tag{1.12}$$

We can see from this that in the comoving frame of the fluid, the energy-momentum tensor will be diagonal. The equations of motion for a relativistic fluid then follow from considering parts of the conservation of the energy momentum tensor contracted with the comoving velocity u^a. We find that

$$u^a \nabla_a \rho + (\rho + p)\nabla_a u^a = 0 \ , \tag{1.13}$$

$$(\rho + p)u^b \nabla_b u^a + (g^{ab} + u^a u^b)\nabla_b p = 0 \ , \tag{1.14}$$

which are the relativistic forms of the conservation and Euler equations from standard fluid dynamics. We could recover the standard equations by taking the Newtonian limit. If we wish to now solve these equations, it would be necessary to further specify

an equation of state, a relationship $P = P(\rho)$ relating the pressure and the density for the fluid.

Finally, in 2, we consider the real scalar field, which is a spin zero particle acting in a potential $V(\phi)$. This is some scalar function of position ϕ, which we note is a zeroth rank tensor. This can be described by the lagrangian

$$\mathcal{L} = \frac{1}{2}\nabla_a\phi\nabla^a\phi - V(\phi) \ , \tag{1.15}$$

and has energy-momentum tensor

$$T_{ab} = \nabla_a\phi\nabla_b\phi - g_{ab}(\frac{1}{2}\nabla_a\phi\nabla^a\phi + V(\phi)) \ , \tag{1.16}$$

where we may also note that the covariant derivative of a scalar field is simply the partial derivative.

1.2.6 Einstein Field Equations

In order to describe the overall dynamics of the universe in general relativity, we must find the field equations which link the matter content to the spacetime curvature.

The spacetime curvature is described by the **Riemman tensor**, $R^a{}_{bcd}$ defined as

$$\nabla_a\nabla_b v^c - \nabla_b\nabla_a v^c = R^c{}_{dab}v^d \ , \tag{1.17}$$

where v^c is an arbitrary vector. This is equivalent to saying that the Riemann tensor is the commutator of the second covariant derivative. From the expression above the Riemann tensor could then further be written purely in terms of the Christoffel symbols and their derivatives.

The Riemann tensor has various symmetries, including $R^a{}_{(bcd)} = 0$, $R_{abcd} = R_{cdab}$ and $R^a{}_{b[cd]} = 0$. These symmetries reduce the number of independent components to 20, which capture all of the information about the curvature of the spacetime. If the spacetime has no curvature it is flat, and this is equivalent to $R^a{}_{bcd} = 0$.

We may then define the **Ricci tensor** as the contraction over the first and third indices of the Riemann tensor

$$R_{ab} = R^d{}_{adb} \ , \tag{1.18}$$

which is a symmetric $(0, 2)$ tensor. Further, we define the **Ricci scalar** as the contraction of the Ricci tensor

$$R = R^a{}_a \ . \tag{1.19}$$

Finally, we can define the **Einstein tensor** in terms of the Ricci tensor and scalar, as

$$G_{ab} = R_{ab} - \frac{1}{2} R g_{ab} \ . \tag{1.20}$$

Having defined the Einstein tensor and the energy-momentum tensor, we can now write down the **Einstein field equations**. These are a set of ten coupled partial differential equations which describe the dynamics and gravitation of our universe by relating the curvature and the matter content. They are

$$G_{ab} + \Lambda g_{ab} = \kappa T_{ab} \ . \tag{1.21}$$

This includes a new term, Λ, which is known as the **cosmological constant**. κ is a constant equal to

$$\kappa \equiv \frac{8\pi G}{c^4} \ , \tag{1.22}$$

which we will often find convenient to set equal to 1 by suitable choice of units. Λ was originally introduced by Einstein to permit a static model of the universe, but later removed once observational and mathematical evidence ruled out the static model. However, more recent considerations have led to its reintroduction into the Einstein equations. If we consider the maximally symmetric solutions to the Einstein equations, we find that Λ corresponds to the space-time curvature, with $\Lambda = 0$ giving us Minkowski, flat, space which is the limit of GR in which we recover special relativity and then Newtonian dynamics. If we have $\Lambda > 0$ then the maximally symmetric solution is a closed universe with constant curvature, called de Sitter space, whilst if we have $\Lambda < 0$ we have instead an open universe with constant curvature, known as anti-de Sitter space.

These equations are in fact the most general field equations possible in four dimensions, if we require that the field equations are derivable from an action, and depend only on the metric and its first two derivatives. This is known as **Lovelock's theorem**. Therefore, as we will see, in order to modify the behaviour of gravity we would need to relax one of these requirements. The Einstein field equations can then be derived from an action principle, by varying the following action with respect to the metric

$$\mathcal{S} = \frac{1}{2\kappa}\int \sqrt{-g}(R - 2\Lambda)d^4x + \int \sqrt{-g}\mathcal{L}_m d^4x \ , \tag{1.23}$$

where the first term is the gravitational part of the action, known as the Einstein-Hilbert action, and the second is the action of the matter lagrangian. g is the determinant of the metric. We would then define the energy-momentum tensor as

$$T_{ab} = \frac{-2}{\sqrt{-g}}\frac{\delta \mathcal{S}_m}{\delta g^{ab}} \ , \tag{1.24}$$

where $\mathcal{S}_m$ is the matter action.

1.3 Cosmology

The discovery of the theory of general relativity has been a powerful tool for understanding cosmology. In this section we will give a summary of some aspects of modern cosmology. There are many thorough textbooks on the subject available for further detail, including [18–21].

1.3.1 The Friedmann-Lemaître-Robertson-Walker metric

The Einstein equations in full generality are a set of ten coupled partial differential equations. In order to make meaningful progress in the study cosmology, we need to enforce certain features of the metric which will simplify the equations and allow us to find solutions.

The standard assumptions that we will make are that on large scales the universe is isotropic and homogeneous. This is known as the cosmological principle, and underpins much of modern cosmology. The statement that the universe is isotropic means that the universe looks the same in every direction. Whilst this is not true on small scales, observations of the cosmic microwave background [22] are consistent with statistical isotropy on large scales, to a high degree. Homogeneity on the other hand means that the universe should look the same at every point. This is not possible to test directly, but if we assert that we should not live at a special point in the universe (the Copernican Principle), then the observations of isotropy from Earth allow us to conclude isotropy from every point, which is sufficient to then conclude homogeneity.

Once we have enforced homogeneity and isotropy in our universe, we are left with only possibility for the metric, the Friedmann-Lemaître-Robertson-Walker or FLRW metric, which has the line element

$$ds^2 = -dt^2 + a^2(t)\left(\frac{dr^2}{1-kr^2} + r^2\left(d\theta^2 + \sin^2\theta d\phi^2\right)\right), \tag{1.25}$$

where k is the parameter describing the curvature of the spatial 3-spaces. When $k < 0$, it is hyperbolic (often referred to as open), when $k > 0$ they are spherical (closed), and when $k = 0$ we have a spatially flat universe. We note that this is distinct from the overall *space-time* curvature, which is controlled by Λ, and ultimately describes whether the universe will expand forever (open) or recollapse (closed). Current observational evidence suggests that the universe has at most very small deviations from flatness, and we will work in the case $k = 0$ in much of what follows, in which case the metric takes the simple form

$$ds^2 = -dt^2 + a^2(t)(dx^2 + dy^2 + dz^2)\ . \tag{1.26}$$

The function $a(t) \geq 0$ is known as the scale factor, and describes the size of the universe. From knowledge of this function, we are able to determine the past, present and future of our universe. Thus the primary goal of much of Cosmology is to determine the evolution of the scale factor, by solving the Einstein equations. The scale factor is itself not directly measurable, but we can instead measure ratios - for example $\frac{a(t)}{a(t_0)}$, where $a(t_0)$ is the scale factor today. Since the metric can be rescaled, we will often conveniently set $a(t_0) = 1$. If we have $a(t) = 0$, then we have a singularity - the universe has zero size. This occurs in many models at $t = 0$ as an initial singularity or 'big bang', but may also occur at other times, for example as a 'big crunch', where the universe recollapses in a finite time.

There are other important observables related to the scale factor. The Hubble parameter, H(t), provides a measure of the rate of expansion,

$$H(t) = \frac{\dot{a}(t)}{a(t)}\ , \tag{1.27}$$

and the value today, H_0 is commonly known as the Hubble parameter. There are many different methods used to estimate the value of the Hubble parameter, and although the original methods used produced extremely imprecise values, modern measurements

have produced increasingly precise measurements of H_0 [23, 12, 24] resulting in values in the region of

$$H_0 \approx 70\ km\ s^{-1}\ Mpc^{-1}\ . \tag{1.28}$$

However, there is an important tension in the available data. The recent precise calculation of H_0 from the Planck collaboration [12] provides a value of $H_0 = 67.4 \pm 0.5$ and the SHoES programme [24] also provides a precise calculation, finding $H_0 = 74.03 \pm 1.42$. These calculations, based on different methods and observations, are not consistent. A third calculation using data from the Hubble space telescope, [23] finds $H_0 = 69.8 \pm 0.8 \pm 1.7$, which is consistent with both other calculations, but does not resolve the tension between them.

Related to the Hubble parameter, we also have the deceleration parameter

$$q(t) = -\frac{a\ddot{a}}{\dot{a}^2} = -\left(\frac{\dot{H}}{H^2} + 1\right)\ , \tag{1.29}$$

which indicates the universe is decelerating if $q > 0$, although current observations suggest the universe is instead accelerating, and therefore $q < 0$. A higher order term still is the jerk, defined as

$$j(t) = \dddot{a} a H^3\ . \tag{1.30}$$

and we note that H, q and j can be viewed as the first coefficients in the Taylor expansion of the scale factor.

In general relativity, we find that if a source emits radiation at time t_o, with wavelength λ_e, the wavelength received by an observer, λ_o, at time t_e is different, depending on the relative motion of the source and observer. This difference is quantified by the redshift, z,

$$1 + z = \frac{\lambda_o}{\lambda_e} = \frac{a(t_o)}{a(t_e)}\ , \tag{1.31}$$

where we will normally set t_o as the present time, so $a(t_o) = 1$.

1.3.2 Friedmann Equations

Now that we have established the FLRW metric, we can use it to solve our general relativistic equations of motion. The first step is to consider the form of $T_{\mu\nu}$ that we

require. It turns out that the properties of homogeneity and isotropy require that matter must take the form of a perfect fluid, as discussed in 1.2.5. We can prove this by considering first $T_{ab}(t, x, y, z)$ as an arbitrary symmetric tensor, where we can view each component as some function of the coordinates. The condition of spatial homogeneity, i.e. that the universe must look the same at every point, then forces that the Energy-Momentum tensor must in fact be a function of t only, i.e. $T_{ab}(t)$. We now consider the condition of spatial isotropy. We can consider T_{0i} and T_{i0} as spatial 3-vectors - by isotropy they must be invariant under spatial transformations. However, there are no non-zero isotropic 3-vectors, and therefore $T_{0i} = T_{i0} \equiv 0$. We can also consider T_{ij} as a spatial 3-tensor, which, again must be isotropic. Since the only isotropic spatial 3-tensors are proportional to δ_{ij}, we have $T_{ij} \propto p(t)\delta_{ij} \propto p(t)g_{ij}$ for some function p. Finally, we call the remaining component $T_{00} = \rho(t)$, which leaves us with the perfect fluid form of the Energy-momentum tensor, $T^a_b = diag(-\rho(t), p(t), p(t), p(t))$, as required.

Returning to the Einstein Field Equations

$$R_{\mu\nu} - \frac{1}{2}Rg_{\mu\nu} + \Lambda g_{\mu\nu} = \kappa T_{\mu\nu} \ , \tag{1.32}$$

and inserting this form of matter, together with the FLRW metric we find our cosmological equations of motion

$$\left(\frac{\dot{a}}{a}\right)^2 + \frac{k}{a^2} = \frac{\Lambda}{3} + \frac{\kappa}{3}\rho \ , \tag{1.33}$$

which is the 00 component of the Einstein equations, known as the Friedmann equation, and

$$\frac{\ddot{a}}{a} = -\frac{\kappa}{6}(\rho + 3p) + \frac{\Lambda}{3} \ , \tag{1.34}$$

from the ii component, which is known as the acceleration equation. Together these are sometimes known as the Friedmann equations, and they describe the evolution of the scale factor, and the perfect fluid described by the energy density ρ and pressure, p. These are the only independent components of the Einstein equations, and represent a significant reduction in complexity, from ten coupled, non-linear PDES, to just two ordinary differential equations.

We have a further equation, arising from the conservation of the energy-momentum tensor for a perfect fluid, which is known as the continuity equation

$$\dot{\rho} = -3\frac{\dot{a}}{a}(\rho + p) \ . \tag{1.35}$$

However, the continuity equation is in fact not independent of the Friedmann equations, and could be derived by differentiating (1.33) and combining appropriately with (1.34). Although only two of the three equations are independent, and so only two are needed to completely solve any situation, depending on the setup, it is helpful to use different combinations of the three.

We now have two independent equations, but with three variables, $a(t)$, ρ, p. Therefore, in order to solve the system, we need to specify a relationship between the energy density and the pressure. Typically this is done by specifying a specific equation of state, in which we express $p = p(\rho)$, for some specific form. The Friedmann equations can then be solved for a and ρ. The most commonly used cosmological equation of state is a simple linear one

$$p = w\rho \ , \tag{1.36}$$

where w is a constant which controls the behaviour of our perfect fluid. Choosing this equation of state, we then find that the continuity equation becomes

$$\dot{\rho} = -3\frac{\dot{a}}{a}(1 + w)\rho \ , \tag{1.37}$$

which can be integrated as

$$\rho = \rho_0 a^{-3(1+w)} \ . \tag{1.38}$$

At this point it is useful to consider the meaning of different values of w. The first step is to observe that if we take $w = -1$, then we have $\rho = \rho_0$, a constant. This is the same behaviour as the cosmological constant term in the Friedmann equations, meaning that we can view the cosmological constant as arising instead from the matter distribution, as a $w = -1$ perfect fluid. Similarly, $w = -1/3$ provides a term behaving as $\rho \propto a^{-2}$, which is the same behaviour as the curvature terms in (1.33) and (1.34) (the latter non-existent), and so we can instead view curvature as arising from the matter distribution. We may also consider some values of w which describe particular types of matter of importance. $w = 0$ results in $p = 0$, which describes 'dust', or

non-relativistic, pressureless matter, whilst $w = 1/3$ describe relativistic particles and radiation, and $w = 1$ describes a stiff fluid, such as a scalar field. Values of $w < -1$ are often known as 'phantoms', but have negative kinetic energy, and are generally regarded as unphysical. Values of $w > 1$ are known as 'ultrastiff', and are used in certain models. It is also worth noting at this point that since the Friedmann equations are linear in ρ, there is no difference between interpreting the cosmological constant and spatial curvature as arising from matter or from space-time curvature.

There is a commonly used alternative way of writing the Friedmann equations, by defining what are known as the (fractional) density parameters

$$\Omega_m = \frac{\rho}{3H^2}, \quad \Omega_k = -\frac{k}{a^2H^2}, \quad \Omega_\Lambda = \frac{\Lambda}{3H^2} \ , \tag{1.39}$$

in which case we can rewrite the Friedmann equation as a constraint equation

$$\Omega_m + \Omega_k + \Omega_\Lambda = 1 \ , \tag{1.40}$$

and we see that each term describes the fractional contribution of each term to the energy content of the universe. It has been possible to measure the value of the density parameters today, and the most recent measurements [12] show that $\Omega_{m,0} \approx 0.31$, $\Omega_{\Lambda,0} \approx 0.69$, and $\Omega_{k,0} < 0.001$. This means that we believe that the significant majority of the universe's current energy content arises from the cosmological constant, also known as dark energy. We also have strong evidence that the universe is extremely spatially flat.

Once we have found the energy density as a function of the scale factor as in (1.38), the next step is to attempt to integrate a second time and solve for the scale factor as a pure function of time, which it is possible to do in a range of scenarios. Historically, the dominant belief was in a static universe with neither beginning nor end, that is with $a(t) \equiv a_0$, a constant. This is the Einstein static universe [25], which lead to the original introduction of the cosmological constant, as it requires $k > 0$ and $\Lambda > 0$, constant matter density to which the value of Λ is tuned. The static universe is then given by

$$a = \sqrt{\frac{k}{\Lambda}} \ , \quad \Lambda = 4\pi G\rho_m \ . \tag{1.41}$$

However, it was subsequently noticed that this universe would be unstable to perturbations - a slight disturbance would be enough to destroy its static nature. Another simple

solution is the de Sitter universe. This is an exponentially expanding vacuum universe with non-zero cosmological constant, where the scale factor (in the case $k = 0$)is given by

$$a(t) = e^{\sqrt{\frac{\Lambda}{3}}t} \ . \tag{1.42}$$

The de Sitter universe is the late time attractor of the ΛCDM model, since as the universe expands all other cosmological components will be diluted away until we have a vacuum universe. If instead we had taken the negative square root, we would have an infinitely collapsing solution, but it is unstable. There is also a vacuum solution with no cosmological constant, provided we have negative curvature. This is the Milne solution, and has

$$a(t) \propto t \ . \tag{1.43}$$

If we consider a flat universe with no cosmological constant, we can use (1.38) and (1.33) to find

$$a(t) = \left(\frac{3(1+w)}{2}H_0 t\right)^{\frac{2}{3(1+w)}} \ , \tag{1.44}$$

and where $H_0 = \sqrt{\frac{\kappa\rho_0}{3}}$ is the value of the Hubble parameter today.

The standard model of cosmology, known as ΛCDM, describes a universal history consisting largely of periods where the energy content of the universe is dominated by a particular form, first radiation, then matter, and now dark energy, or Λ. Since the matter content, apart from near the change of eras, is dominated by one form, we can consider the universe as containing only a single form of matter. The earliest phase is radiation domination, which occurred at very early times and lasted until redshifts of $z \sim 3300$, which is the time known as matter-radiation domination. This era is approximately described by the Tolman solution, which has

$$a(t) = (2H_0 t)^{\frac{1}{2}} \ , \tag{1.45}$$

which is (1.44) with the equation of state for radiation, $w = 1/3$.

The second major era is that of matter domination, in which the dominant energy contribution arises from $w = 0$ dust. The period of matter domination is believed to have lasted from the matter-radiation crossover at $z \sim 3300$ until the onset of Λ domination at $z \sim 2/3$, at which point the current phase of accelerated expansion began. An approximate solution for this era during the time when Λ can be neglected

is the Einstein-de Sitter solution,

$$a(t) = \left(\frac{3}{2}H_0 t\right)^{\frac{2}{3}} \ . \tag{1.46}$$

This was favoured as a model for the universe when it was believed that $\Lambda = 0$. However, more recent evidence suggests that $\Lambda > 0$, in which case the Friedmann equations can still be solved explicity if $k = 0$. In the case of dust we then find

$$a(t) = \left(\frac{\Omega_{m,0}}{1-\Omega_{m,0}}\right)^{\frac{1}{3}} \sinh^{\frac{2}{3}}\left(\frac{3}{2}H_0\sqrt{1-\Omega_{m,0}}t\right) \ , \tag{1.47}$$

which is especially important for describing the universal history during the time when matter and Λ are both non-negligible. This has as it's limits the expected Einstein-de Sitter solution when t is small, i.e. matter domination, and the accelerating de Sitter universe at large times, i.e. during Λ domination.

To make further progress, for example in the case $k \neq 0$ we make a change of parameter, from coordinate time, t, to conformal time, η, defined by

$$\eta = \int \frac{dt}{a(t)} \ . \tag{1.48}$$

We can then find parametric solutions in certain cases, for example in the case of dust and a closed universe, $k > 0$ we have

$$a(\eta) = \frac{\Omega_{m,0}}{2(\Omega_{m,0}-1)}(1-\cos(\sqrt{k}\eta)) \ , \tag{1.49}$$

$$t(\eta) = \frac{\Omega_{m,0}}{2H_0(\Omega_{m,0}-1)^{\frac{3}{2}}}(\sqrt{k}\eta - \sin(\sqrt{k}\eta)) \ , \tag{1.50}$$

which reaches a maximum value of a at $\eta = \frac{2\pi}{\sqrt{k}}$ before recollapsing as expected for a closed universe, whilst for an open universe $k < 0$, we have a continuously expanding solution

$$a(\eta) = \frac{\Omega_{m,0}}{2(1-\Omega_{m,0})}(\cos(\sqrt{|k|}\eta) - 1) \ , \tag{1.51}$$

$$t(\eta) = \frac{\Omega_{m,0}}{2H_0(1-\Omega_{m,0})^{\frac{3}{2}}}(\sin(\sqrt{|k|}\eta) - \sqrt{|k|}\eta) \ . \tag{1.52}$$

A final parametric solution of interest is the two-fluid solution, for example to describe the period of radiation-matter equality at $z \sim 3300$, which takes the form

$$a(\eta) = \frac{1}{4}H_0^2\Omega_{m,0}\eta^2 + H_0\sqrt{1-\Omega_{m,0}}\eta \ , \tag{1.53}$$

$$t(\eta) = \frac{1}{12}H_0^2\Omega_{m,0}\eta^3 + \frac{1}{2}H_0\sqrt{1-\Omega_{m,0}}\eta^2 \ . \tag{1.54}$$

1.3.3 Other solutions in Cosmology

If we relax the assumptions of homogeneity and isotropy, it is still possible to find cosmological solutions in some cases, provided we still impose sufficiently 'nice' requirements on our spacetime. If we relax the requirement of isotropy, then there are a wide range of anisotropic universes, known as the Bianchi spacetimes. There are eleven types of Bianchi universe, labelled from I to IX (type VI and VII each have two subtypes), with the different types being defined by certain intrinsic properties of their isometry groups. The reduced symmetry of the Bianchi universes allows new and interesting behaviours to arise, particularly in the early universe, whilst a result due to Wald [26] showed that the existence of $\Lambda > 0$ is sufficient to cause these anisotropic universe to isotropise at late times. Specifically, Wald showed that all Bianchi models with $\Lambda > 0$, except for Type IX where Λ is small relative to the space-time curvature, evolve exponentially to the isotropic de Sitter solution.

The simplest type is the Bianchi type I spacetimes, which represent a generalisation of flat FLRW to having separate scale factors in each spatial direction, the line element for which is

$$ds^2 = -dt^2 + a^2(t)dx^2 + b^2(t)dy^2 + c^2(t)dz^2 \ , \tag{1.55}$$

and we recover isotropy (and hence $k = 0$ FLRW) by setting $a = b = c$. Although we do not go into further details in this thesis, it is worth noting that the $k > 0$ FLRW is recovered as a special case of Bianchi IX, and $k < 0$ FLRW similarly as a special case of Bianchi VII$_a$.

Of course, the Bianchi universes do not represent the only cosmological solutions. Even in the class of homogeneous spacetimes, there is an exceptional family known as the Kantowski-Sachs universes which fall outside of the Bianchi classification, by virtue of the spatial components having topology $\mathbb{R} \times S^2$. If we further relax the requirement of homogeneity, then we may encounter the Lemaître-Tolman-Bondi spacetimes which is

a spherically symmetric solution to the Einstein equations in the presence of dust. This solution has been used in various ways, including to measure the effect of overdense regions and voids in an expanding universe, or to investigate the behaviour of an inhomogeneous big bang. Similarly, the so-called 'Swiss-cheese' model is constructed by removing spherical sections from FLRW, and filling them with another spherically symmetric solution with suitable boundary behaviour. Even further, the Szekeres-Szafron family of solutions [27] has no specific symmetries, but retains some helpful algebraic properties and takes the general form

$$ds^2 = -dt^2 + e^{2\alpha}dz^2 + e^{2\beta}(dx^2 + dy^2), \tag{1.56}$$

where α and β are functions of all four coordinates. Many of the other solutions discussed, including FLRW itself, arise as special cases of the Szekeres-Szafron family.

1.3.4 Problems in Cosmology

The standard model of Cosmology, ΛCDM, is in very good agreement with most observational data. However, there remain problems with it which yet to meet satisfactory resolution, and we summarise a couple of them below.

As we discussed earlier, observations of the Cosmic Microwave Background strongly support the idea that the universe is isotropic. However, if we attempt to ask why the universe appears so isotropic, we encounter the Horizon problem. The CMB is an observable remnant of the early universe, formed when photons decoupled from the primordial plasma approximately 380,000 years after the big bang. In order to consider how particles may have interacted in the past, we define the particle horizon as

$$\eta_{ph} = \int_{\ln a_i}^{\ln a} (aH)^{-1} d\ln a \ , \tag{1.57}$$

where $a_i \equiv 0$ is the initial big bang singularity. We also call $(aH)^{-1}$ the Hubble radius. This is equivalent to the amount of conformal time, $\eta = \int_{t_1}^{t_2} \frac{1}{a} dt$, which has passed since the initial singularity until today. The particle horizon is the maximum comoving distance travelled by light since the beginning of the universe, and thus tells us whether two photons could have interacted at any point in the past. If their particle horizons do not intersect, then they cannot have been in causal contact at any point in the past. If we do this calculation in the standard model of cosmology, with an increasing

Hubble radius and perfect fluid matter component with $w > -1/3$ (which is necessary physically in order to obey the strong energy condition) then we encounter a serious problem. We find that the big-bang singularity occurred at conformal time 0, (1.57) is dominated by its upper limit, and therefore that $\eta_{ph} \sim (aH)^{-1}$, i.e. that there has been a finite amount of conformal time since $t = 0$, and as a consequence that most points on the sky have non-overlapping particle horizons. In fact, this affects any points separated by more than about 1 deg of sky, resulting in 10^4 patches of the CMB with non-overlapping horizons. But if these patches have non-overlapping particle horizons, then they were never in causal contact, so why does the universe appear so isotropic? This is the horizon problem.

The cosmological constant was originally introduced by Einstein in order to permit the existence of a static universe, the evidence built against such a model, and he eventually discarded the cosmological constant entirely, preferring instead an expanding universe without Λ. However more recent cosmological evidence has reintroduced the cosmological constant in order to explain the observed accelerating expansion of the Universe. Λ appears in the Einstein equations, and can be interpreted equivalently as either a 'bare' geometric term, or as a perfect fluid with energy density

$$\rho_\Lambda = \frac{\Lambda}{8\pi G} \ . \tag{1.58}$$

This cosmological interpretation of Λ has no theoretical determination of the size, rather from observations we can determine that

$$\rho_\Lambda^{1/4} \sim 10^{-3} eV \ , \tag{1.59}$$

which does not lead to any problem on the classical level. However, if we consider the quantum field theory contributions to the vacuum energy, we find that there are zero-point energy contributions that are many orders of magnitude larger. If we fix an energy cutoff, E, for our quantum theory, then an effective cosmological constant arises

$$\rho_{vac} = \frac{1}{2}\int_0^E \frac{d^3\mathbf{k}}{(2\pi)^3}\sqrt{k^2+m^2} \sim E^4 \ . \tag{1.60}$$

Depending on the level at which we set the cutoff energy, we now find that

$$\rho_{vac}^{1/4} \sim 10^{11} eV \qquad \text{up to} \qquad \rho_{vac}^{1/4} \sim 10^{27} eV \ , \tag{1.61}$$

so that the value of the cosmological constant from these quantum calculations is 60-120 orders of magnitude larger than the observed value. Further, even if the cosmological constant could be fixed at an appropriately small value, it would still be vulnerable to quantum fluctuations of large size compared to the value of Λ. This, then, is the cosmological constant problem, finding a way to reconcile the observed value of Λ with the size of the quantum contributions to the vacuum energy.

1.3.5 Inflation

In order to resolve some of the cosmological issues, such as the horizon problem, which arise in the early universe of the standard model of cosmology, on proposed solution is inflation. This is a hypothetical period of accelerated expansion, occurring after the big bang but before the onset of radiation domination. Inflation was first proposed by Guth in 1981 [28], as a solution to these cosmological problems, followed swiftly by many further models which corrected certain problems with the early formulations, particularly regarding the mechanisms for exiting the inflationary phase [13, 29]. Nowadays, there are many different models of inflation, ranging from simple models of single field inflation, in which inflation is driven by a single scalar field, known as the inflaton, acting in some appropriate potential, to far more complex models involving multiple fields, through to eternal inflation in which the inflationary phase of the universe occurs forever in most of the universe, with only pockets of the universe ever exiting inflation resulting in a multiverse outcome [30].

If there is a period of accelerated expansion in the early universe, then by definition $\ddot{a} > 0$, which is equivalent to the statement that

$$\frac{d}{dt}(aH)^{-1} < 0 \ , \tag{1.62}$$

that is that the Hubble radius is shrinking during the accelerating phase. If we also take the energy content of the universe to be provided by a strong energy condition violating perfect fluid, so that $w < -1/3$, then we find that (1.57) is instead dominated by its *lower* limit, and that the initial big bang singularity occured at $-\infty$ conformal time. This means that instead of a finite particle horizon, we instead have infinite conformal time between the big bang and now, so there is enough “time" for all particles to have been in causal contact, thus resolving the Horizon problem.

The simplest way to perform inflation, is via a single scalar field acting in an appropriate potential. The equations of motion for a single scalar field ϕ in a potential $V(\phi)$ in flat FLRW space are:

$$H^2 = \frac{1}{2}\dot{\phi}^2 + V(\phi) \ , \tag{1.63}$$

which is the Friedmann equation with units chosen such that $\frac{8\pi G}{3} \equiv 1$, and

$$\ddot{\phi} + 3H\dot{\phi} + V'(\phi) = 0 \ , \tag{1.64}$$

from the continuity equation. These are obtained straightforwardly, because a scalar field can be viewed as a perfect fluid with $\rho_\phi = \frac{1}{2}\dot{\phi}^2 + V(\phi)$ and $p_\phi = \frac{1}{2}\dot{\phi}^2 - V(\phi)$. The inflaton begins far away from the minimum, at which point its behaviour is dominated by the potential, driving exponential-like expansion of the universe in a way similar to a cosmological constant. For this phase, the potential undergoes slow-roll behaviour, and we can make the slow-roll approximations

$$\frac{1}{2}\dot{\phi}^2 << V(\phi) \qquad \text{and} \qquad \ddot{\phi} << |3H\dot{\phi}| \ , \tag{1.65}$$

meaning that the equations of motion reduce to

$$3H^2 \approx v(\phi) \qquad \text{and} \qquad 3H\dot{\phi} \approx -V'(\phi) \ , \tag{1.66}$$

which are readily soluble with a specific choice of $V(\phi)$. Inflation ends once the inflaton reaches the bottom of the potential, and the behaviour instead becomes dominated by the kinetic terms. At this point it is expected that a period of reheating occurs, the inflaton decays, and standard physics takes over [31]. There are many different classes of potential that can drive inflation, but the simplest is power-law inflation, in which the inflationary potential takes the form

$$V(\phi) = V_0\phi^n \qquad n > 0 \ , \tag{1.67}$$

that is, a simple monomial. Typical choices might be $n = 2$ or $n = 4$, the latter of which was Linde's original model of chaotic inflation [32]. As an example of how the

system can then be solved, if we choose $n = 2$, we find

$$\phi(t) = \phi_0 - \sqrt{\frac{V_0}{12}}t \ , \tag{1.68}$$

$$a(t) = a_0 \exp\{4(\phi_0^2 - \phi^2(t))\} \ . \tag{1.69}$$

There are many other models of inflation, for example, the alpha-attractor models [33, 34] which are families of potentials originally motivated by string theory and supergravity considerations in accordance with cosmological observations. The α in question is a parameter corresponding to the cutoff from the underlying supergravitational theory, whilst they are called attractors because some of the fundamental observational predictions of these models remain stable even as the choice of potential may vary significantly. Of particular importance is the predictions of the primordial scalar spectral index, n_s and the tensor-to-scalar ratio, r. The predictions of both of these parameters from the alpha-attractor models lie directly within the observationally favoured region of the phase-space from the WMAP [35] and Planck [12] observations of the Cosmic Microwave Background. The basic families of single field alpha attractors include the T-model

$$V(\phi) = V_0 \tanh^{2n}\left(\frac{\phi}{\sqrt{6\alpha}}\right) \ , \tag{1.70}$$

and the E-model

$$V(\phi) = V_0(1 - e^{-\sqrt{\frac{2}{3\alpha}}\phi})^{2n} \ , \tag{1.71}$$

whilst many other common choices of inflationary potential emerge as specific cases of these.

1.3.6 Modified Gravity

Although we can attempt to resolve some of the problems in ΛCDM through adding a new physical process, such as inflation, active at some point during the history of the universe, many proposed solutions arise instead from attempting to modify the theory of general relativity itself. It can already be seen that GR is not a complete theory of gravitation, as it breaks down at extreme curvatures, resulting in singularities in the theory. In addition, it is not compatible with quantum theory, and no unified description is known. Therefore we might expect to be able to resolve some of these problems by modifying GR itself. Typically this is done by using a more complicated

action than the simple Einstein-Hilbert, which may include the introduction of new fields. This will then result in higher order terms appearing in the equations of motion, leading to new behaviour in certain scenarios, whilst not deviating significantly from GR in local tests.

Modifications to gravity can take many forms, but one of the earliest modifications of GR arose from allowing the gravitational 'constant', G, to vary. This is the Brans-Dicke theory [36], in which G^{-1} is replaced by a new scalar field ϕ, and a corresponding kinetic term introduced into the action, which becomes:

$$\mathcal{S} = \frac{1}{16\pi}\int \sqrt{-g}(\phi R - \frac{\omega}{\phi}\partial_a\phi\partial^a\phi)d^4x + \int \sqrt{-g}\mathcal{L}_m d^4x \ . \tag{1.72}$$

Varying this action then produces a generalisation of the Einstein Field equations, as well as an additional equation of motion relating ϕ to the energy-momentum tensor, and the entire theory recovers general relativity in the limit $\omega \to \infty$. This, however, is not the most general theory in the class of 'scalar-tensor' theories. ω can be permitted to vary as a function of ϕ, and a potential for the scalar field can be introduced, which then acts as a dynamical generalisation for the cosmological constant. A more general scalar tensor action is then

$$\mathcal{S}_{\mathcal{ST},\mathcal{J}} = \frac{1}{16\pi}\int \sqrt{-g}\left\{\left(\phi R - \frac{\omega(\phi)}{\phi}\partial_a\phi\partial^a\phi + \Lambda(\phi)\right) + \alpha_m\mathcal{L}_m\right\}d^4x \ , \tag{1.73}$$

where α_m is a coupling constant for the matter lagrangian. Generalising further still, the most general four-dimensional scalar-tensor theory with second-order equations of motion is known as Horndeski gravity. Horndeski generalises (1.73) by replacing the coefficient of R by a function of ϕ and $X = \partial_a\phi\partial^a\phi$, and the introduction of several new terms. Collectively, the modifications then depend upon four functions, known as $G_n(\phi, X)$ for $2 \leq n \leq 5$, and the total action takes the form

$$\begin{aligned}\mathcal{L} \ &= G_2(\phi,X) + G_3(\phi,X)\Box\phi + G_4(\phi,X)R + G_{4,X}(\phi,X)\left[(\Box\phi)^2 - \phi_{;ab}\phi^{;ab}\right] \\ &+ \ G_5(\phi,X)G_{ab}\phi^{;ab} - \frac{1}{6}G_{5,X}(\phi,X)\left[(\Box\phi)^3 + 2\phi_{;a}^{\ ;b}\phi_{;b}^{\ ;c}\phi_{;c}^{\ ;a} - 3\phi_{;ab}\phi^{;ab}\Box\phi\right],\end{aligned} \tag{1.74}$$

where $\Box$ is the d'Alembertian operator. We can see that we recover the simpler theories as specific cases, with the scalar-tensor action in (1.73) coming from $G_3 = G_5 = 0$, $G_2 = -\frac{\omega(\phi)}{\phi}X$, $G_4 = \phi$. The Horndeski action has a rich variety of possible behaviours, however recent observational tests have placed strong bounds on several of

the parameters. Chief amongst these was the detection, by the LIGO collaboration, of gravitational waves from the neutron star binary collision GW170817 [37] and the electromagnetic counterpart GW170817A [38]. The combination of these observations allows strong bounds to be placed on the deviation of the speed of propagation of gravitational waves, c_T, from the speed of light $c = 1$. Writing $c_T^2 = 1 + \alpha_T$, a an extremely tight bound of $|\alpha_T| \lesssim 1 \times 10^{-15}$ [39] has been placed, fixing the deviation at essentially zero. This has serious implications for Horndeski models and, absent any finely tuned cross-cancellation of specific terms, the final three terms in (1.74) must vanish identically, leaving a much reduced form of the action as viable

$$\mathcal{L} \ = G_2(\phi, X) + G_3(\phi, X)\Box\phi + G_4(\phi)R, \tag{1.75}$$

although this form of the action leaves viable several common modifications, including the Brans-Dicke scalar-tensor theory and its generalisation (1.73).

An intriguing aspect of scalar-tensor theories is that there exist conformal transformations from (1.73), known as the Jordan frame action, to another frame known as the Einstein frame, in which the action of the transformed fields takes the standard form of the Einstein-Hilbert action together with a minimally coupled canonical scalar field, but with a non-constant coupling to the matter lagrangian.

$$\mathcal{S}_{\mathcal{ST},\mathcal{E}} = \frac{1}{16\pi}\int \sqrt{-\tilde{g}}\left\{\left(\frac{\tilde{R}}{G} - \frac{1}{2}\tilde{\partial}_a\tilde{\phi}\tilde{\partial}^a\tilde{\phi} + V(\tilde{\phi})\right) + \tilde{\alpha_m}(\phi))\mathcal{L}_m\right\} d^4x \ . \tag{1.76}$$

This conformal equivalence is very useful for analysis of scalar-tensor theories, since known solutions in GR can be conformally transformed into solutions of the scalar-tensor theory. It is important to note however, that the non-constancy of α_m in (1.76) results in deviation from general relativity in the behaviour of matter fields. The matter energy momentum tensor is not conserved, and the equivalence principle is broken. This, as we shall see, is a feature of many modified gravitational theories.

An alternative modification, although in some ways related to scalar-tensor theories, is $F(R)$ gravity [40], in which the Ricci scalar in the Einstein-Hilbert action is replaced by some function of the Ricci scalar, $F(R)$

$$\mathcal{S} = \frac{1}{2\kappa}\int \sqrt{-g}(F(R) - 2\Lambda)d^4x + \int \sqrt{-g}\mathcal{L}_m d^4x \ . \tag{1.77}$$

This results in higher-order equations of motion, in which the left-hand side of the Einstein equations are altered, whilst maintaining the covariance and Lorenz invariance of the Einstein-Hilbert action. Varying this results in the equations of motion

$$F'(R)R_{\mu\nu} - \frac{1}{2}F(R)g_{\mu\nu} - \nabla_\mu\nabla_\nu F'(R) + g_{\mu\nu}\nabla^\zeta\nabla_\zeta F'(R) = \kappa T_{\mu\nu} \ , \tag{1.78}$$

which are in general fourth order equations of motion, but can be seen to reduce to general relativity in the case $F(R) = R$. As mentioned above, these models are closely related to scalar tensor models, as there exists a conformal transformation which maps $F(R)$ theories to GR with minimally coupled scalar fields, and legendre transformations which result in theories like Brans-Dicke with $\omega = 0$ [41]. This makes models of this kind of extreme interest in cosmology, as they provide a geometric origin for behaviours such as inflation. Many $F(R)$ models exhibit interesting features, but a specific example of great interest is

$$F(R) = R + \alpha R^2 \ , \tag{1.79}$$

which produces inflationary behaviour known as Starobinsky inflation [42] in the early universe, which is in very good agreement with current observational data [43]. By the conformal transformation mentioned above, this model is equivalent to a minimally coupled scalar field acting in the potential

$$V(\phi) = V_0\left(1 - e^{-\sqrt{\frac{2}{3\alpha}}\phi}\right)^2 \ , \tag{1.80}$$

which we note is the case of the α-attractor E-model with $n = 1$ given in (1.71).

However, although $F(R)$ gravity is a natural extension of the Einstein-Hilbert action, the Ricci scalar is not the only term that we could add to the action. Indeed, R is not even the only scalar formed from the Riemann tensor that we might consider. We could also consider the "squared" scalars $R_{ab}R^{ab}$ and $R_{abcd}R^{abcd}$, which allow us to then consider the action

$$\mathcal{S} = \frac{1}{2\kappa}\int\sqrt{-g}F(R, R_{ab}R^{ab}, R_{abcd}R^{abcd})d^4x + \int\sqrt{-g}\mathcal{L}_m d^4x \ . \tag{1.81}$$

Many solutions have been found in these extended theories, including homogeneous and isotropic solutions familiar from GR, as well as solutions in both the isotropic and anisotropic cases in which the scale factors take the form of power laws [44], and

many others. As an example of deviations from GR, it has been found that in theories of the form $f(R, R^{ab}R_{ab}) = R + \alpha(R^{ab}R_{ab})^n$ initial isotropic singularities are stable under various types of perturbation, whilst in GR they would be unstable [45]. Further progress can be made in some situations by consideration of the Gauss-Bonnet term [40] which is given by

$$G = R^2 - 4R^{ab}R_{ab} + R^{abcd}R_{abcd}. \tag{1.82}$$

G is a purely topological surface term, and therefore does not contribute to the action if it appears linearly. Therefore if one of the three arguments of F appears as a simple linear term added to some function of the other two, then we can eliminate that argument in favour of the other two and G, and integrate out the linear G contribution to leave just two arguments. Unfortunately this is not possible for the most general form of F, as arbitrary functions of G are not themselves total derivatives.

The above answers the question of how to generalise GR by adding additional curvature terms to the action. However, the Einstein equations contain two parts, the Ricci tensor and scalar on the left, and the energy-momentum tensor on the right-hand side. We could therefore consider the addition of terms dependent on T_{ab} to the Einstein Hilbert action, and there are two natural types to consider, based on either the trace of the energy-momentum tensor, $T = T^a_{\ a}$ [46] or the scalar square, $T^{ab}T_{ab}$ [47, 48]. This type of modification introduces new higher-order matter contributions to the Einstein equations, and hence impact the cosmology by introducing new non-linear behaviour of matter in the Friedmann equations. It is worth confirming that these types of modification do indeed have different behaviour, as can be seen by considering a perfect fluid with equation of state $w = -1/3$. In this case the trace of the energy momentum tensor vanishes, $T = 0$ and so we would expect no modification to the underlying cosmology, but the square, $T^{ab}T_{ab}$ does not vanish. If we consider the case of $F(R, T^{\mu\nu}T_{\mu\nu})$ gravity, known as "Energy-momentum squared gravity", we have the action

$$S = \frac{1}{2\kappa}\int \sqrt{-g}(F(R, T^{\mu\nu}T_{\mu\nu}) - 2\Lambda)\ d^4x + \int L_m\sqrt{-g}\ d^4x\ , \tag{1.83}$$

and varying this we find the modified Einstein Field equations

$$F_R R_{\mu\nu} - \frac{1}{2}F g_{\mu\nu} + \Lambda g_{\mu\nu} + (g_{\mu\nu}\nabla_\alpha\nabla^\alpha - \nabla_\mu\nabla_\nu)F_R = \kappa(T_{\mu\nu} - \frac{1}{\kappa}F_{\mathbf{T^2}}\theta_{\mu\nu})\ , \tag{1.84}$$

where subscripts of R and $\mathbf{T}^2$ represent differentiation of F with respect to the relevant argument, and θ is a tensor dependent on the energy momentum tensor as

$$\theta_{\mu\nu} \equiv \frac{\delta(T_{\alpha\beta}T^{\alpha\beta})}{\delta g^{\mu\nu}} \ . \tag{1.85}$$

Theories of this kind have now been studied in several contexts, often using forms such as $F(R, \mathbf{T}^2) = R + \eta\mathbf{T}^{2n}$. In this context [47] investigated solutions for charged black holes in the theory, and [49] considered similar models as arising from quantum fluctuations of the metric tensor. The cosmology of these models is particularly interesting, as, for example, the case with $n = 1$ results in quadratic modifications to the Friedmann equations, bearing resemblance to those corrections arising in Braneworld or Loop Quantum Cosmology models. In the third and fourth chapters of this thesis, we investigate the cosmology of certain models in $F(R, T^{\mu\nu}T_{\mu\nu})$ gravity.

Chapter 2

Singular inflation with more general potentials

2.1 Introduction

2.1.1 Singularities

Singularities, whereby some quantity becomes ill-defined, often by taking some infinite value, are a feature of great interest in the study of general relativity and cosmology. There exist many different kinds of behaviour referred to as singularities, ranging from simple co-ordinate singularities which arise only as a result of our choice of co-ordinate system, such as in the case of the famous Schwarzschild solution for a spherically symmetric, non-rotating, uncharged black-hole which has metric

$$ds^2 = -\left(1 - \frac{r_s}{r}\right) dt^2 + \left(1 - \frac{r_s}{r}\right)^{-1} dr^2 + r^2 d\Omega^2 \ , \tag{2.1}$$

which appears to become singular at $r = r_s$. However, this singularity turns out not to be a physical singularity, and can be removed by a suitable change of variable. This stands in contrast to the case at $r = 0$ which is not a simple co-ordinate singularity, but a spacetime curvature singularity at which various co-ordinate independent quantities diverge. A typical scalar quantity that one might consider in this case is the Kretschmann scalar, $K = R^{abcd}R_{abcd}$, which becomes infinite at $r = 0$ in Schwarzschild.

In a cosmological context, the most natural singularity to consider is the Big Bang. In ΛCDM, the universe began at some finite point in the past from an initial singularity of infinite density, where $a = 0$ [18]. Given, then, that the history of the universe began with a singularity, the natural question to ask is whether there may be a further singularity in the future, and if so what form it might take. A natural mirror of the Big Bang singularity is the Big Crunch, a future density singularity, an example of which occurs in a closed universe described by the FLRW metric with $k > 0$ and the energy content described by a perfect fluid with $w > -1/3$, for example dust $w = 0$. In this the universal expansion reaches a maximum value before recollapsing in finite time to a singularity of infinite density and zero size.

However, these density singularities are not the only cosmological singularities. The Big Rip is a type of future singularity in which the scale factor and its derivatives become infinite in a finite amount of time [50]. It occurs when the energy content of the universe is made up of a phantom, $w < -1$ perfect fluid, and could be viewed as the opposite of a Big Crunch - the universe becomes infinite in extent but has zero density.

Both classes of future singularity mentioned above might be regarded as 'strong' singularities, representing a cosmological event which is a fundamental end to the universe, we can consider weaker future singularities. The "sudden singularities" of [51], in which both $a(t)$ and $\dot{a}(t)$ remain finite, but $\ddot{a}(t)$ becomes infinite in some finite time. In this case, the density, ρ, remains finite, but the pressure, p, becomes infinite. Futhermore $\rho + 3P > 0$ at this point, so the strong energy condition is not violated. We can observe this behaviour if we consider the solution for the scale factor given in [52]

$$a(t) \;=\; \left(\frac{t}{t_s}\right)^q (a(t_s) - 1) + 1 - \left(1 - \frac{t}{t_s}\right)^n, \tag{2.2}$$

where t_s is the time at which the sudden singularity occurs, and $0 < q \leq 1$, $1 < n < 2$. From this we can then see by substituting this solution into the friedmann equations, that at time t_s, $a(t_s)$ remains finite, as does $\rho(t_s)$, but $\ddot{a}(t_s) \to \infty$, $p(t_s) \to \infty$. Weaker singularities still can be constructed, in which the divergence occurs in an arbitrarily high derivative of the scale factor [53], as indeed occurs if we allow $2 < n < 3$ in this example.

These sudden singularities are weaker than the Big Rip and Big Crunch type singularities in several ways:

1. Geodesics are extendible through sudden singularities [54]. This can be seen as the geodesic equations depend only on the first derivative of the scale factor, which remains finite - it is only higher derivatives which diverge.

2. They obey most of the classical energy conditions. The exception is the dominant energy condition, but even this is satisfied by the generalised sudden singularities. [55]

3. The singularities are not "crushing" - objects approaching the singularity are not crushed to zero volume, and the Ricci scalar remains finite, although higher derivatives may not.

Finally, we might wish to consider a method of classifying cosmological singularities. In [56], future cosmological singularities occuring at some finite time t_s, are sorted into four types.

Type I - as $t \to t_s$, $a \to \infty$ $\rho,\ p \to \infty$

Type II - as $t \to t_s$, $a \to a_s$ $\rho \to \rho_s,\ p \to \infty$

Type III - as $t \to t_s$, $a \to a_s$ $\rho \to \infty,\ p \to \infty$

Type IV - as $t \to t_s$, $a \to a_s$, $\rho \to 0,\ p \to 0$, higher derivatives of H diverge

Sudden singularities are classified as Type II, whilst the generalised sudden singularities are Type IV. Type I singularities would include the Big Rip, and Type III would include singularities such as the Big Freeze [57], which arises in certain models of Cosmology where the matter takes the form of a Chaplygin gas.

2.1.2 Singular inflation

One solution to problems, such as the horizon problem, which arise in the early universe of the standard ΛCDM mode of cosmology is inflation. This involves the addition of fields that will, in the early universe, have caused very rapid expansion. This allows for greater conformal time to have passed than otherwise thought, meaning that the disparate regions in fact were in causal contact in the early universe. The simplest way to model inflation is by the addition of a single canonical and minimally coupled scalar field acting in some potential to General Relativity. The resulting equations of

motion are as given above. Perhaps the most straightforward example of an inflationary potential is the powerlaw $V(\phi) = \phi^n$, which is simple to write down and has been highly studied. Even in this case, however, complexities can arise.

[58] showed that sudden singularities arise for a simple scalar field in a power-law potential $V(\phi) = A\phi^n$ for n non-integer. The singularities occur in the $\lfloor n \rfloor + 2$ th derivative of ϕ, and can be observed by taking $\lfloor n \rfloor$ derivatives of the scalar field equation of motion (2.10). The non-integer power means that the differentiated equation contains a negative power of ϕ which will diverge if it can be shown that $\phi = 0$ in finite time. This was shown to occur. Potentials of this form can be used to describe large-field inflationary theories, which would subsequently result in evolution to a sudden singularity. Inflation with fractional power law potentials has been discussed before, eg [59]. This suggests that it is worthwhile investigating the range of potentials that result in sudden singularities in order to determine which inflationary models may exhibit this behaviour, and in 2.2 we investigate which properties of the potential will result in a sudden singularity.

2.1.3 Minimally Coupled Scalar Fields

We consider a simple cosmological model, consisting of a flat, homogeneous and isotropic universe with the matter content described by a single minimally coupled scalar field. The metric is then given by the $k = 0$ FLRW metric

$$ds^2 = -dt^2 + a^2(t)\left(dx^2 + dy^2 + dz^2\right) \ . \tag{2.3}$$

The matter content is described by the scalar field Lagrangian,

$$L_\phi = \frac{1}{2}\dot{\phi}^2 - V(\phi) \ , \tag{2.4}$$

where $V(\phi)$ is a chosen potential. The pressure and density of our scalar field are then

$$\rho = \frac{1}{2}\dot{\phi}^2 + V(\phi) \ , \tag{2.5}$$

$$p = \frac{1}{2}\dot{\phi}^2 - V(\phi) \ . \tag{2.6}$$

$$\tag{2.7}$$

By inserting these into the Friedmann equations and the continuity equation, we find the scalar field equations of motion.

$$3H^2 = \frac{1}{2}\dot{\phi}^2 + V(\phi) \ , \tag{2.8}$$

$$\dot{H} = -\frac{1}{2}\dot{\phi}^2 \ , \tag{2.9}$$

$$\ddot{\phi} = -3H\dot{\phi} - V'(\phi) \ . \tag{2.10}$$

2.2 Finite time singularities in more general potentials

In [58] it was shown that singular inflation occurs for a scalar field with potential $V(\phi) = \phi^n$ for non-integer n and generic initial conditions. They showed that for $\phi_0 > 0$ and $\dot{\phi}_0 > 0$ first $\dot{\phi}$ must become negative in finite time and that in finite time beyond this ϕ itself must reach zero. By the nature of the potential, as $\phi \to 0$ then $V(\phi)$ remains finite, but $V'(\phi)$ diverges, resulting in the singular behaviour in $\ddot{\phi}$. We have worked to generalise these results in order to increase the known family of potentials which will result in singular inflationary behaviour. In the following work we determine sufficient conditions on $V(\phi)$ to ensure firstly that $\dot{\phi}$ reaches 0 in finite time, before finding further conditions which suffice to ensure that ϕ itself reaches 0 in finite time, resulting in a sudden singularity in the future.

2.2.1 Showing $\dot{\phi} \to 0$ in finite time

It can be shown that $\dot{\phi}$ must become negative in finite time when the potential is such that $V(\phi) > 0$, $V(\phi)$ is increasing, and $V'(\phi)$ has finitely many stationary points, all for $\phi > 0$. Consider initial conditions $\phi_0 > 0$ and $\dot{\phi}_0 > 0$.

In the case that the number of stationary points of $V'(\phi)$ is non-zero, since the initial conditions were generic, we can simply evolve forwards a finite time until the system passes the final stationary point and consider the system again with a new ϕ_0 and $\dot{\phi}_0$ and a potential that is either increasing or decreasing.

Consider the case with $V'(\phi)$ decreasing. Then the scalar field equation of motion is

$$\ddot{\phi} = -3H\dot{\phi} - V'(\phi) < 0 \ , \tag{2.11}$$

where the inequality arises as both terms are negative for this region. Integrating twice gives

$$\phi(t) < \phi_0 + \dot{\phi}_0 t \ , \tag{2.12}$$

and as $V'(\phi)$ is decreasing,

$$\ddot{\phi} < -V'(\phi) < -V'(\phi_0 + \dot{\phi}_0 t) \ . \tag{2.13}$$

Integrating again gives that

$$\dot{\phi} \leq \dot{\phi}_0 + \frac{V(\phi_0)}{\dot{\phi}_0} - \frac{V(\phi_0 + \dot{\phi}_0 t)}{\dot{\phi}_0} \ . \tag{2.14}$$

Since $V(\phi)$ is increasing in ϕ, the final term must eventually pass the constant term and at this point $\dot{\phi} = 0$. Note that in fact in this case the requirement that the potential be increasing is actually stronger than is necessary - all that is really required is that at some point it reaches the (fixed) constant value. This could happen if it tended to some limit above this value or in various other situations.

If $V'(\phi)$ is increasing then we can provide the following bound, as with $\dot{\phi} > 0$, ϕ must be increasing in this region:

$$\ddot{\phi} < -V'(\phi_0) \ . \tag{2.15}$$

Integrating, we find

$$\dot{\phi} \leq \dot{\phi}_0 - V'(\phi_0)t \ , \tag{2.16}$$

which must go to zero in finite time.

2.2.2 Showing $\phi \to 0$ in finite time

To show that ϕ itself becomes zero in finite time is more complicated. In the case of sudden singularities we can show that one must arise in the case above when $V'(\phi)$ is

decreasing beyond some finite time. For the generalised sudden singularities it is less straightforward.

Consider first the case that after finite time $V'(\phi)$ is decreasing. This corresponds to the case in [58] where $0 < n < 1$, and proceeds in similar fashion. We show that there is a finite time T beyond which $\dot{\phi}(t) < \dot{\phi}(T) < 0$ for all $t > T$. Since at $\dot{\phi} = 0$, $\ddot{\phi} = -V'(\phi) < 0$ it is clear that we can find a T such that $\dot{\phi}(T) < 0$ and after this remains negative. In addition T can be chosen such that $\ddot{\phi}(T) < 0$.

Since by equation (2.9) we have that $H(t)$ must be decreasing we can consider (2.10), supposing for contradiction that there is t_1 such that $t_1 > T$ and that $\dot{\phi}(t_1) = \dot{\phi}(T)$. For this to occur we must then have $\ddot{\phi} > 0$:

$$\ddot{\phi}(t_1) = -3H(t_1)\dot{\phi}(t_1) - V'(\phi(t_1)) \tag{2.17}$$

$$< -3H(T)\dot{\phi}(T) - V'(\phi(T)) = \ddot{\phi}(T) < 0 \ , \tag{2.18}$$

and so this cannot occur. This then places a lower bound on the rate of decrease of ϕ, which is sufficient to ensure that it must reach 0 in finite time, and causes a sudden singularity to occur. There are several families of potential which satisfy these conditions and thus exhibit a sudden singularity. One example of these is the family $V(\phi) = \tanh(A(\phi)^n)$ for $0 < n < 1$, where A is a suitable constant with mass dimension $-n$, which renders the argument of tanh dimensionless, and for which $\phi \to 0$ as shown below (figure 2.1). It is also worth noting that numerical simulations suggest these potentials also exhibit $\phi \to 0$ for $n > 1$, although these do not quite fulfil the conditions on $V(\phi)$ given above. A further possibility is the similar potentials $(\tanh(A\phi))^n$ for $0 < n < 1$, where A is an appropriate constant with mass dimension -1, which are of the form considered in the α-attractor model [60].

For higher order singularities (corresponding to the case $n > 1$ in the power law potentials discussed in [58]) the situation is less clear. One can show that

$$F(\phi) \equiv \int \frac{1}{V'(\phi)} d\phi < C - t \ , \tag{2.19}$$

where C is a constant. This is done by assuming that at some time t_1 after $\dot{\phi}$ has become negative we have $\ddot{\phi} > 0$ for all $t > t_1$. If this is not the case then ϕ must decrease even faster, so it is sufficient to consider this case. Rearranging (2.10) we can

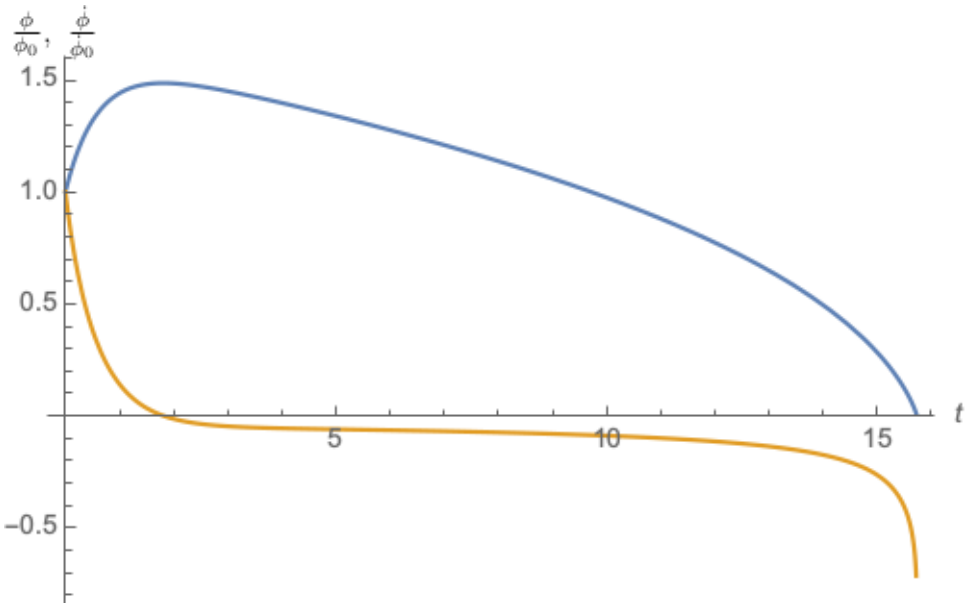

Fig. 2.1 Numerical simulation for a universe containing a scalar field with $V(\phi) = \tanh((\frac{\phi}{\phi_0})^{1/3})$. The y-axis gives the values of the field and its derivative, both normalised by their initial values. The upper, blue line is the value of $\frac{\phi}{\phi_0}$ whilst the lower, orange line is that of $\frac{\dot{\phi}}{\dot{\phi}_0}$. As can be seen, $\phi = 0$ is reached in finite time.

write

$$\dot{\phi} \leq \frac{-V'(\phi)}{3H} \ , \tag{2.20}$$

and integrating again gives the result.

This bound is not terribly intuitive, but allows us to at least see that if $F(\phi)$ has its only root at $\phi = 0$ and $F(\phi_0) > 0$ then in finite time the sign of F must change and so it must pass through the root at $\phi = 0$. More broadly, if it has multiple roots, at least one of which is less than or equal to 0 and below which F is decreasing, then again, ϕ must take the corresponding non-positive value in finite time and hence have passed through 0.

As a final point, we note that the singularity need not occur at $\phi = 0$. Since we have shown that after some t, ϕ must reach 0, it must also necessarily pass through all values less than ϕ_0. This means that we can allow the sudden singularity to be translated to any value of $\phi < \phi_0$. This means that for suitable ϕ_{sing}, potentials such as $V(\phi) = A(\phi - \phi_{\text{sing}})^n$ for n non-integer and A a positive constant, would also exhibit sudden singularities.

2.3 Conclusion

In this chapter we investigated a type of weak future singularity known as sudden, or generalised sudden, singularities. We have studied them in the context of inflationary models driven by a single scalar field minimally coupled to the Einstein-Hilbert action in $k = 0$ FLRW spacetime. These singularities provide a mechanism by which a single scalar field undergoes a significant transition and change in behaviour, without the cosmology itself necessarily undergoing the destruction that results from stronger types of singularity. Indeed, it is known that there are even examples of sudden singularities which need not disrupt bound systems [61]. As such, these potentials can provide a possible mechanism for an exit from inflation.

We have found that for an inflationary potential $V(\phi)$, then $\dot{\phi}$ will become negative in finite time if for $\phi > 0$, $V(\phi) > 0$, $V'(\phi) > 0$ and $V'(\phi)$ has at most finitely many stationary points. Furthermore, we have found that if additionally $V''(\phi) < 0$ after some finite time, then this is sufficient to ensure that ϕ itself reaches 0 in some finite time, and that if $V'(\phi)$ exhibits a singularity at $\phi = 0$, this singularity is reached in finite time. This extends the power law example of singular inflation [58] to further classes of potential, including those connected to popular α-attractor models of inflation, and providing a possible mechanism for inflation under these models to come to an end.

Chapter 3

Cosmological Models in $F(T_{\mu\nu}T^{\mu\nu})$ Gravity

The work presented in this chapter was published as [62], in collaboration with John D. Barrow.

3.1 Introduction

The twin challenges of naturally explaining two periods of accelerated expansion during the history of the universe engage the attentions of many contemporary cosmologists. The first period may have had a beginning and necessarily came to an end when the universe was young and hot: it is called a period of 'inflation' and it leaves observable traces in the cosmic microwave background radiation that are believed to have been detected. The second period of acceleration began only a few billion years ago and is observed in the Hubble flow traced by type IA supernovae; it is not known if it will ever come to an end or is changing in any way. There are separate non-unique mathematical descriptions of each of these periods of acceleration but there is no single explanation of both of them, nor any insight into whether or not they are related, or even random, occurrences. For these reasons, there is continuing interest in all the different ways in which expanding universes can undergo periods of accelerated expansion. In the case of late-time acceleration the simplest description of an effectively anti-gravitating

stress, known as 'dark energy', is provided by introducing a cosmological constant (Λ) into general relativity with a value arbitrarily chosen to match observations.

The best-fit theory of this sort is dubbed ΛCDM and in its simplest form is defined by six constants (which determine Λ) that can be fixed by observation. One of those parameters is Λ and its required value is difficult to explain: it requires a theory that contributes an effective vacuum stress of magnitude $\Lambda \sim (t_{pl}/t_0)^2 \sim 10^{-120}$ at a time of observation $t_0 \sim 10^{17}$s, where $t_{pl} \sim 10^{-43}$s is the Planck time [63]. Other descriptions that lead to slowly evolving scalar fields in place of a constant Λ have also been explored, together with a range of modified gravity theories that contribute anti-gravitating stresses. There are many such modifications and extensions of Einstein's general relativity and they can be tuned to provide acceleration at early or late times. So far, almost all of these modifications to general relativity have focussed on generalising the gravitational Lagrangian away from the linear function of the spacetime curvature, R, responsible for the Einstein tensor in Einstein's equations. A much-studied family of theories of this sort are those deriving from a Lagrangian of the form $F(R)$, where F is some analytic function. By contrast, in this chapter we will explore some of the consequences of generalising the form of the matter Lagrangian in a nonlinear way, to some analytic function of $T_{\mu\nu}T^{\mu\nu}$, where $T_{\mu\nu}$ is the energy-momentum tensor of the matter stresses. This is more radical than simply introducing new forms of fluid stress, like bulk viscosity or scalar fields, into the Einstein equations in order to drive acceleration in Friedmann-Lemaître-Robertson-Walker (FLRW) universes.

In 3.2 we discuss and motivate higher order contributions to gravity from matter terms. In 3.3 we derive the equations of motion for a generic $F(R, T_{\mu\nu}T^{\mu\nu})$ modification of the action with bare cosmological constant, before specialising to the case $F(R, T_{\mu\nu}T^{\mu\nu}) = R + \eta(T_{\mu\nu}T^{\mu\nu})^n$. We then investigate several features of the isotropic cosmology in this theory in 3.4 and, finally, move to the anisotropic Bianchi type I setting in 3.5.

3.2 Background

3.2.1 Field equations

Einstein's theory of general relativity (GR) with cosmological constant Λ can be derived from the variation of the action,

$$S = \frac{1}{2\kappa}\int \sqrt{-g}(R - 2\Lambda)d^4x + \int \sqrt{-g}L_m d^4x, \tag{3.1}$$

where $\kappa = 8\pi G$ and L_m is the matter Lagrangian, which we will take to describe a perfect fluid; $R \equiv R^a_a$, where R^a_b is the Ricci tensor, and g is the determinant of the metric itself. Here, and in all that follows, we use units in which $c = 1$.

An isotropic and homogeneous universe may be described by the FLRW metric:

$$ds^2 = -dt^2 + a^2(t)\left(\frac{dr^2}{1-kr^2} + r^2\left(d\theta^2 + \sin^2\theta d\phi^2\right)\right), \tag{3.2}$$

where k, the curvature parameter, takes the values $\{-1, 0, +1\}$ corresponding to open, flat and closed 3-spaces, respectively; t is the comoving proper time and $a(t)$ is the expansion scale factor.

There are many proposals to modify or extend the ΛCDM cosmological picture. These fall broadly into two categories, depending on which side of the Einstein field equations is modified. We can modify the right-hand side of the Einstein equations by adding new forms of matter that will drive expansion either at early times, as in the theory of inflation, or at late times, such as in quintessence or k-essence scenarios [64]. Alternatively, we can modify the left-hand side of the Einstein equations in order to modify the effect of gravity itself. There are several ways to do this, including $F(R)$ theories [65] in which the Ricci scalar in (3.1) is replaced by some function $f(R)$, so-called $F(T)$ theories in which we modify the teleparallel equivalent of general relativity [66], or scalar-tensor theories in which a scalar field is coupled to the Ricci scalar.

3.2.2 Higher-order matter contributions

The type of generalisation of general relativity we will explore in this chapter looks to include higher-order contributions to the right-hand side of the Einstein equations, where the material stresses appear. This results in field equations that include new terms that enter at high densities and pressures, which may be anti-gravitational in their effects. Typically, they affect the cosmological model at high densities and may alter the conclusions regarding the appearance of spacetime singularities in the finite cosmological past. Conversely, we might expect their effects at late times and low cosmological densities to be very small. Even within general relativity, there is scope to include high-order matter contributions, as the Einstein equations have almost no content unless some prescription or constraint is given on the forms of matter stress. Thus, in the general-relativistic Friedmann models, we can introduce non-linear stresses defined by relations between pressure, p, and density, ρ, of the form $\rho + p = \gamma\rho^n$, [67], or $f(\rho)$, [68], where $\gamma \geq 0$ and n are constants, or include a bulk viscous stress into the equation of state of the standard form $p = (\gamma - 1)\rho - 3H\varsigma(\rho)$,where H is the Hubble expansion rate and $\varsigma \geq 0$ is the bulk viscosity coefficient [69]. The so-called Chaplygin and generalised Chaplygin gases are just special cases of these bulk viscous models, and choices of n or $\varsigma \propto \rho^m$ introduce higher-order matter corrections. Similarly, the choice of self-interaction potential $V(\phi)$ for a scalar field can also introduce higher-order matter effects into cosmology. Analogously, in scalar-tensor theories like Brans-Dicke (BD) which are defined by a constant BD coupling constant, ω, generalisations are possible to the cases where ω becomes a function of the BD scalar field.

In all these extensions of the standard relativistic perfect fluid cosmology there will be several critical observational tests which will constrain them. In particular, in higher-order matter theories the inevitable deviations that can occur from the standard thermal history in the early radiation era will change the predicted abundances of helium-4 and deuterium and alter the detailed structure of the microwave background power spectrum. Also, as studied for Brans-Dicke theory [70, 71], changes in the cold dark matter dominated era evolution can shift the time when matter and radiation densities are equal. This is the epoch when matter perturbations begin to grow and sensitively determines the peak of the matter power spectrum. At a later nonlinear stage of the evolution, higher-order gravity theories will effect the formation of galactic halos. This has been investigated for bulk viscous cosmologies [72]. A further observational constraint on the modifications arises from the fact that if we expect these modifications

to give rise to high-energy density effects, we would expect to see modifications to behaviour of the interior stars and other compact objects. This will place further constraints on the permitted magnitude of such modifications, or the requirement of some screening mechanism to otherwise evade the constraints. The effect of one of the models we will study on stellar behaviour has been investigated [73], where they concluded that the model can recover appropriate solutions for stellar objects, without introducing overly problematic behaviour. However, further discussion of these observational constraints will form the subject of future work and will not be discussed in detail here.

If we depart from general relativity, then various simple quantum gravitational corrections are possible, and have been explored. The most well known are the loop quantum gravity (LQG) [74] and brane-world [75] scenarios that contribute new quadratic terms to the Friedmann equation for isotropic cosmologies by replacing ρ by $\rho(1 \pm O(\rho^2))$ in the Friedmann equation, where the $-$ contribution is from LQG and the $+$ is from brane-world scenarios. The impact on anisotropic cosmological models is more complicated and not straightforward to calculate [76, 77]. In particular, we find that simple forms of anisotropic stress are no longer equivalent to a $p = \rho$ fluid as we are used to finding in general relativity. Our study will be of a type of higher-order matter corrections which modify the Friedmann equations in ways that include both of the aforementioned types of phenomenological modification to the form of the Friedmann equations, although the underlying physical theory does not incorporate the LQC or brane-world models or reduce to them in a limiting case.

Standard $F(R)$ theories of gravity [65] can be generalised to include a dependence of the form

$$S = \frac{1}{2\kappa} \int \sqrt{-g} F(R, L_m) d^4x. \tag{3.3}$$

This is in some sense an extremal extension of the Einstein-Hilbert action, as discussed in [78]. If the coupling between matter and gravity is non-minimal, then there will be an extra force exerted on matter, resulting in non-geodesic motion and a violation of the equivalence principle. This type of modification has been investigated in several contexts, particularly when the additional dependence on the matter Lagrangian arises from F taking the form $F(R, \mathcal{T})$ where $\mathcal{T}$ is the trace of the energy-momentum tensor [46].

A theory, closely related to $F(R,\mathcal{T})$ gravity, that allows the gravitational Lagrangian to depend on a more complicated scalar formed from the energy-momentum tensor is provided by $F(R,\mathbf{T}^2)$, where $\mathbf{T^2} \equiv T_{\mu\nu}T^{\mu\nu}$ is the scalar formed from the square of the energy-momentum tensor. This was first discussed in [48], and the special case with

$$F(R,\mathbf{T^2}) = R + \eta\mathbf{T^2}, \tag{3.4}$$

where η is a constant, was also discussed in [47], where the authors investigated the possibility of a bounce at early times when $\eta < 0$ (although in that paper they used the opposite sign convention to us for η), and also found an exact solution for charged black holes in the extended theory. In [49] a similar form, with additional cross terms between the Ricci and Energy-momentum tensors, was discussed as arising from quantum fluctuations of the metric tensor. Recently the authors of [79] investigated the late time acceleration of universes described by this model in the dust-only case, and used observations of the Hubble parameter to constrain the parameters of the theory.

We would expect the theory derived from (3.4) to provide different physics to the $F(R,\mathcal{T})$ case. Indeed, one example of this is the case of a perfect fluid with equation of state $p = -\frac{1}{3}\rho$. The additional terms in $F(R,\mathcal{T})$ will vanish as $\mathcal{T} = 0$, but in the $F(R,\mathbf{T^2})$ theory the extra terms in $\mathbf{T^2}$ will not vanish and we will find new cosmological behaviour. In 3.3, we will investigate the cosmological solutions in a more general setting, where the $\mathbf{T^2}$ term may be raised to an arbitrary power.

3.3 Field Equations for $F(R,T_{\mu\nu}T^{\mu\nu})$ Gravity with Cosmological Constant

In [80] the Friedmann equations were derived in the case where F is given by (3.4), for a flat FLRW cosmology. A 'bare' cosmological constant was also included on the left-hand side of the field equations (rather than as an effective energy-momentum tensor for the vacuum). In [81], the field equations were derived without a cosmological constant and specialised to two particular models. We first derive the equations of motion with a cosmological constant for general F, before specialising to theories where the additional term takes the form $(\mathbf{T^2})^n$, and determining the FLRW equations

with general curvature. In GR, the cosmological constant can be considered to be, equivalently, either a 'bare' constant on the left-hand side of the Einstein equations, or part of the matter Lagrangian. As discussed in [80], the two are no longer equivalent in this theory, due to the non-minimal nature of the curvature-matter couplings. A similar inequivalence also occurs in other models that introduce non-linear matter terms, including loop quantum cosmology. We will assume that the cosmological constant arises in its bare form as part of the gravitational action. This gives the modified action

$$S = \frac{1}{2\kappa}\int \sqrt{-g}(F(R, T^{\mu\nu}T_{\mu\nu}) - 2\Lambda)\ d^4x + \int L_m\sqrt{-g}\ d^4x, \tag{3.5}$$

where L_m is taken to be the same as the matter component contributed by $T_{\mu\nu}$. Since the gravitational Lagrangian now depends on $\mathbf{T^2}$, we note that the new terms in the variation of the action will arise from the variation of this square, via $\delta(T_{\mu\nu}T^{\mu\nu})$. To calculate this, we define $T_{\mu\nu}$ by

$$T_{\mu\nu} = -\frac{2}{\sqrt{-g}}\frac{\delta(\sqrt{-g}L_m)}{\delta g^{\mu\nu}}. \tag{3.6}$$

We enforce the condition that L_m depends only on the metric components, and not on their derivatives, to find

$$T_{\mu\nu} = g_{\mu\nu}L_m - 2\frac{\partial L_m}{\partial g^{\mu\nu}}. \tag{3.7}$$

Varying with respect to the inverse metric, we define

$$\theta_{\mu\nu} \equiv \frac{\delta(T_{\alpha\beta}T^{\alpha\beta})}{\delta g^{\mu\nu}} = -2L_m(T_{\mu\nu} - \frac{1}{2}g_{\mu\nu}T) - TT_{\mu\nu} + 2T^{\alpha}_{\mu}T_{\nu\alpha} - 4T^{\alpha\beta}\frac{\partial^2 L_m}{\partial g^{\mu\nu}\partial g^{\alpha\beta}}, \tag{3.8}$$

where T is the trace of the energy-momentum tensor. Varying the action in this way, we find

$$\delta S = \frac{1}{2\kappa}\int \left[F_R\delta R + F_{T^2}\delta(T_{\mu\nu}T^{\mu\nu}) - \frac{1}{2}g_{\mu\nu}F\delta g^{\mu\nu} + \Lambda + \frac{1}{\sqrt{-g}}\delta(\sqrt{-g}L_m)\right] d^4x, \tag{3.9}$$

where subscripts denote differentiation with respect to R and $\mathbf{T^2}$, respectively.

From this variation we obtain the field equations:

$$F_R R_{\mu\nu} - \frac{1}{2}Fg_{\mu\nu} + \Lambda g_{\mu\nu} + (g_{\mu\nu}\nabla_\alpha\nabla^\alpha - \nabla_\mu\nabla_\nu)F_R = \kappa(T_{\mu\nu} - \frac{1}{\kappa}F_{\mathbf{T^2}}\theta_{\mu\nu}). \tag{3.10}$$

These reduce, as expected, to the field equations for $F(R)$ gravity in the special case where $F(R, \mathbf{T^2}) = F(R)$ [65] and to the Einstein equations with a cosmological constant when $F(R, \mathbf{T^2}) = R$.

We will assume that the matter component can be described by a perfect fluid,

$$T_{\mu\nu} = (\rho + p)u_\mu u_\nu + p g_{\mu\nu}, \tag{3.11}$$

where ρ is the energy density and p the pressure; hence

$$T_{\mu\nu}T^{\mu\nu} = \rho^2 + 3p^2. \tag{3.12}$$

Furthermore, we take the Lagrangian $L_m = p$. This means that the final term in the definition of $\theta_{\mu\nu}$ vanishes and allows us to calculate the form of $\theta_{\mu\nu}$ independently of the function F. Substituting (3.11) into (3.8), we find

$$\theta_{\mu\nu} = -(\rho^2 + 4p\rho + 3p^2)u_\mu u_\nu. \tag{3.13}$$

We now proceed to specify a particular form for $F(R, \mathbf{T^2})$ which includes and generalises the models used in [81] and for energy-momentum-squared gravity in [80] (EMSG). This form is

$$F(R, T_{\mu\nu}T^{\mu\nu}) = R + \eta(T_{\mu\nu}T^{\mu\nu})^n, \tag{3.14}$$

where n need not be an integer. This corresponds to EMSG in the case $n = 1$, and to Models A and B of [81] when $n = 1/2$ and $n = 1/4$, respectively; it reduces the field equations to

$$R_{\mu\nu} - \frac{1}{2}Rg_{\mu\nu} + \Lambda g_{\mu\nu} = \kappa(T_{\mu\nu} + \frac{\eta}{\kappa}(T_{\alpha\beta}T^{\alpha\beta})^{n-1}\left[\frac{1}{2}(T_{\alpha\beta}T^{\alpha\beta})g_{\mu\nu} - n\theta_{\mu\nu}\right]), \tag{3.15}$$

which we rewrite as

$$G_{\mu\nu} + \Lambda g_{\mu\nu} = \kappa T^{\text{eff}}_{\mu\nu}, \tag{3.16}$$

where $G_{\mu\nu}$ is the Einstein tensor, to show the relationship to general relativity. Continuing with the perfect fluid form of the energy-momentum tensor, this expands to

give:

$$G_{\mu\nu} + \Lambda g_{\mu\nu} = \kappa((\rho + p)u_\mu u_\nu + p g_{\mu\nu}) \\ + \eta(\rho^2 + 3p^2)^{n-1}\left[\frac{1}{2}(\rho^2 + 3p^2)g_{\mu\nu} + n(\rho + p)(\rho + 3p)u_\mu u_\nu\right]. \tag{3.17}$$

3.4 Isotropic Cosmology

If we assume a FLRW universe with curvature parameter k, we find the generalised Friedmann equation,

$$\left(\frac{\dot{a}}{a}\right)^2 + \frac{k}{a^2} = \frac{\Lambda}{3} + \kappa\frac{\rho}{3} + \frac{\eta}{3}(\rho^2 + 3p^2)^{n-1}\left[(n - \frac{1}{2})(\rho^2 + 3p^2) + 4n\rho p\right], \tag{3.18}$$

and acceleration equation

$$\frac{\ddot{a}}{a} = -\kappa\frac{\rho + 3p}{6} + \frac{\Lambda}{3} - \frac{\eta}{3}(\rho^2 + 3p^2)^{n-1}\left[\frac{n+1}{2}(\rho^2 + 3p^2) + 2n\rho p\right]. \tag{3.19}$$

If the matter field obeys a barotropic equation of state, $p = w\rho$ with w constant, then the non-GR terms are all of the form ρ^{2n} multiplied by a constant. Thus, the generalised Friedmann equation becomes

$$\left(\frac{\dot{a}}{a}\right)^2 + \frac{k}{a^2} = \frac{\Lambda}{3} + \kappa\frac{\rho}{3} + \frac{\eta\rho^{2n}}{3}A(n, w), \tag{3.20}$$

where A is a constant depending on the choice of n and w, given by

$$A(n, w) \equiv (1 + 3w^2)^{n-1}\left[(n - \frac{1}{2})(1 + 3w^2) + 4nw\right], \tag{3.21}$$

and the acceleration equation becomes

$$\frac{\ddot{a}}{a} = -\kappa\frac{1 + 3w}{6}\rho + \frac{\Lambda}{3} - \frac{\eta\rho^{2n}}{3}B(n, w), \tag{3.22}$$

where B a constant given by

$$B(n, w) \equiv (1 + 3w^2)^{n-1}\left[\frac{n+1}{2}(1 + 3w^2) + 2nw\right]. \tag{3.23}$$

Finally, we determine the generalised continuity equation, by differentiating the generalised Friedmann equation,

$$\dot{\rho} = -3\frac{\dot{a}}{a}\rho(1+w)\left[\frac{\kappa + \eta\rho^{2n-1}n(1+3w)(1+3w^2)^{n-1}}{\kappa + 2\eta\rho^{2n-1}nA(n,w)}\right], \tag{3.24}$$

where we have written it in a form that makes clear the generalisation of the GR case.

We can see immediately that there is an interesting difference between the FLRW equations in GR and in EMSG. When $\eta = 0$ there are solutions with finite $a, \dot{a}$,and ρ but infinite values of p and $\ddot{a}$. These are called sudden singularities [82, 51, 83] and can be constructed explicitly. In EMSG, where $\eta \neq 0$, the appearance of the pressure, p, explicitly in the Friedmann equation changes the structure of the equations and the same type of sudden singularity is no longer possible at this order in derivatives of a.

3.4.1 Integrating the continuity equation

We now attempt to determine the cosmological behaviour of some cases where the modified continuity equation can be integrated exactly. We find four simply integrable cases: two of these are for fixed w independent of the value of n, the other two occur for specific values of w dependent on the choice of n, although we note that some of these integrable cases may coincide, depending on our choice of the exponent, n. Several of these analytic cases will turn out to be of physical relevance, whilst we note that in other cases one could solve numerically.

The first case that can be integrated is for the equation of state corresponding to dark energy, $w = -1$, where the entire right-hand side of (3.24) vanishes, and so $\rho \equiv \rho_0$, a constant. In this case we expect to find a solution to the modified Friedmann equation that is the same as the solution in GR except with altered constants, which results in a de Sitter solution where $H \equiv \frac{\dot{a}}{a} =$ constant, and the universe expands exponentially.

Next, we consider the case $w = -\frac{1}{3}$, which corresponds to an effective perfect fluid representing a negative curvature, so the numerator in the modified continuity equation

becomes simply κ, and we can integrate (3.24) since

$$\dot{\rho}\left(\frac{1}{\rho}+\frac{2\eta n A(n,\frac{-1}{3})}{\kappa}\rho^{2n-2}\right) = -2\frac{\dot{a}}{a}, \tag{3.25}$$

$$\frac{d}{dt}\left(\ln(\rho)-\frac{\eta n(\frac{4}{3})^n}{(2n-1)\kappa}\rho^{2n-1}\right) = \frac{d}{dt}(\ln(a^{-2})), \tag{3.26}$$

$$\rho\exp\left(-\frac{\eta n(\frac{4}{3})^n}{(2n-1)\kappa}\rho^{2n-1}\right) = Ca^{-2}, \tag{3.27}$$

with $C>0$ a constant of integration.

We can also integrate the continuity equation when the correction factor in (3.24) is equal to 1, which occurs when

$$(1+3w)(1+3w^2)^{n-1} = 2A(n,w). \tag{3.28}$$

The continuity equation then reduces to the standard GR form for these special values, $w=w_*$, and so we have

$$\rho = Ca^{-3(1+w_*)}. \tag{3.29}$$

The final possibility that we consider is when

$$n(1+3w)(1+3w^2)^{n-1} = A(n,w), \tag{3.30}$$

in which case we can write (3.24) as

$$\frac{d}{dt}\left(\ln(\kappa\rho+n\eta\rho^{2n}(1+3w_*)(1+3w_*^2)^{n-1})\right) = \frac{d}{dt}(\ln(a^{-3(1+w_*)})), \tag{3.31}$$

which integrates to

$$\kappa\rho+n\eta\rho^{2n}(1+3w_*)(1+3w_*^2)^{n-1} = Ca^{-3(1+w_*)}. \tag{3.32}$$

We note that, depending on the choice of exponent n, some of the second pair of solutions may exist for multiple choices of w, or may coincide with each other, or with the $w=-1$, $w=-\frac{1}{3}$ cases. Also, for some choices of n, there may be no solutions at all.

Finally, note that only one of these solutions allows easy integration of the modified Friedmann equation (3.20). This is the case when $w = -1$ and so $\rho = \rho_0$. In this case the Friedmann-like equation becomes

$$\left(\frac{\dot{a}}{a}\right)^2 + \frac{k}{a^2} = \lambda(\Lambda, n), \tag{3.33}$$

where λ is a constant given by

$$\lambda(\Lambda, n) \equiv \frac{\Lambda}{3} + \kappa\frac{\rho_0}{3} - \frac{\eta\rho_0^{2n}}{6}4^n. \tag{3.34}$$

The solution to the modified Friedmann equation is then given by

$$a(t) = \frac{1}{2\sqrt{\lambda}}(C\sqrt{\lambda} + \frac{k}{C\sqrt{\lambda}})\cosh(\sqrt{\lambda}t) \pm (C\sqrt{\lambda} - \frac{k}{C\sqrt{\lambda}})\sinh(\sqrt{\lambda}t)\ , \tag{3.35}$$

where C is a new constant of integration. Equivalently, we can write this solution in terms of exponentials as

$$a(t) = \frac{1}{2\sqrt{\lambda}}\left(C\sqrt{\lambda}e^{\sqrt{\lambda}t} + \frac{k}{C\sqrt{\lambda}}e^{-\sqrt{\lambda}t}\right)\ , \tag{3.36}$$

as well as its time reversal, $t \to -t$. Assuming $\lambda > 0$, we can see that this reduces to the expected de Sitter solution from general relativity in the case $k = 0$, as we would expect. If $\lambda < 0$ then, writing instead $\lambda \to -\lambda$, there is a real solution only for negative curvature, where we must choose $k = -C^2\lambda$, giving the anti-de Sitter solution

$$a(t) = C\cos(\sqrt{\lambda}t). \tag{3.37}$$

It is important to note that because of the form of λ, unlike in the unmodified case, we do not necessarily require a negative cosmological constant to find this solution. We would expect this anti-de Sitter analogue to appear whenever $\eta > 0$, for suitable choices of ρ_0 and n.

This solution is very similar to the case of $w = -1$ in GR, where we can rewrite the cosmological constant as a perfect fluid with this equation of state. This is possible in GR because the continuity equations for non-interacting multi-component fluids decouple, allowing us to treat them independently. Unfortunately, because of the additional non-linear terms arising in these $F(R, \mathbf{T^2})$ models (except in the special

case $n = 1/2$), we cannot decouple different fluids in this way and then subsequently superpose them in our Friedmann-like equations. This means that we cannot replace the curvature or cosmological constant terms with perfect fluids with $w = -1/3$ and -1 as in classical GR. However, for some choices of n and η, the correction terms can themselves provide an additional late-time or early inflationary repulsive force, removing the need for an explicit cosmological constant.

3.4.2 Energy-momentum-squared gravity: the case $n = 1$

If we fix our choice of n, then we can say more about the behaviour of the specific solutions that arise. In what follows we consider primarily the case $n = 1$ which was originally discussed in [80], under the name 'energy-momentum squared gravity'. After specialising to $n = 1$, we can say more about the solutions to the continuity equation found in the previous section, and investigate the modified Friedmann equations. The form of the Friedmann equations, after setting $n = 1$ in (3.20), (3.22) and (3.24), is:

$$\left(\frac{\dot{a}}{a}\right)^2 + \frac{k}{a^2} = \frac{\Lambda}{3} + \kappa\frac{\rho}{3} + \frac{\eta\rho^2}{6}(3w^2 + 8w + 1) \ , \tag{3.38}$$

$$\frac{\ddot{a}}{a} = \frac{\Lambda}{3} - \kappa\frac{1+3w}{6}\rho - \frac{\eta\rho^2}{3}(3w^2 + 2w + 1) \ , \tag{3.39}$$

$$\dot{\rho} = -3\frac{\dot{a}}{a}\rho(1+w)\frac{\kappa + \eta\rho(1+3w)}{\kappa + \eta\rho(3w^2 + 8w + 1)} \ . \tag{3.40}$$

The new terms in the Friedmann equations are quadratic in the energy density, which we would expect to dominate in the very early universe as $\rho \to \infty$. Additionally, if we choose $\eta < 0$, then the modified Friedmann equations in this model are similar to the effective Friedmann equations arising in loop quantum cosmology, [74], where

$$\left(\frac{\dot{a}}{a}\right) = \frac{\kappa}{3}\rho\left(1 - \frac{\rho}{\rho_{\text{crit}}}\right), \tag{3.41}$$

which may warrant further investigation. An analogous higher-order effect occurs in brane world cosmologies, where there is an effective equation of state with [84–87]

$$p^{eff} = \frac{1}{2\Lambda}(\rho^2 + 2p\rho); \quad \Lambda > 0 \text{ constant.} \tag{3.42}$$

We briefly summarise the values of w for which the results of the previous section allow us to integrate the Friedmann equation and find the values of w that satisfy (3.28) and (3.30). If we set $n = 1$ then (3.28) reduces to

$$3w^2 + 5w = 0, \tag{3.43}$$

which has solutions $w = -\frac{5}{3}$ and $w = 0$. The $w = 0$ solution describes 'dust' matter. The case $w = -5/3$ corresponds to some form of phantom energy, which will result in a Big Rip singularity, [88], at finite future time.

Alternatively, solving (3.30) for $n = 1$ gives

$$3w^2 + 2w - 1 = 0, \tag{3.44}$$

which has solutions $w = -1$ and $w = \frac{1}{3}$. The first of these has already been found for all n as the first case above, whilst the second gives a solution corresponding to blackbody radiation. Hence, we have exact solutions to the continuity equation for the cases $w = \{-\frac{5}{3}, -1, -\frac{1}{3}, 0, \frac{1}{3}\}$ which include the physically important cases of dust and radiation.

The equation of state $p = 0$ corresponds to pressureless dust or non-relativistic cold dark matter, and as shown above, we recover the same dependence of the energy density on the scale factor as in the GR case,

$$\rho = Ca^{-3}. \tag{3.45}$$

If we combine this with the modified acceleration and Friedmann equations for $w = 0$ we find

$$a\ddot{a} + 2\dot{a}^2 + k = \frac{\Lambda}{2}a^2 + \frac{\kappa}{4C}a^{-1}. \tag{3.46}$$

If we consider only flat space ($k = 0$) then we find

$$a(t) = (4\Lambda)^{-\frac{1}{3}}((C^2+D+1)\cosh\left(\sqrt{\frac{3\Lambda}{2}}t\right)+(C^2+D-1)\sinh\left(\sqrt{\frac{3\Lambda}{2}}t\right)-2C)^{\frac{1}{3}}, \tag{3.47}$$

where D is a constant of integration, and we have eliminated a further constant by a covariant translation of the time coordinate. We can then find ρ explicitly, using (3.45). We can see, however, that this form of the solution does not capture the case

$\Lambda = 0$. In this case, instead we find the solution

$$a(t) = \left(\frac{3}{8C}\right)^{\frac{1}{3}} (C^2t^2 - 16D)^{\frac{1}{3}}, \tag{3.48}$$

which gives the GR dust behaviour of $a \sim t^{\frac{2}{3}}$ at large t.

In the case of $w = -\frac{1}{3}$, we can write

$$\rho \exp\left(-\frac{4\eta}{3\kappa}\rho\right) = Ca^{-2}. \tag{3.49}$$

After differentiation and multiplication by a^2, we can write

$$\frac{\dot{a}}{a} = \frac{\dot{\rho}}{\rho}(1 - \frac{4\eta}{3\kappa}\rho) \ , \tag{3.50}$$

and so in the case $k = 0$ we can write the Friedmann equation in terms of ρ without any exponentials, as

$$\left(\frac{\dot{\rho}}{\rho}\right)^2 \left(1 - \frac{4\eta}{3\kappa}\rho\right)^2 \frac{1}{4C^2} = \frac{\Lambda}{3} + \frac{\kappa}{3}\rho - \frac{2\eta}{9}\rho^2. \tag{3.51}$$

Finally, in the case of $w = \frac{1}{3}$, which corresponds to radiation, [80] gave a solution in the case of flat space, $a(t) \propto \sqrt{\cosh(\lambda t)}$ where now $\lambda \equiv \sqrt{\frac{4\Lambda}{3}}$. We see that in this case we can write the continuity equation as

$$\kappa\rho + 2\eta\rho^2 = Ca^{-4}, \tag{3.52}$$

and that in the Friedmann and acceleration equations, the density terms are of equal magnitude but opposite sign. We can then sum the two to find our equation for $a(t)$

$$\left(\frac{\dot{a}}{a}\right)^2 + \frac{\ddot{a}}{a} + \frac{k}{a^2} = \frac{2\Lambda}{3}, \tag{3.53}$$

which we solve by use of the substitution $y = a^2$ to find

$$a^2(t) = \frac{1}{4\Lambda}((1 + 9k^2 - 12\Lambda D)\cosh(\lambda t) + (1 - 9k^2 + 12\Lambda D)\sinh(\lambda t) + 6k) \ , \tag{3.54}$$

for all Λ, k non-zero, with $\lambda \equiv \sqrt{\frac{4\Lambda}{3}}$, as above. In the $\Lambda = 0$ subcase, we find the solutions

$$a^2(t) = \begin{cases} Dt - kt^2 & k \neq 0 \\ Dt & k = 0 \end{cases} . \tag{3.55}$$

3.4.3 de Sitter-like solutions

de Sitter solutions arise in EMSG theory. They have constant density and Hubble parameter, which includes the case $w = -1$. In ΛCDM we expect this to arise in two situations. The first is when we have $\rho \equiv 0$, that is an empty universe whose expansion is controlled solely by Λ, and the second is the similar dark-energy equation of state $w = -1$ for which the perfect fluid behaves as a cosmological constant. In EMSG we find that there is an extra family of de Sitter solutions. We describe them first for general n, then specialise to EMSG.

Since we are searching for solutions with $H \equiv H_0$ and $\rho \equiv \rho_0$, from (3.20) we must have $k = 0$, and the Friedmann equation then reduces to an algebraic one for H^2 in terms of ρ_0. Similarly, since $\dot{H} = 0$, (3.22) reduces to another relation for H^2. Equating the two to remove H^2 and simplifying, we find that ρ_0 must satisfy

$$\rho_0(1+w)(\kappa + n\eta(1+3w^2)^{n-1}(1+3w)\rho_0^{2n-1}) = 0. \tag{3.56}$$

There are the two standard solutions, $w = -1$ and $\rho_0 = 0$, but the additional factor gives us another family of solutions, with

$$\rho_0^{2n-1} = -\frac{\kappa}{n\eta(1+3w^2)^{n-1}(1+3w)}. \tag{3.57}$$

In the case of EMSG, when we choose $n = 1$, this condition reduces to

$$\rho_0 = -\frac{\kappa}{\eta(1+3w)} , \tag{3.58}$$

which gives us a constant density, exponentially expanding solution for every equation of state, w, excluding $w = -\frac{1}{3}$, for an appropriate sign of η. The existence of this extra de Sitter solution is reminiscent of its appearance in GR cosmologies with bulk viscosity [69]

This unusual situation suggests that we investigate the stability of these $n = 1$ solutions. We consider a homogeneous linear perturbation about the constant density solution by writing

$$\rho = \rho_0(1 + \delta(t)), \tag{3.59}$$

$$H = H_0(1 + \epsilon(t)), \tag{3.60}$$

The perturbed continuity equation is then given by

$$\rho_0\dot{\delta} = -3(1+w)H_0(1+\epsilon)\rho_0(1+\delta)\frac{\kappa + \eta\rho_0(1+\delta)(1+3w)}{\kappa + \eta\rho_0(1+\delta)(3w^2+8w+1)}. \tag{3.61}$$

If we use the expression for ρ_0 given in (3.58), we can reduce this to

$$\dot{\delta} = -3(1+w)(1+3w)H_0(1+\epsilon)(1+\delta)\delta\frac{1}{(3w^2+5w)(1+\frac{3w^2+8w+1}{3w^2+5w}\delta)}. \tag{3.62}$$

From the perturbation of the modified Friedmann equation we find that $\epsilon \sim \delta$ which means that after expanding to first order in δ, we have

$$\dot{\delta} = -3H_0\delta\frac{(1+w)(1+3w)}{(3w+5)w}, \tag{3.63}$$

so small perturbations evolve as

$$\delta(t) \propto \exp\left(-3H_0\frac{(1+w)(1+3w)}{(3w+5)w}t\right) . \tag{3.64}$$

The exponent coefficient in (3.64) is plotted in Figure 3.1, where we can see that these de Sitter-like solutions are indeed stable for a wide range of w values. This gives us an exponentially expanding universe for (almost) any equation of state as long as we set the density to the correct constant value. In particular, these solutions will be stable for $w < -\frac{5}{3}$, $-1 < w < -\frac{1}{3}$ and $w > 0$, and unstable for $-\frac{5}{3} < w < -1$ and $\frac{-1}{3} < w < 0$. It is also the case that, depending on the sign of the parameter η, some of these solutions will be unphysical, as they require negative energy density. For $\eta < 0$, there will be no physical solutions for $w < -\frac{1}{3}$, whilst for $\eta > 0$ there will be no solutions for $w > -\frac{1}{3}$.

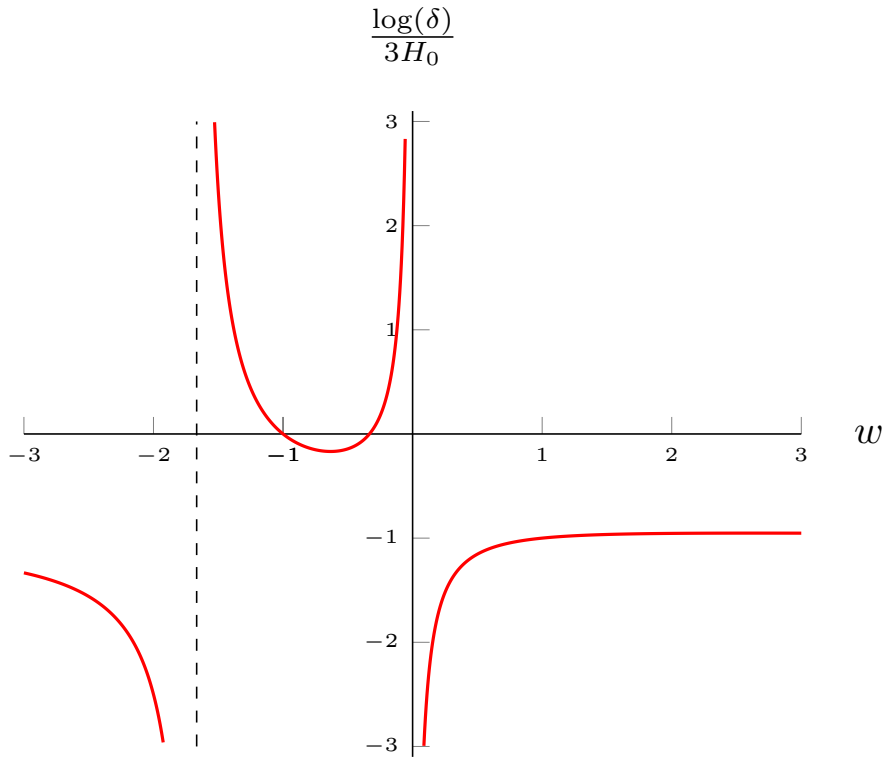

Fig. 3.1 The plot shows the value of the exponent, and hence the stability of the solutions, in (3.64) (where we have divided by $3H_0t$). The asymptotes are found at $w = -\frac{5}{3}$ and $w = 0$, whilst the zeroes are at $w = -1$ and $w = -\frac{1}{3}$. The solutions will be stable for values of w where the graph is negative, and unstable otherwise.

3.4.4 Early times: the bounce and high-density limits

Examining the modified Friedmann equation (3.38) in the case $k \geq 0$, we can see that as the left-hand side of the equation is a sum of positive terms, we must have

$$\Lambda + \kappa\rho + \eta\rho^2 A(1, w) \geq 0, \tag{3.65}$$

which can be split into two cases, for $\eta A(1, w) < 0$ and $\eta A(1, w) > 0$, respectively. The first case occurs for

$$\eta < 0 \quad \text{and} \quad \{w < \alpha_- \text{ or } w > \alpha_+\}, \tag{3.66}$$

$$\eta > 0 \quad \text{and} \quad \{\alpha_- < w < \alpha_+\}, \tag{3.67}$$

where

$$\alpha_{\pm} = \frac{-4 \pm \sqrt{13}}{3} \ , \tag{3.68}$$

are the roots of

$$A(1, w) \equiv 3w^2 + 8w + 1 = 0. \tag{3.69}$$

In this case we have a maximum possible density given by

$$\rho_{max} = \frac{\kappa}{2A(1, w)\eta} \left(-1 + \sqrt{1 - \frac{4\eta\Lambda A(1, w)}{\kappa^2}} \right) , \tag{3.70}$$

indicating that a bounce occurs in this case, avoiding an initial singularity. In the second case, where $\eta A(1, w) > 0$, there is no bounce and no maximum energy density.

We now consider the solutions when $k = 0$ in the high-density limit, where we assume the correction terms dominate over the ρ and Λ terms. We consider the case of general n, and find an analytic solution. The Friedmann and acceleration equations reduce to

$$\left(\frac{\dot{a}}{a}\right)^2 = \frac{\eta}{3}\rho^{2n} A(n, w), \tag{3.71}$$

$$\frac{\ddot{a}}{a} = -\frac{\eta}{3}\rho^{2n} B(n, w). \tag{3.72}$$

From these, we can eliminate ρ to find

$$\left(\frac{\dot{a}}{a}\right)^2 + \frac{A(n, w)}{B(n, w)} \frac{\ddot{a}}{a} = 0. \tag{3.73}$$

which has the solution

$$a(t) = D[(A + B)t - C]^{\frac{A}{A+B}} \ , \tag{3.74}$$

where C and D are new constants of integration. We can then solve for the density:

$$\rho(t) = \left(\frac{3A}{\eta}\right)^{\frac{1}{2n}} ((A + B)t - C))^{-\frac{1}{n}}. \tag{3.75}$$

This solution is real (and thus not unphysical) only if $A(n, w)/\eta$ is positive. In the case of EMSG, this condition reduces to the requirement that η and $3w^2 + 8w + 1$ must

have the same sign. So, the two regions where this solution exists are,

$$\eta > 0 \quad \text{and} \quad \{w < \alpha_- \text{ or } w > \alpha_+\}, \tag{3.76}$$

$$\eta < 0 \quad \text{and} \quad \{\alpha_- < w < \alpha_+\}, \tag{3.77}$$

where

$$\alpha_\pm = \frac{-4 \pm \sqrt{13}}{3}\ , \tag{3.78}$$

are the roots of $3w^2+8w+1$. These are complementary to the conditions for the bounce to occur, as previously discussed. This is as we would expect, with the high-density approximation failing at a maximum density, as in the case of a bounce.

3.5 Anisotropic Cosmology

There are several ways of introducing anisotropy into our cosmological models. We will consider the simplest generalisation of FLRW, in which we have a flat, spatially homogeneous universe, with anisotropic scale factors. This is the Bianchi type I universe, with metric given by [89]

$$ds^2 = -dt^2 + a^2(t)dx^2 + b^2(t)dy^2 + c^2(t)dz^2, \tag{3.79}$$

where $a(t)$, $b(t)$ and $c(t)$ are the expansion scale factors in the x, y and z directions, respectively.

Assuming that the energy-momentum tensor takes the form of a perfect fluid with principal pressures, p_1, p_2 and p_3, so $L_m = \frac{1}{3}(p_1 + p_2 + p_3)$, we can derive the field equations for Bianchi I universes in our higher-order matter theories:

$$\frac{\dot{a}\dot{b}}{ab}+\frac{\dot{b}\dot{c}}{bc}+\frac{\dot{c}\dot{a}}{ca} = \kappa\rho+\frac{\eta}{6}(\rho^2+\sum_{i=1}^{3}p_i^2)^{n-1}\left[(6n-3)\rho^2+8n\rho\sum_{i=1}^{3}p_i+2n(\sum_{i=1}^{3}p_i)^2-3\sum_{i=1}^{3}p_i^2\right], \tag{3.80}$$

$$\frac{\dot{b}\dot{c}}{bc}+\frac{\ddot{b}}{b}+\frac{\ddot{c}}{c} = -\kappa p_1+\frac{\eta}{6}(\rho^2+\sum_{i=1}^{3}p_i^2)^{n-1}\left[2n(\rho+p_1-p_2-p_3)(2p_1-p_2-p_3)-3\sum_{i=1}^{3}p_i^2\right], \tag{3.81}$$

$$\frac{\dot{c}\dot{a}}{ca}+\frac{\ddot{c}}{c}+\frac{\ddot{a}}{a} = -\kappa p_2+\frac{\eta}{6}(\rho^2+\sum_{i=1}^{3}p_i^2)^{n-1}\left[2n(\rho+p_2-p_3-p_1)(2p_2-p_3-p_1)-3\sum_{i=1}^{3}p_i^2\right], \tag{3.82}$$

$$\frac{\dot{a}\dot{b}}{ab}+\frac{\ddot{a}}{a}+\frac{\ddot{b}}{b}=-\kappa p_3+\frac{\eta}{6}(\rho^2+\sum_{i=1}^{3}p_i^2)^{n-1}\left[2n(\rho+p_3-p_1-p_2)(2p_3-p_1-p_2)-3\sum_{i=1}^{3}p_i^2\right]. \tag{3.83}$$

In the case of an isotropic pressure fluid ($p_1 = p_2 = p_3 = p$):

$$\frac{\dot{a}\dot{b}}{ab}+\frac{\dot{b}\dot{c}}{bc}+\frac{\dot{c}\dot{a}}{ca}=\kappa\rho+\frac{\eta}{2}(\rho^2+3p^2)^{n-1}((2n-1)\rho^2+8n\rho p+(6n-3)p^2), \tag{3.84}$$

$$\frac{\dot{b}\dot{c}}{bc}+\frac{\ddot{b}}{b}+\frac{\ddot{c}}{c}=-\kappa p-\frac{\eta}{2}(\rho^2+3p^2)^{n-1}3p^2, \tag{3.85}$$

$$\frac{\dot{c}\dot{a}}{ca}+\frac{\ddot{c}}{c}+\frac{\ddot{a}}{a}=-\kappa p-\frac{\eta}{2}(\rho^2+3p^2)^{n-1}3p^2, \tag{3.86}$$

$$\frac{\dot{a}\dot{b}}{ab}+\frac{\ddot{a}}{a}+\frac{\ddot{b}}{b}=-\kappa p-\frac{\eta}{2}(\rho^2+3p^2)^{n-1}3p^2. \tag{3.87}$$

The first of these is the generalised Friedmann equation.

Qualitatively, we expect that the higher-order density and pressure terms will dominate at early times to modify or remove (depending on the sign of η) the initial singularity when $n > 1/2$, but will have negligible effects at late times, when the dynamics will approach the flat isotropic FLRW model. At early times, we know that in GR the singularity will be anisotropic and dominated by shear anisotropy whenever $-\rho/3 < p < \rho$. In order to determine the dominant effects as $t \to 0$ we will simplify to the case of isotropic perfect fluid pressures ($p_1 = p_2 = p_3 = w\rho$). Now, we determine the dependence of the highest-order matter terms on the scale factors, a, b and c from the generalisation of the conservation equation (3.24) with an anisotropic metric (3.79). For the case with general n, this is

$$\dot{\rho}=-\left(\frac{\dot{a}}{a}+\frac{\dot{b}}{b}+\frac{\dot{c}}{c}\right)\rho(1+w)\left[\frac{\kappa+\eta\rho^{2n-1}n(1+3w)}{\kappa+2\eta\rho^{2n-1}A(n,w)}\right], \tag{3.88}$$

and so the behaviour of the density is just

$$\rho\propto(abc)^{-\Gamma}, \tag{3.89}$$

where

$$\Gamma(n,w)=(1+w)\left[\frac{\kappa+\eta\rho^{2n-1}n(1+3w)}{\kappa+2\eta\rho^{2n-1}A(n,w)}\right]. \tag{3.90}$$

The higher-order density terms will dominate the evolution at early times when $n > 1/2$ and we see that, in these cases, Γ is independent of ρ and η as $\rho \to \infty$,since in this limit,

$$\Gamma(n, w) \to \frac{n(1+3w)(1+w)}{2A(n, w)}. \tag{3.91}$$

In the cosmology obtained by setting $n = 1$ in (3.80)-(3.83) we will have domination by the nonlinear matter terms, which will drive the expansion towards isotropy as $t \to 0$ if ρ^2 diverges faster than $(abc)^{-2}$ as $abc \to 0$. Thus, the condition for an isotropic initial singularity in $n = 1$ theories is that $\Gamma(1, w) > 2$, or

$$\frac{(1+3w)(1+w)}{2A(1, w)} > 2\ . \tag{3.92}$$

When this condition holds as $t \to 0$, the dynamics will approach the flat FLRW metric with

$$a(t) \propto b(t) \propto c(t) \propto t^{2/\Gamma(1,w)}. \tag{3.93}$$

When $\Gamma(1, w) < 2$, the dynamics will approach the vacuum Kasner metric with

$$(a, b, c) = (t^{q_1}, t^{q_2}, t^{q_3}), \tag{3.94}$$

$$\sum_{i=1}^{3} q_i = \sum_{i=1}^{3} q_i^2 = 1. \tag{3.95}$$

This condition simplifies to four cases:

$w > 0$	anisotropic singularity
$\alpha_+ < w < 0$	isotropic singularity
$\alpha_- < w < \alpha_+$	anisotropic singularity
$w < \alpha_-$	isotropic singularity

Here, the constants α_+ and α_- take the values determined earlier in (3.78).

In general, for arbitrary n, the higher-order correction terms on the right-hand side of the field equations (3.17) are proportional to $\eta\rho^{2n}$ when $p = w\rho$, and so the condition for an isotropic singularity as $t \to 0$ becomes

$$\Gamma(n, w) > 2n, \tag{3.96}$$

and the dynamics approach

$$a(t) \propto b(t) \propto c(t) \propto t^{2/\Gamma(n,w)}. \tag{3.97}$$

The case for general n and w is problematic to simplify succinctly due to the exponential dependence on n. However, we can consider specific physically relevant equations of state individually.

For dark energy ($w = -1$) and curvature ($w = -\frac{1}{3}$) 'fluids', we find that $\Gamma(n) = 0$, for all n, and so the condition for an isotropic initial singularity will depend only on whether n itself is positive or negative.

For $w = 0$, dust, we find

$$\Gamma(n, 0) = \frac{n}{2n - 1}, \tag{3.98}$$

for $n \neq \frac{1}{2}$. which leads to isotropy only when $\frac{1}{2} < n < \frac{3}{4}$.

For radiation, $w = \frac{1}{3}$, an isotropic singularity will occur if

$$\frac{n}{(\frac{4}{3})^{n-1}(2n - \frac{1}{2})} > 2n, \tag{3.99}$$

whilst for $w = 1$ we find that the condition for isotropy is

$$\frac{n}{4^{n-1}(2n - \frac{1}{2})} > 2n. \tag{3.100}$$

In both of the latter cases, we require $n \neq \frac{1}{4}$.

A similar effect will occur in more general anisotropic universes, like those of Bianchi type VII_h or IX, which are the most general containing open and closed FLRW models, respectively. In type IX, the higher-order matter terms will prevent the occurrence of chaotic behaviour with $w < 1$ fluids on approach to an initial or final singularity in a $\mathbf{T}^{2n}$ theory when $n > 1$. Thus we see that in these theories the general cosmological behaviour on approach to an initial and (in type IX universes) final singularity is expected to be isotropic in the wide range of cases we have determined, when $\Gamma(n, w) > 2n$. This simplifying effect of adding higher-order effects can also be found in the study of other modifications to GR, for example those produced by the addition of quadratic $R_{ab}R^{ab}$ terms to the gravitational Lagrangian, [90, 91]. These

also render isotropic singularities stable for normal matter (unlike in GR). If T_{ab} is not a perfect fluid but has anisotropic terms (for example, because of a magnetic field or free streaming gravitons [92]) they will add higher-order anisotropic stresses.

3.6 Conclusions

We have considered a class of theories which generalise general relativity by adding higher-order terms of the form $(T^{\mu\nu}T_{\mu\nu})^n$ to the matter Lagrangian, in contrast to theories which add higher-order curvature terms to the Einstein-Hilbert Lagrangians, as in $f(R)$ gravity theories. The family of theories which lead phenomenologically to higher-order matter contributions to the classical gravitation field equations of the sort studied here includes loop quantum gravity, and bulk viscous fluids, k-essence, or brane-world cosmologies in GR. This generalisation of the matter stresses is expected to create changes in the evolution of simple cosmological models at times when the density or pressure is high but to recover the predictions of general relativistic cosmology at late times in ever-expanding universes where the density is small. However, we find that there is a richer structure of behaviour if we generalise GR by adding arbitrary powers of the scalar square of the energy-momentum tensor to the action. In particular, we find a range of exact solutions for isotropic universes, discuss their behaviours with reference to the early- and late-time evolution, accelerated expansion, and the occurrence or avoidance of singularities. Finally, we discuss extensions to the simplest anisotropic cosmologies and delineated the situations where the higher-order matter terms will dominate over the anisotropic stresses on approach to cosmological singularities. This leads to a situation where the general cosmological solutions of the field equations for our higher-order matter theories are seen to contain isotropically expanding universes, in complete contrast to the situation in general relativistic cosmologies. In future work we will discuss the observational consequences of higher-order stresses for astrophysics.

Chapter 4

Screening Λ in a new modified gravity model

The work presented in this chapter was published as [93], in collaboration with Özgür Akarsu, John D. Barrow, N. Merve Uzun and J. Alberto Vasquez.

4.1 Introduction

The standard Lambda cold dark matter (ΛCDM) model is the most successful and economical cosmological model that accounts for the dynamics and the large-scale structure of the observable universe. Furthermore, it is in good agreement with the most of the currently available data [94–96]. Nevertheless, it suffers from profound theoretical issues relating to the cosmological constant Λ [97–99] and, on the observational side, from tensions of various degrees of significance between some existing data sets [100–109]. Firstly, the value of H_0 measured from the cosmic microwave background (CMB) data by the Planck Collaboration [95] in the basic ΛCDM model is 3.4 σ lower than the model-independent local value reported from supernovae by Riess et al. [110]; secondly, the Lyman-α forest measurements of the baryon acoustic oscillations (BAO) by the Baryon Oscillation Spectroscopic Survey (BOSS) prefer a smaller value of the pressureless matter density parameter than is preferred by the CMB data within ΛCDM [111]. Such tensions are of great importance since detection of even small deviations from ΛCDM could imply profound modifications to the fundamental theories

underpinning this model. We do, however, acknowledge that there are concerns about the possibility of systematic errors in the Lyman-α results, including those arising in the flux calibration due to Balmer lines, and sensitivity to the choice of spectrographic template used to estimate the continuum [111]. For instance, the BOSS collaboration reported a clear detection of dark energy (DE) in [106], consistent with positive Λ for $z < 1$, but with a preference for a DE yielding negative energy density values for $z > 1.6$. They then argued that the Lyman-α data from $z \sim 2.3$ can be accommodated by a non-monotonic evolution of $H(z)$, and thus of $\rho_{\rm tot}(z)$ within general relativity (GR), which is difficult to realise in any model with non-negative DE density. However, a *physical* DE with negative energy density would be physically problematic, which suggests that DE might instead be an *effective source* arising from a modified theory of gravity (see [64, 112, 41, 40, 113–115] for reviews on DE and modified theories of gravity). In line with this, [1] argues that the Lyman-α data can be addressed using a physically motivated modified gravity model that alters the Friedmann equation for $H(z)$ itself, and that a further tension, also relevant to the Lyman-α data, can be alleviated in models in which Λ is dynamically screened, implying an effective DE passing below zero and concurrently exhibiting a pole in its equation of state (EOS) at large redshift. The possible modifications to the $H(z)$ of ΛCDM can be represented by $3H^2(z) = \rho_{\rm m,0}(1+z)^3[1-u(z)] + \Lambda - v(z)$, involving functions $u(z)$ and $v(z)$ that represent two principal modifications. Interpreting all the terms other than $\rho_{\rm m,0}(1+z)^3$ as arising from DE, i.e. writing $3H^2(z) = \rho_{\rm m,0}(1+z)^3 + \rho_{\rm DE}$, would lead to an effective DE of the form $\rho_{\rm DE} = \Lambda - \rho_{\rm m,0}u(z)(1+z)^3 - v(z)$. Accordingly, $u(z) > 0$ and $v(z) > 0$ would drive $\rho_{\rm DE}$ towards negative values, and so Λ could be screened and $\rho_{\rm DE} < 0$ when we have $\rho_{\rm m,0}u(z)(1+z)^3 + v(z) > \Lambda$. Dynamical $u(z)$ and $v(z)$ functions are familiar from scalar-tensor theories, in which $u(z)$ stands for a varying effective gravitational coupling strength in the Jordan frame (or non-conservation, say, of the pressureless matter in the Einstein frame [116]), while $v(z)$ stands for the new terms due to the scalar field associated with varying gravitational 'constant', G. In such models, when the effective gravitational coupling strength gets weaker with increasing redshift, $\rho_{\rm DE}$ (as defined above) becomes negative at large redshifts [116–119]. A range of other examples of $\rho_{\rm DE}$ crossing below zero exist, including theories in which Λ relaxes from a large initial value via an adjustment mechanism [120, 121], cosmological models based on Gauss-Bonnet gravity [122], braneworld models [123, 75], loop quantum cosmology [124, 125], and higher dimensional cosmologies that accommodate dynamical reduction of the internal space [126–130]. In this chapter, as a new example of such zero-crossing

models, we study a particular theory of modified gravity: Energy-Momentum Squared Gravity (EMSG) [48, 47, 79, 62, 131, 73, 132], which generalises the form of the matter Lagrangian in a non-linear way and ensures that both $u(z)$ and $v(z)$ are dynamical. We will make a specific choice of model within the theory, in order to establish whether it is a good candidate for such behaviour.

From the Einstein-Hilbert action of GR, it is possible to consider a generalisation involving non-linear matter terms, by adding some analytic function of a new scalar $T^2 = T_{\mu\nu}T^{\mu\nu}$ formed from the energy-momentum tensor (EMT), $T_{\mu\nu}$, of the matter stresses [48]. Such generalisations of GR result in new contributions by the usual material stresses to the right-hand side of the generalised Einstein field equations, $v(z)$, and lead in general to non-conservation of the material stresses, $u(z)$, without the need to invoke new forms of matter (for other similar types of theories, [78, 46]). A particular example of EMSG is when $f(T^2) = \alpha T^2$, which has been studied in various contexts in [47, 62, 131, 73]. EMSG of this form in the presence of dust leads to $u(z) = 0$ and $v(z) = -\alpha\rho_{\rm m}^2 = -\alpha\rho_{\rm m,0}^2(1+z)^6 > 0$ for $\alpha < 0$, as in loop quantum cosmology [124, 125], which would lead to negative DE in the past, whilst the case $\alpha > 0$ corresponds to the braneworld scenarios [75]. However, if the quadratic energy density term is large enough to be effective today, then it would be the dominant term after just a few redshift units from today ($z = 0$) and hence spoil the successful description of the early universe.

A generalisation of the above model with $f(T^2) = \alpha T^2$, is Energy-Momentum Powered Gravity (EMPG), where $f(T^2) = \alpha(T^2)^\eta$, as studied in [79, 62]. This modification becomes effective at high energy densities, as in the early universe [62, 131], for the cases with $\eta > 1/2$, and at low energy densities, as in the late universe, when $\eta < 1/2$ [79]. For instance, $\eta = 0$ leads mathematically to exactly the same background dynamics as ΛCDM and $\eta \simeq 0$ to a wCDM-type cosmological model, despite the only physical source in the model being dust [79]. A recent study constraining the model from the low-redshift cosmological data can be found in [133] and a dynamical systems analysis in [134]. EMPG results in both $u(z)$ and $v(z)$ arising dynamically and could be investigated for producing effective DE passage below zero at large redshifts. Nevertheless, it is generally not possible to obtain explicit exact solutions for $\rho_{\rm m}(z)$, and hence of $\rho_{\rm de}(z)$, which renders EMPG inconvenient for the present study [79, 62]. The particular case $\eta = 1/2$, dubbed, 'Scale Independent EMSG', is one of the exceptions, along with the case $\eta = 1$ (EMSG with $f(T^2) = \alpha T^2$), which provides explicit exact

solutions for $H(z)$ required for a detailed observational test. In this model, the new terms in the field equations enter with the same power as the usual terms in GR, yet the standard energy is not conserved, and this leads to $u(z) = (1+z)^{3\alpha} - 1$ and $v(z) = \rho_{\mathrm{m},0}(1+z)^{3+3\alpha}$, which could provide the desired features in the $\alpha < 0$ case. Nevertheless, this model is studied in detail in [132] (though in somewhat different context) and α is well constrained observationally to be so close to zero that Scale Independent EMSG is unable to resolve the issues noted above.

In what follows we consider a new type of EMSG, called Energy-Momentum Log Gravity, EMLG, constructed by the choice of $f(T_{\mu\nu}T^{\mu\nu}) = \alpha \ln(\lambda\, T_{\mu\nu}T^{\mu\nu})$, where $\lambda > 0$ and α are real constants, to the Einstein-Hilbert action with cosmological constant Λ. [1] This form, which determines $u(z)$ and $v(z)$ in a specific way depending on α, has appealing features. It gives rise to new contributions that appear similar to those of a perfect fluid with constant equation of state parameter on the right-hand side of the Friedmann equations, reminiscent of a source with constant inertial mass density, and furthermore it allows us to obtain an explicit exact solution of the pressureless matter energy density in terms of redshift, so that we can conduct an exact theoretical investigation of the model using the observational data without further simplifications. We look for observationally viable cosmologies, in particular, for an extension of the standard ΛCDM model. We find that the observational data does not exclude the ΛCDM limit of our model but slightly prefers $u(z) > 0$ (related to the non-conservation of pressureless matter) and $v(z) < 0$ (related to the new terms of the pressureless matter in the field equations), where $u(z) > 0$ arises with the appropriate sign to produce an effective dynamical DE passing below zero (a screening of Λ) at high redshifts, as desired to address the tension with the Lyman-α measurements within the standard ΛCDM model. We also discuss the fact that the EMLG model relaxes, at some level, the persistent tension that appears between different measurements of H_0 within the standard ΛCDM model.

[1] A related logarithmic modification is considered in the context of $f(R,T)$ gravity [46] (where $T = g^{\mu\nu}T_{\mu\nu}$) in a recent paper [135] after our work. They extend the Starobinsky action [42] by including the logarithmic trace of the energy-momentum tensor, $f(T) \propto \ln(T)$, and study the cosmological dynamics.

4.2 Energy-Momentum Log Gravity

We begin with the action constructed by the addition of the term $f(T_{\mu\nu}T^{\mu\nu})$ to the Einstein-Hilbert (EH) action with a cosmological constant, Λ, as follows

$$S = \int \left[\frac{1}{2\kappa}(R - 2\Lambda) + f(T_{\mu\nu}T^{\mu\nu}) + \mathcal{L}_{\rm m}\right]\sqrt{-g}\,\mathrm{d}^4x, \tag{4.1}$$

where κ is Newton's constant scaled by a factor of 8π (and we henceforth set $\kappa = 1$), R is the Ricci scalar, g is the determinant of the metric $g_{\mu\nu}$, $\mathcal{L}_{\rm m}$ is the Lagrangian density corresponding to the matter source described by the energy-momentum tensor $T_{\mu\nu}$, and we have used units such that $c = 1$. We retain the cosmological constant, Λ, in the model since according to Lovelock's theorem it arises as a constant of nature. [2]

We take the variation of the action with respect to the inverse metric $g^{\mu\nu}$ as

$$\begin{aligned}\delta S = \int \mathrm{d}^4x\sqrt{-g}\Bigg[&\frac{1}{2}\delta R + \frac{\partial f}{\partial(T_{\mu\nu}T^{\mu\nu})}\frac{\delta(T_{\sigma\epsilon}T^{\sigma\epsilon})}{\delta g^{\mu\nu}}\delta g^{\mu\nu} \\ &-\frac{1}{2}g_{\mu\nu}\left(R - \Lambda + f(T_{\sigma\epsilon}T^{\sigma\epsilon})\right)\delta g^{\mu\nu} + \frac{1}{\sqrt{-g}}\frac{\delta(\sqrt{-g}\mathcal{L}_{\rm m})}{\delta g^{\mu\nu}}\Bigg],\end{aligned} \tag{4.2}$$

and, as usual, we define the EMT in terms of the matter Lagrangian $\mathcal{L}_{\rm m}$ as follows

$$T_{\mu\nu} = -\frac{2}{\sqrt{-g}}\frac{\delta(\sqrt{-g}\mathcal{L}_{\rm m})}{\delta g^{\mu\nu}} = g_{\mu\nu}\mathcal{L}_{\rm m} - 2\frac{\partial\mathcal{L}_{\rm m}}{\partial g^{\mu\nu}}. \tag{4.3}$$

Accordingly, the modified Einstein field equations read

$$G_{\mu\nu} + \Lambda g_{\mu\nu} = T_{\mu\nu} + f g_{\mu\nu} - 2\frac{\partial f}{\partial(T_{\mu\nu}T^{\mu\nu})}\theta_{\mu\nu}, \tag{4.4}$$

[2] Lovelock's theorem [136, 137] states that the only possible second-order Euler-Lagrange expression obtainable in a four-dimensional space from a scalar density of the form $\mathcal{L} = \mathcal{L}(g_{\mu\nu})$ is $E_{\mu\nu} = \sqrt{-g}\,(\lambda_1 G_{\mu\nu} + \lambda_2 g_{\mu\nu})$, where λ_1 and λ_2 are constants, leading to Newton's gravitational constant $G \equiv \kappa/8\pi$ and cosmological constant Λ in Einstein's field equations $G_{\mu\nu} + \Lambda g_{\mu\nu} = \kappa T_{\mu\nu}$ (see [138, 41, 139] for further reading).

where $G_{\mu\nu} = R_{\mu\nu} - \frac{1}{2}Rg_{\mu\nu}$ is the Einstein tensor and $\theta_{\mu\nu}$ is a new tensor defined as

$$\begin{aligned}\theta_{\mu\nu} &= T^{\sigma\epsilon}\frac{\delta T_{\sigma\epsilon}}{\delta g^{\mu\nu}} + T_{\sigma\epsilon}\frac{\delta T^{\sigma\epsilon}}{\delta g^{\mu\nu}} \\ &= -2\mathcal{L}_{\rm m}\left(T_{\mu\nu} - \frac{1}{2}g_{\mu\nu}\mathcal{T}\right) - \mathcal{T}T_{\mu\nu} \\ &\quad + 2T^{\gamma}_{\mu}T_{\nu\gamma} - 4T^{\sigma\epsilon}\frac{\partial^2\mathcal{L}_{\rm m}}{\partial g^{\mu\nu}\partial g^{\sigma\epsilon}}\ ,\end{aligned} \tag{4.5}$$

with $\mathcal{T}$ being the trace of the EMT, $T_{\mu\nu}$. We note that the EMT given in (4.3) does not include the second variation of $\mathcal{L}_{\rm m}$, and hence the last term of (4.5) vanishes. As the definition of the matter Lagrangian that gives rise to the perfect-fluid EMT is not unique, one could choose either $\mathcal{L}_{\rm m} = p$ or $\mathcal{L}_{\rm m} = -\rho$, which result in the same EMT. In the present study, we consider $\mathcal{L}_{\rm m} = p$.

We proceed with a specific form of the model,

$$f(T_{\mu\nu}T^{\mu\nu}) = \alpha\ln(\lambda\, T_{\mu\nu}T^{\mu\nu}), \tag{4.6}$$

where λ has the dimension inverse energy density squared so that $\lambda\, T_{\mu\nu}T^{\mu\nu}$ is dimensionless. This choice comes with some particular advantageous features. In the cosmological application of the model, this is the only functional choice of $f(T_{\mu\nu}T^{\mu\nu})$ that gives rise to new contributions of a perfect fluid on the right hand side of the Einstein field equations yielding constant effective inertial mass density (See Section 4.3.1 for details). Also, it has an explicit exact solution, including the form of $\rho(z)$ which is important for analytical investigations. This contrasts with many EMSG-type models, in which this is usually not possible due to the non-linear coupling of the matter sources to gravity. For instance, in [79] cosmic acceleration in a dust only EMPG model was investigated, where the exact solution of $z(\rho_{\rm m})$ was obtained, but the corresponding explicit solution of $\rho_{\rm m}(z)$ could usually only be obtained through an approximation procedure, except for a few particular cases ([62, 132]).

Consequently, the action we use is

$$S = \int\left[\frac{1}{2}(R - 2\Lambda) + \alpha\ln(\lambda\, T_{\mu\nu}T^{\mu\nu}) + \mathcal{L}_{\rm m}\right]\sqrt{-g}\,{\rm d}^4x, \tag{4.7}$$

where α is a constant that determines the gravitational coupling strength of the EMLG modification of GR. Accordingly, the modified Einstein equations (4.4) for this action

now read,

$$G_{\mu\nu} + \Lambda g_{\mu\nu} = T_{\mu\nu} + \alpha g_{\mu\nu} \ln(\lambda\, T_{\sigma\epsilon} T^{\sigma\epsilon}) - 2\alpha \frac{\theta_{\mu\nu}}{(T_{\sigma\epsilon} T^{\sigma\epsilon})}. \tag{4.8}$$

From (4.8), the covariant divergence of the EMT becomes

$$\nabla^{\mu} T_{\mu\nu} = -\alpha g_{\mu\nu} \nabla^{\mu} \ln(\lambda\, T_{\sigma\epsilon} T^{\sigma\epsilon}) + 2\alpha \nabla^{\mu} \left(\frac{\theta_{\mu\nu}}{T_{\sigma\epsilon} T^{\sigma\epsilon}} \right). \tag{4.9}$$

We note that, unless $\alpha = 0$, the right-hand side of this equation does not vanish in general, and thus the EMT is not conserved, i.e. $\nabla^{\mu} T_{\mu\nu} = 0$ is not satisfied.

4.3 Cosmology in EMLG

In this chapter, we investigate the cosmological behaviour of this gravitational model. We proceed by considering the spatially maximally symmetric spacetime metric, given by the Friedmann metric,

$$\mathrm{d}s^2 = -\mathrm{d}t^2 + a^2 \left[\frac{\mathrm{d}r^2}{1 - kr^2} + r^2 (\mathrm{d}\theta^2 + \sin^2\theta \mathrm{d}\phi^2) \right], \tag{4.10}$$

where the spatial curvature parameter k takes values in $\{-1,\, 0,\, 1\}$ corresponding to open, flat and closed 3-spaces respectively, and the scale factor $a = a(t)$ is a function of cosmic time t only. For cosmological matter sources describing the physical component of the universe, we consider the perfect fluid form of the EMT given by

$$T_{\mu\nu} = (\rho + p) u_{\mu} u_{\nu} + p g_{\mu\nu}, \tag{4.11}$$

where $\rho > 0$ is the energy density and p is the thermodynamic pressure satisfying the barotropic equation of state (EoS) as

$$\frac{p}{\rho} = w = \text{constant}, \tag{4.12}$$

and u_{μ} is the four-velocity satisfying the conditions $u_{\mu} u^{\mu} = -1$, and $\nabla_{\nu} u^{\mu} u_{\mu} = 0$.

Using (4.11) and (4.12), we calculate $\theta_{\mu\nu}$ defined in (4.5) and the self-contraction of the EMT for the perfect fluid with barotropic EoS (4.12) as follows

$$\theta_{\mu\nu} = -\rho^2(3w+1)(w+1)u_\mu u_\nu, \tag{4.13}$$

$$T_{\mu\nu}T^{\mu\nu} = \rho^2(3w^2+1). \tag{4.14}$$

Next, using (4.13) and (4.14) along with the metric (4.10) in the modified Einstein field equations (4.8) we obtain the following pair of linearly independent modified Friedmann equations, for a single fluid cosmology,

$$3H^2 + \frac{3k}{a^2} = \rho + \Lambda + \alpha'\rho_0 + \alpha'\rho_0\frac{2}{\gamma}\ln\left(\rho/\rho_0\right), \tag{4.15}$$

$$\begin{aligned} -2\dot{H} - 3H^2 - \frac{k}{a^2} =& w\rho - \Lambda \\ & - \alpha'\rho_0\frac{2}{\gamma}\ln\left[\sqrt{3w^2+1}\ \left(\rho/\rho_0\right)\right], \end{aligned} \tag{4.16}$$

where we set $\lambda = \rho_0^{-2}$ without loss of generality.[3] Here $H = \dot{a}/a$ is the Hubble parameter and the subscript $_0$ denotes the present-day values of the parameters. $\gamma = \gamma(w)$ is a parameter defined by

$$\gamma = \ln(3w^2+1) - 2\frac{(3w+1)(w+1)}{(3w^2+1)}, \tag{4.17}$$

which is negative for $-0.27 < w < 2.52$ and positive otherwise. We also define the dimensionless constant

$$\alpha' = -\alpha\,\gamma\rho_0^{-1}. \tag{4.18}$$

Note that in the action (4.7), the terms $\alpha\ln(\lambda\,T_{\mu\nu}T^{\mu\nu})$ and $\mathcal{L}_\mathrm{m}$ are both related to the material content of the universe and that the EMT included in the modification term $\alpha\ln(\lambda\,T_{\mu\nu}T^{\mu\nu})$ is the same as the one obtained from the variation of $\mathcal{L}_\mathrm{m}$, so the model contains only a single matter source. However, the terms arising due to the EMLG modification couple to gravity with a different strength, α', to the normalised gravitational coupling strength (i.e. $\kappa = 1$) of the standard GR terms. Furthermore,

[3]Defining $\lambda = \eta\rho_0^{-2}$, where $\eta > 0$ is a coefficient, we can write $\ln(\lambda\,T_{\mu\nu}T^{\mu\nu}) = \alpha\ln(\eta) + \ln(T_{\mu\nu}T^{\mu\nu}/\rho_0^2)$. The term $\alpha\ln(\eta)$ then acts like a cosmological constant, and so simply rescales Λ in the action (4.7) and field equations (4.8). Additionally, λ has no contribution to the continuity equation (4.9) since $\nabla^\mu\ln(\lambda\,T_{\sigma\epsilon}T^{\sigma\epsilon}) = \nabla^\mu\ln(T_{\sigma\epsilon}T^{\sigma\epsilon})$. Therefore, choosing a particular value for η, i.e. $\eta = 1$ as we have done, does not lead to any loss of generality as our model already includes Λ in the action.

we note that α' is a function not only of the true constant of the EMLG modification, α, but also the current energy density, ρ_0, and the EoS parameter, w, describing the type of the matter source, so $\alpha' = \alpha'(\alpha, \rho_0, w)$. The latter two dependencies imply a violation of the equivalence principle, which means our modification must obey constraints from solar system tests of this principle. It would also have implications in fundamental physics. For example, the violation of equivalence principle is intimately connected with some of the basic aspects of the unification of gravity with particle physics such as string theories [140] and theories of varying constants [141–143]. The consequences of this property of the model are beyond the scope of the current study, which focuses on the dynamics of a mono-fluid universe, where the only material source is dust (pressureless fluid) with the purpose of modifying ΛCDM by considering the new terms arising from EMLG as a correction.

The corresponding local energy-momentum conservation equation (4.9) is

$$\dot{\rho} + 3H(1+w)\rho\left[\frac{\gamma\rho(3w^2+1) - 2\alpha'\rho_0(3w+1)}{\gamma\rho(3w^2+1) + 2\alpha'\rho_0(3w^2+1)}\right] = 0. \tag{4.19}$$

The expression in square brackets is the modification arising from EMLG and is equal to unity in the case $\alpha' = 0$, corresponding to GR. We can see that the covariant energy-momentum conservation $\nabla^\mu T_{\mu\nu} = 0$, which in GR would lead to $\rho \propto a^{-3(1+w)}$, does not hold for any $w \neq -1$ when $\alpha' \neq 0$, whilst the case $w = -1$, corresponding to conventional dark energy, i.e., vacuum energy, is unmodified by EMLG.

4.3.1 Constant effective inertial mass density

It is worth noting here that, for a perfect fluid with barotropic equation of state, both $\theta_{\mu\nu}$ and $T_{\mu\nu}T^{\mu\nu}$ are proportional to ρ^2 and therefore the last term in (4.8) is independent of the energy density scale, instead depending only on the four-velocity of the fluid and type of the fluid (i.e., the EoS of the matter source). Furthermore, for usual cosmological applications, when a comoving (i.e. $u_\mu u^\mu = -1$ and $\nabla_\nu u^\mu u_\mu = 0$) fluid with a constant EoS parameter w is considered, this term becomes a constant determined by the model parameter α and the equation of state under consideration. On the other hand, the second term on the right-hand side of (4.8) will always contribute equally but with opposite signs to the time and space components of the equation in Lorentzian spacetimes, that is to the energy density and pressure equations arising

from the metric given in (4.10), and therefore the addition of these equations results in the modifications from the second term on the right-hand side of (4.8) cancelling each other. Consequently, this produces a characteristic feature of the model: if we define the new terms that arise due to the EMLG modification in the energy density equation (4.15) as an effective energy density

$$\rho' = \alpha'\rho_0 + \alpha'\rho_0\frac{2}{\gamma}\ln\left(\rho/\rho_0\right) \ , \tag{4.20}$$

and those in the pressure equation (4.16) as an effective pressure

$$p' = -\alpha'\rho_0\frac{1}{\gamma}\ln(3w^2+1) - \alpha'\rho_0\frac{2}{\gamma}\ln\left(\rho/\rho_0\right), \tag{4.21}$$

then the *effective inertial mass density* defined as $\rho' + p'$ is always constant; specifically,

$$\rho' + p' = \alpha'\rho_0[1 - \gamma^{-1}\ln(3w^2+1)], \tag{4.22}$$

for $p/\rho = w =$ constant. This feature of the model leads to $\rho' = \alpha'\rho_0[1-\gamma^{-1}\ln(3w^2+1)] - p'$ meaning that ρ' changes sign when $p' = \alpha'\rho_0[1-\gamma^{-1}\ln(3w^2+1)]$, showing our model's relevance to the studies [1, 106] suggesting that a DE model achieving negative energy density values for redshifts larger than a certain value (e.g., $z \gtrsim 2$ as suggested by [1, 103, 106]) might improve the fit to observational data. It might be mentioned that the sign change of ρ' does not signal any pathologies since it is an *effective* energy density, not the physical energy density. For example, in the case of dust, $w = 0$, we have

$$\rho' = \alpha'\rho_{\mathrm{m},0} - p', \tag{4.23}$$

and accordingly $\rho' < 0$ when $p' > \alpha'\rho_{\mathrm{m},0}$.

4.3.2 Preliminary constraints on α

We now determine some preliminary constraints on α by considering separately two standard cosmological matter sources: radiation and dust. We begin by writing (4.19) in terms of α:

$$\dot{\rho} = -3(1+w)H\rho\left[\frac{\rho(3w^2+1)+2\alpha(3w+1)}{\rho(3w^2+1)-2\alpha(3w^2+1)}\right]. \tag{4.24}$$

A viable cosmological model should satisfy $H > 0$, $\dot{H} < 0$, $\rho > 0$ and $\dot{\rho} < 0$. Here $H > 0$ and $\dot{H} < 0$ together lead to an expanding universe in line with observations. $\dot{\rho} < 0$ means that the energy density is decreasing with time, and therefore $H > 0$ and $\dot{\rho} < 0$ together guarantee that the density is larger at early times and decreases as the universe expands. As seen from (4.24), taking $H > 0$, $\dot{\rho} < 0$ implies

$$(1+w)\rho\left[\frac{\rho(3w^2+1)+2\alpha(3w+1)}{\rho(3w^2+1)-2\alpha(3w^2+1)}\right] > 0. \tag{4.25}$$

Substituting $w = 1/3$ into (4.25), we obtain the interval

$$-\frac{\rho_{\rm r}}{3} < \alpha < \frac{\rho_{\rm r}}{2}\ , \tag{4.26}$$

over which it is guaranteed that the energy density of radiation, $\rho_{\rm r}$, increases as we go to earlier times. Next, we also substitute $w = 0$ into (4.25) and obtain the interval

$$-\frac{\rho_{\rm m}}{2} < \alpha < \frac{\rho_{\rm m}}{2}\ , \tag{4.27}$$

over which it is guaranteed that $\rho_{\rm m}$ (energy density of dust) decreases as the universe expands. From (4.15) and (4.16), one can see that the energy density corresponding to the spatial curvature evolves as $\rho_k = \frac{3k}{a^2}$. We note that this is equivalent to a matter source with an EoS parameter $w = -1/3$ via $\nabla^\mu T_{\mu\nu} = 0$ in GR, but it is not the case in our model since, unless $\alpha' = 0$, $\nabla^\mu T_{\mu\nu} \neq 0$ for a matter source with $w = -1/3$ (see (4.33) in Sec. 4.3.3 for the solution). Finally, in order to align with standard cosmology, we wish to avoid spatial curvature domination over dust in the early universe. This means that, using the continuity equation (4.24) for dust and the fact that $\rho_k \propto a^{-2}$, we must have

$$3\left[\frac{\rho_{\rm m}+2\alpha}{\rho_{\rm m}-2\alpha}\right] > 2\ , \tag{4.28}$$

leading to the following permitted interval

$$-\frac{\rho_{\rm m}}{10} < \alpha < \frac{\rho_{\rm m}}{2}, \tag{4.29}$$

which is a tighter bound than the one given in (4.27).

4.3.3 Solving the continuity equation explicitly for $\rho(z)$

As mentioned in Sec. 4.2, one of the difficulties in studying EMSG type models is that it is usually not possible to obtain the explicit exact solution of ρ in terms of scale factor a (or redshift z). For instance, in [79] which investigated cosmic acceleration in a dust only universe via EMPG, the explicit solution of $\rho_{\rm m}(z)$ could only be obtained through an approximation procedure. In this section, we investigate the cases providing explicit solutions of $\rho(z)$ and show that EMLG model (4.6) provides an exact solution for the dust only universe.

Defining

$$\beta(w) = \frac{3w+1}{3w^2+1}, \tag{4.30}$$

we rewrite (4.19) as

$$\frac{\dot{\rho}}{\rho}\left[\frac{\rho-2\alpha}{\rho+2\alpha\beta}\right] = -3(1+w)\frac{\dot{a}}{a}, \tag{4.31}$$

which can be solved implicitly as

$$\rho\left(1+\frac{2\alpha}{\rho}\beta\right)^{\frac{1}{\beta}+1} \propto a^{-3(1+w)}. \tag{4.32}$$

We can then proceed by examining the behaviour of $\beta(w)$.

We notice first that β attains a maximum value of $3/2$ at $w = 1/3$, and a minimum of $-1/2$ at $w = -1$; however, β is not injective, and so there exist two values of w that provide the same right-hand side of (4.32). However, as the left hand side also has a w dependence, the behaviour of our perfect fluid for the two equations of state will not coincide.

At $w = -1/3$, we must note that $\beta = 0$. At this point we consider the limiting behaviour of (4.32), which takes exponential form:

$$\rho e^{\frac{2\alpha}{\rho}} \propto a^{-2}. \tag{4.33}$$

We could also recover this by integrating (4.19) directly with $w = -1/3$. This equation of state no longer corresponds to the behaviour of curvature terms as in GR, but describes the evolution of cosmic strings. We also note the similarities between the

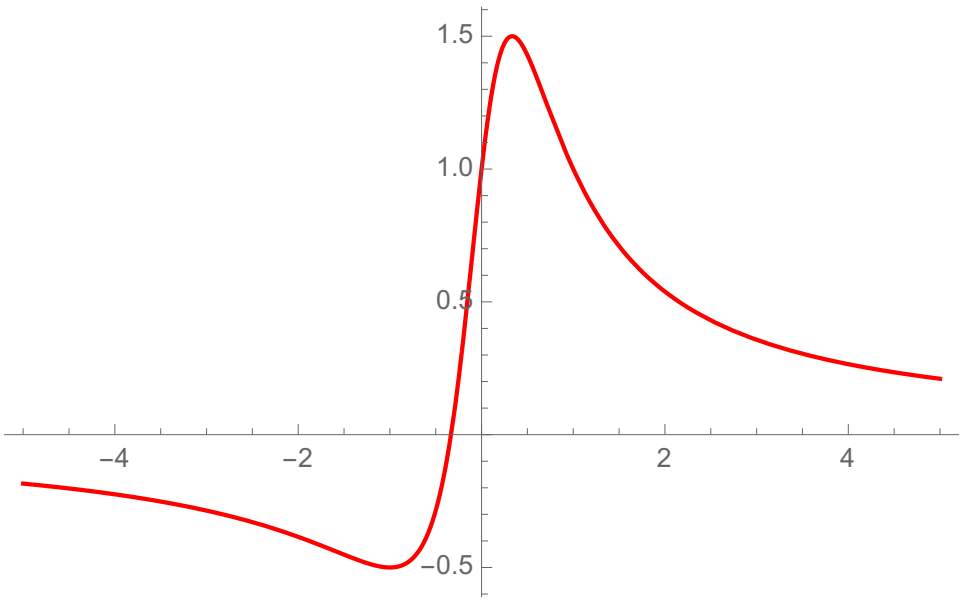

Fig. 4.1 The behaviour of the parameter β (y-axis) for different equation of state parameters w (x-axis), i.e., $\beta(w)$. The region of most interest has $-1 \leq w \leq 1$.

behaviour for $w = -1/3$ in this model and that in EMPG, as discussed in [62]. However, we cannot solve the radiation dominated Universe explicitly.

This implicit solution (4.32) depends on the behaviour of the parameter β, and in general we would not expect to find explicit solutions for the energy density in terms of the scale factor. In fact, we will be able to find explicit closed form solutions in certain physically relevant cases when (4.32) reduces to a polynomial in ρ of degree at most four. If we write the exponent as $\frac{A}{B} = \frac{1}{\beta} + 1$ as a fraction in its lowest terms (A, $B \in \mathbb{Z}$, $B \neq 0$) we can determine the conditions on A and B such that the resulting equation is an appropriate polynomial. Once this is done, we can further constrain the exponent by considering the values which β may take. It emerges that the only appropriate values that the exponent can take are integers in the list $\{-3, -2, -1, 2, 3, 4\}$. Two of these cases are of specific interest. The -1 case corresponds to $w = -1$, the equation of state for the conventional vacuum energy, in which case the exponent on the right hand side vanishes and we find that the energy density in this case, ρ_{-1} is a constant, equal to its value today $\rho_{-1,0}$, that is:

$$\rho_{-1} \equiv \rho_{-1,0} \ , \tag{4.34}$$

as in the GR case.

The second case of interest is $\beta = 1$, in which case (4.32) reduces to a quadratic. This arises for the physically relevant cases of dust, $w = 0$ and stiff fluid, $w = 1$. This allows us to find an exact solution for the energy density in these cases, the specific form of which is discussed in the subsequent section.

The remaining cases each result from a pair of values of w, but these values are irrational and thus unlikely to be of physical importance. Typically, one of the two values lies within the $-1 < w < 1$ range, and the other outside.

It is also important to note that although we have explicit solutions for these cases, and can examine features of (4.32) for others, we are not able to compare the behaviour of a single cosmological model using these solutions since they are each valid only for a single fluid Universe. In this study, we will investigate the late-time acceleration of the universe, accordingly, neglect the radiation and assume that there is only dust as the material source, for which, fortunately, EMLG provides us with explicit solution for $\rho(a)$. In Section 4.4.5, we will also briefly discuss possible analytical solutions of a Universe including radiation.

4.3.4 Dust-filled Universe

Since we will concentrate our discussions on the late-time acceleration of the universe, we assume that the radiation density is negligible, and the universe is spatially flat and filled only with dust. Accordingly, substituting $w = 0$ and $k = 0$ into the modified Friedmann equations (4.15) and (4.16), they reduce to the following

$$3H^2 = \rho_{\rm m} + \Lambda + \alpha'\rho_{\rm m,0} - \alpha'\rho_{\rm m,0}\ln\left(\rho_{\rm m}/\rho_{\rm m,0}\right), \tag{4.35}$$

$$-2\dot{H} - 3H^2 = -\Lambda + \alpha'\rho_{\rm m,0}\ln\left(\rho_{\rm m}/\rho_{\rm m,0}\right). \tag{4.36}$$

And for $w = 0$, the continuity equation (4.19) is satisfied as

$$\dot{\rho}_{\rm m} + 3H\rho_{\rm m}\left(\frac{\rho_{\rm m} + \alpha'\rho_{\rm m,0}}{\rho_{\rm m} - \alpha'\rho_{\rm m,0}}\right) = 0, \tag{4.37}$$

and hence as discussed above, we obtain the explicit solution

$$\begin{aligned}\rho_{\rm m} =& \frac{1}{2}\rho_{\rm m,0}(1+\alpha')^2(1+z)^3 - \alpha'\rho_{\rm m,0} \\ &+ \frac{1}{2}\rho_{\rm m,0}\sqrt{-4\alpha'^2 + \left[(1+\alpha')^2(1+z)^3 - 2\alpha'\right]^2}\,,\end{aligned} \tag{4.38}$$

provided that $-1 < \alpha' \leq 1$, and using that $a = (1+z)^{-1}$. We note that as $\alpha' \to 0$, in our solution $\rho_{\rm m} \to \rho_{\rm m,0}(1+z)^3$, the usual pressureless matter evolution, so we recover the standard ΛCDM model along with GR. We also note that (4.35) with $\Lambda = 0$ at the present time reads $3H_0^2 = \rho_{\rm m,0} + \alpha'\rho_{\rm m,0}$ and consequently $\Omega_{\rm m,0}(1+\alpha') = 1$. Here we define the present day density parameters of dust and Λ as $\Omega_{\rm m,0} = \frac{\rho_{\rm m,0}}{3H_0^2}$ and $\Omega_{\Lambda,0} = \frac{\Lambda}{3H_0^2}$. From the most recent observational results $\Omega_{\rm m,0} \approx 0.3$ and therefore we estimate that $\alpha' \approx 2.3$. However, our solution (4.38) is not valid for this α' value. Thus, to be able to use the solution (4.38), we must include Λ in our model, so that (4.35) implies that $\Omega_{\rm m,0}(1+\alpha') + \Omega_{\Lambda,0} = 1$. We note that the intervals we deduced in Section 4.3.2 for a viable cosmology are a subset of the interval needed for the validity of solution (4.38) today. Namely, curvature domination discussion in (4.29) with the definition (4.18) leads to a narrower interval for α'. Considering that interval of α', $-0.20 < \alpha' < 1$, we find $1 - 2\,\Omega_{\rm m,0} < \Omega_{\Lambda,0} < 1 - 0.8\,\Omega_{\rm m,0}$. Consequently, we estimate that the solution given in (4.38) is valid for $0.40 \lesssim \Omega_{\Lambda,0} \lesssim 0.76$. Furthermore, as $z \to -1$, the energy density $\rho \to -\alpha'\rho_{\rm m,0} = \rho_{\rm min}$. This means that if the universe were to expand forever, the energy density would never reach to zero. Instead there would be a minimum energy density limit as $\rho_{\rm min} = -\alpha'\rho_{\rm m,0}$, which in turn implies that α' must be negative in an eternally expanding universe. Finally we note that the solution for equation of state $w = 1$ is the same as the solution for dust, with $a \to a^2$.

4.4 Improved Om diagnostic of EMLG

Cosmological models with late time acceleration, via DE in GR or modified gravity, can be examined with the use of null-diagnostics. One diagnostic is the jerk parameter $j = \frac{\dddot{a}}{aH^3}$, first introduced by Harrison [144] (who denoted it by Q), which is simply equal to unity in ΛCDM (omitting radiation), $j_{\Lambda\rm CDM} = 1$, [145–147]. Hence, any observational evidence which predicts a deviation from unity implies that late time acceleration is not due to the cosmological constant in GR. The second diagnostic is

$Om(z)$ which is defined via an improved version in a recent study [1] as follows:

$$Omh^2(z_i; z_j) = \frac{h^2(z_i) - h^2(z_j)}{(1+z_i)^3 - (1+z_j)^3}, \tag{4.39}$$

where $h(z) = H(z)/100\,\mathrm{km\,s^{-1}Mpc^{-1}}$ is the dimensionless reduced Hubble parameter. We note that Om depends only on $H(z)$, and is therefore easier to determine from observations than j. Consequently, knowing the Hubble parameter at two or more redshifts, one can obtain the value of Omh^2 and conclude whether or not a dark energy modification to GR is the cosmological constant. In ΛCDM, omitting radiation (which is negligible in the late universe) we have

$$h^2 = h_0^2 \left[\Omega_{\mathrm{m},0}(1+z)^3 + 1 - \Omega_{\mathrm{m},0}\right], \tag{4.40}$$

which simply gives a constant as

$$Omh^2(z_i; z_j) = h_0^2 \Omega_{\mathrm{m},0}. \tag{4.41}$$

The estimates given in [1] for the Omh^2 diagnostic consider $H(z_1 = 0) = 70.6 \pm 3.3\mathrm{km\,s^{-1}Mpc^{-1}}$ [148] based on the NGC 4258 maser distance, $H(z_2 = 0.57) = 92.4 \pm 4.5\mathrm{km\,s^{-1}Mpc^{-1}}$ [149] based on the clustering of galaxies in the SDSS-III BOSS DR9, and $H(z_3 = 2.34) = 222 \pm 7\mathrm{km\,s^{-1}Mpc^{-1}}$ [111] based on the BAO in the Lyman-α forest of SDSS DR11 data and read

$$\begin{aligned} Omh^2(z_1; z_2) &= 0.124 \pm 0.045, \\ Omh^2(z_1; z_3) &= 0.122 \pm 0.010, \\ Omh^2(z_2; z_3) &= 0.122 \pm 0.012. \end{aligned} \tag{4.42}$$

Note that these model-independent values of Omh^2 for any two redshifts are stable at about 0.12 which is in tension with, the value $Omh^2 = \Omega_{\mathrm{m},0}h_0^2 = 0.1430 \pm 0.0011$ determined for the base ΛCDM model from the Planck 2018 release [96]. Note that Omh^2 is not affected significantly by $H(z = 0)$ (the accurate value of which is subject to a great debate in the contemporary cosmology) owing to the high-precision measurement of $H(z = 2.34)$ [1].

It is argued in [1] that this tension can be alleviated in models in which Λ was dynamically screened in the past. In line with this, until Section 4.5, we investigate

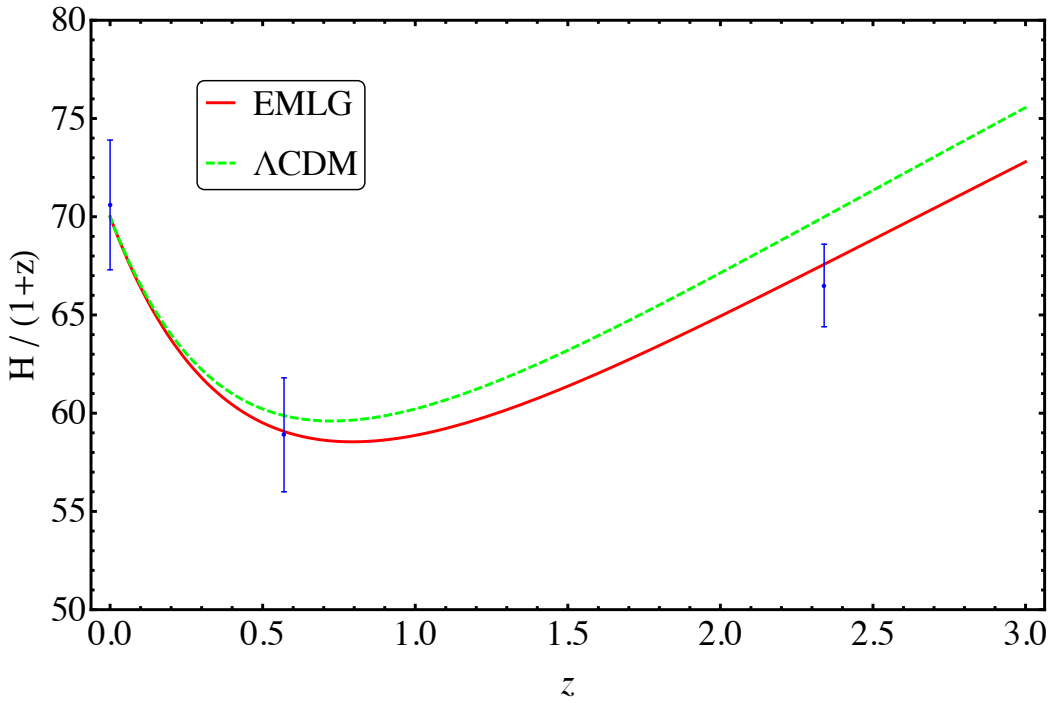

Fig. 4.2 $H(z)/(1+z)$ vs. z graph of the EMLG and ΛCDM. Plotted by using $\Omega_{\mathrm{m},0} = 0.28$, $H_0 = 70\,\mathrm{km\,s^{-1}Mpc^{-1}}$ and $\alpha' = -0.04$. For the three observational $H(z)$ values with errors we consider those in [1]. This is the standard, one redshift, Om parameter, which we plot here to straightforwardly illustrate the comparison between the two models, and the current tension between ΛCDM and some measurements of $H(z)$.

the features of the EMLG model (parametrised by α') in comparison with the ΛCDM model mostly by referring to [1]. Therefore, we intentionally make use of these three $H(z)$ data (rather than the latest data, which would not change our arguments in what follows) as well as the $\Omega_{\mathrm{m},0}$ and H_0 values considered in [1]. This allows us to demonstrate the effect of the EMLG model on Omh^2 diagnostics, with a properly chosen value for α', by a straightforward comparison with [1]. We shall investigate the observational analyses of the EMLG model and compare with the ΛCDM model using the latest cosmological data in Section 4.5.

4.4.1 EMLG cosmology in the light of null-diagnostics

We now consider the Om diagnostic expression defined in (4.39) for our model. Substituting the solution (4.38) into (4.35), we obtain

$$\begin{aligned} h^2 =& h_0^2 \Big\{ 1 - \Omega_{\mathrm{m},0} \Big\{ 1 - \frac{1}{2} \Big[(1+\alpha')^2 (1+z)^3 - 2\alpha' \\ &+ \sqrt{-4\alpha'^2 + \left[(1+\alpha')^2 (1+z)^3 - 2\alpha' \right]^2} \Big] \\ &+ \alpha' \ln \Big\{ \frac{1}{2} \Big[(1+\alpha')^2 (1+z)^3 - 2\alpha' \\ &+ \sqrt{-4\alpha'^2 + \left[(1+\alpha')^2 (1+z)^3 - 2\alpha' \right]^2} \Big] \Big\} \Big\} \Big\} , \end{aligned} \tag{4.43}$$

where we use also the fact that $\Omega_{\Lambda,0} = 1 - (1+\alpha')\Omega_{\mathrm{m},0}$. This leads to

$$\begin{aligned} Omh^2(z_i;z_j) = & h_0^2 \Omega_{\mathrm{m},0} \Big\{ (\alpha'+1)^2 (z_i+1)^3 \\ &+ \sqrt{\left((\alpha'+1)^2 (z_i+1)^3 - 2\alpha' \right)^2 - 4(\alpha')^2} \\ &- 2\alpha' \ln \Big[\frac{1}{2} \Big(-2\alpha' + (\alpha'+1)^2 (z_i+1)^3 \\ &+ \sqrt{\left((\alpha'+1)^2 (z_i+1)^3 - 2\alpha' \right)^2 - 4(\alpha')^2} \Big) \Big] \\ &- (\alpha'+1)^2 (z_j+1)^3 \\ &- \sqrt{\left((\alpha'+1)^2 (z_j+1)^3 - 2\alpha' \right)^2 - 4(\alpha')^2} \\ &+ 2\alpha' \ln \Big[\frac{1}{2} \Big(-2\alpha' + (\alpha'+1)^2 (z_j+1)^3 \\ &+ \sqrt{\left((\alpha'+1)^2 (z_j+1)^3 - 2\alpha' \right)^2 - 4(\alpha')^2} \Big) \Big] \Big\} / \\ & 2 \left[(z_i+1)^3 - (z_j+1)^3 \right] . \end{aligned} \tag{4.44}$$

Following the three $H(z)$ data given in [1], in Fig. 4.2, we plot $H(z)/(1+z)$ with respect to redshift using $\Omega_{\mathrm{m},0} = 0.28$ and $H_0 = 70 \mathrm{km\,s^{-1}Mpc^{-1}}$ for both the ΛCDM model (green) and the EMLG model with $\alpha' = -0.04$ (red), which provides us $H(z)/(1+z)$ in agreement with all data points whereas the one for ΛCDM does not fit to the data point from $z = 2.34$. The true constant of the model in the action (4.7) is, accordingly, $\alpha = -0.02\rho_{\mathrm{m},0}$. The model-independent value of the Om diagnostic estimated in [1] is quite stable at $Omh^2 \simeq 0.12$ and is in tension with the ΛCDM-based value $Omh^2(\Lambda\mathrm{CDM}) \simeq 0.14$. On the other hand, for the EMLG model with

$\Omega_{\mathrm{m},0} = 0.28$, $H_0 = 70\mathrm{km\,s^{-1}Mpc^{-1}}$ and $\alpha' = -0.04$, we find $Omh^2(z_1; z_2) = 0.129$, $Omh^2(z_1; z_3) = 0.127$ and $Omh^2(z_2; z_3) = 0.127$ where $z_1 = 0$, $z_2 = 0.57$ and $z_3 = 2.34$. Note that these are in good agreement with the estimates given in [1].

4.4.2 A comparison via general relativistic interpretation

In [1], it is suggested that lower values for Omh^2 can be obtained in models in which the cosmological constant was screened by a dynamically evolving counter-term $f(z)$ in the past. Accordingly, $H^2(z)$ is modified, with respect to the ΛCDM model, as

$$H^2(z) = \frac{1}{3}\rho_{\mathrm{m},0}(1+z)^3 + \frac{\Lambda}{3} - f(z). \tag{4.45}$$

and at a redshift z_*, $\Lambda/3$ is balanced by $f(z)$ (i.e. $f(z_*) = \Lambda/3$). Comparing (4.45) and (4.35), along with our solution given in (4.38), it emerges that in our model

$$\begin{aligned} f(z) = {} & \frac{1}{6}\rho_{\mathrm{m},0}\left[\left(2-(1+\alpha')^2\right)(1+z)^3\right] \\ & - \frac{1}{6}\rho_{\mathrm{m},0}\sqrt{-4\alpha'^2 + \left[(1+\alpha')^2(1+z)^3 - 2\alpha'\right]^2} \\ & + \frac{1}{3}\rho_{\mathrm{m},0}\alpha' \ln\left\{\frac{1}{2}\left[(1+\alpha')^2(1+z)^3 - 2\alpha'\right.\right. \\ & \left.\left. + \sqrt{-4\alpha'^2 + \left[(1+\alpha')^2(1+z)^3 - 2\alpha'\right]^2}\right]\right\}. \end{aligned} \tag{4.46}$$

It is not possible to calculate the redshift, z_*, exactly from (4.46). However, for $\Omega_{\mathrm{m},0} = 0.28$ and $\alpha' = -0.04$, we can numerically calculate that $z_* = 2.29$ for our model (similar to the value $z_* \simeq 2.4$ given in [1]).

Furthermore, [1] suggests that evolving DE models in which Λ, as part of the dark energy, was screened in the past provide a better fit for the BAO data than the ΛCDM model, as well as alleviating the tension discussed in the preceding two sections. It is also noted that in such evolving DE models, the effective EoS of the DE displays a pole at high redshifts. A pole in w_{DE} implies that the energy density of the DE changes sign at that redshift value. This behavior of the DE is also discussed in another study [106] by the BOSS collaboration using the BBAO, SN and Planck data sets. In the next section, we will investigate the EMLG model from this perspective.

4.4.3 Effective dynamical dark energy

In order to test our model in light of the above discussion, we reconstruct the model by defining an effective DE by rewriting (4.35) and (4.36) in the following form:

$$3H^2 = \rho_{\mathrm{m},0}(1+z)^3 + \rho_{\mathrm{DE}}, \tag{4.47}$$

$$-2\dot{H} - 3H^2 = p_{\mathrm{DE}}. \tag{4.48}$$

Thus, the energy density and pressure of the effective DE are given by

$$\begin{aligned}\rho_{\mathrm{DE}} =& \rho_{\mathrm{m}} + \alpha'\rho_{\mathrm{m},0}\left[1 - \ln\left(\rho_{\mathrm{m}}/\rho_{\mathrm{m},0}\right)\right] \\ & - \rho_{\mathrm{m},0}(1+z)^3 + \Lambda,\end{aligned} \tag{4.49}$$

$$p_{\mathrm{DE}} = \alpha'\rho_{\mathrm{m},0}\ln\left(\rho_{\mathrm{m}}/\rho_{\mathrm{m},0}\right) - \Lambda. \tag{4.50}$$

Next, using (4.38) in these equations we obtain ρ_{DE} and p_{DE} as follows;

$$\begin{aligned}\rho_{\mathrm{DE}} =& \frac{1}{2}\rho_{\mathrm{m},0}\left\{\left[(1+\alpha')^2 - 2\right](1+z)^3\right. \\ & \left. + \sqrt{-4\alpha'^2 + \left[(1+\alpha')^2(1+z)^3 - 2\alpha'\right]^2}\right\} \\ & - \alpha'\rho_{\mathrm{m},0}\ln\left\{\frac{1}{2}\left[(1+\alpha')^2(1+z)^3 - 2\alpha'\right.\right. \\ & \left.\left. + \sqrt{-4\alpha'^2 + \left[(1+\alpha')^2(1+z)^3 - 2\alpha'\right]^2}\right]\right\} + \Lambda,\end{aligned} \tag{4.51}$$

$$\begin{aligned}p_{\mathrm{DE}} =& \alpha'\rho_{\mathrm{m},0}\ln\left\{\frac{1}{2}\left[(1+\alpha')^2(1+z)^3 - 2\alpha'\right.\right. \\ & \left.\left. + \sqrt{-4\alpha'^2 + \left[(1+\alpha')^2(1+z)^3 - 2\alpha'\right]^2}\right]\right\} - \Lambda.\end{aligned} \tag{4.52}$$

The corresponding EoS parameter $w_{\mathrm{DE}} = \frac{p_{\mathrm{DE}}}{\rho_{\mathrm{DE}}}$ is

$$\begin{aligned}w_{\mathrm{DE}} =& -1 + \left\{\rho_{\mathrm{m}} - \rho_{\mathrm{m},0}(1+z)^3 + \alpha'\rho_{\mathrm{m},0}\right\}/ \\ & \left\{\rho_{\mathrm{m}} - \rho_{\mathrm{m},0}(1+z)^3\right. \\ & \left. + \alpha'\rho_{\mathrm{m},0}\left[1 - \ln\left(\rho_{\mathrm{m}}/\rho_{\mathrm{m},0}\right)\right] + \Lambda\right\}.\end{aligned} \tag{4.53}$$

Defining the density parameter of the effective dark energy for today as $\Omega_{\rm DE,0} = \frac{\rho_{\rm DE,0}}{3H_0^2}$, (4.53) together with (4.38) and (4.49) gives

$$\begin{aligned} w_{\rm DE} = &-1 + (1-\Omega_{\rm DE,0})\Bigg[\Big((1+\alpha')^2 - 2\Big)(1+z)^3 \\ &+ \sqrt{-4\alpha'^2 + \left[(1+\alpha')^2(1+z)^3 - 2\alpha'\right]^2}\Bigg] \Bigg/ \\ &\Bigg\{(1-\Omega_{\rm DE,0})\Bigg\{\Big[(1+\alpha')^2 - 2\Big](1+z)^3 - 2\alpha' \\ &+ \sqrt{-4\alpha'^2 + \left[(1+\alpha')^2(1+z)^3 - 2\alpha'\right]^2} \\ &- 2\alpha' \ln\left(\frac{1}{2}\Bigg[(1+\alpha')^2(1+z)^3 - 2\alpha' \right. \\ &\left. + \sqrt{-4\alpha'^2 + \left[(1+\alpha')^2(1+z)^3 - 2\alpha'\right]^2}\Bigg]\right)\Bigg\} \\ &+ 2\Omega_{\rm DE,0}\Bigg\}, \end{aligned} \tag{4.54}$$

where we have used the fact that $\Omega_{\rm m,0} + \Omega_{\rm DE,0} = 1$. The present-day value of the EoS parameter of the effective DE is

$$w_{\rm DE,0} = -1 + \alpha' \frac{1-\Omega_{\rm DE,0}}{\Omega_{\rm DE,0}}. \tag{4.55}$$

We note that it lies in the 'phantom' region ($w < -1$) for $\alpha' < 0$. Specifically, $w_{\rm DE,0} = -1.0156$ for $\alpha' = -0.04$ and $\Omega_{\rm DE,0} = 0.72$. This is consistent with the current bounds on $w_{DE,0}$ from the Planck collaboration observations, which has found $w_{DE,0} = -1.028 \pm 0.032$ [12].

As may be seen from (4.54), the model reduces to ΛCDM for $\alpha' = 0$ giving $w_{\rm DE} = w_{\rm DE,0} = -1$. We now plot illustrative figures by using $\Omega_{\rm m,0} = 0.28$ and $\alpha' = -0.04$. With these values, we see from (4.51) that $\rho_{\rm DE} = 0$ at $z = 2.29$. In accordance with the arguments in [1], within the effective DE source interpretation of our model, Λ is screened at the redshift $z_* = 2.29$ and the effective EoS of the DE exhibits a pole at the same redshift (which is very similar to the estimate $z_* \simeq 2.4$ made in [1]). We depict the pole of $w_{\rm DE}$ at $z = 2.29$ in Fig.4.3, which is due to $\rho_{\rm DE}$ changing sign at that redshift, as can be seen from Fig.4.4. Note that Fig.4.4 shows clearly that the sign change at $z = 2.29$ is in agreement with Fig.11 of [106] revealing that $\rho_{\rm DE}$ passes below zero at a redshift in the interval $1.6 \leq z \leq 3.0$. We also display,

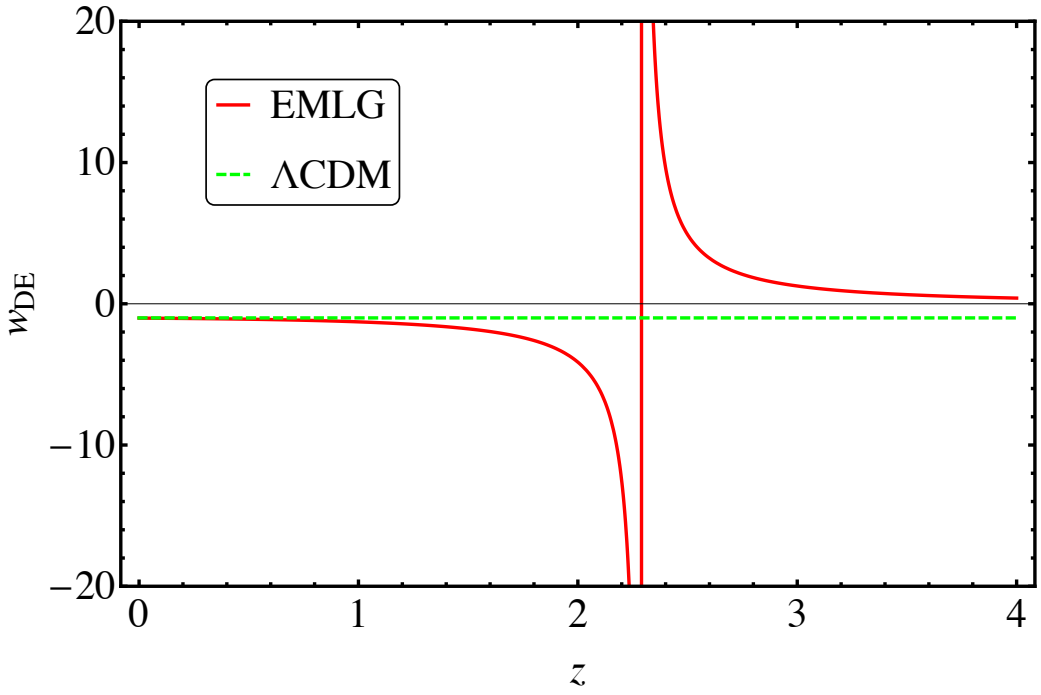

Fig. 4.3 w_{DE} versus z graphs of the EMLG and ΛCDM. Plotted by using $\Omega_{m,0} = 0.28$ and $\alpha' = -0.04$. $|w_{DE}| \to \infty$ at $z = 2.29$ in EMLG.

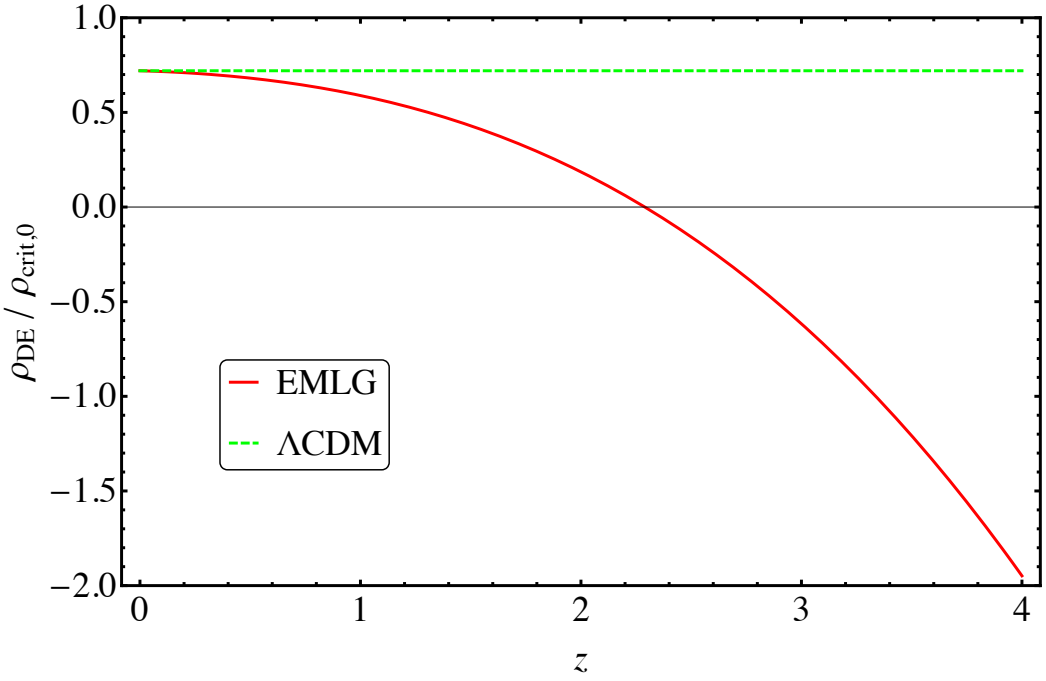

Fig. 4.4 $\rho_{DE}/\rho_{crit,0}$ versus z graphs of the EMLG and ΛCDM. Plotted by using $\Omega_{m,0} = 0.28$ and $\alpha' = -0.04$.

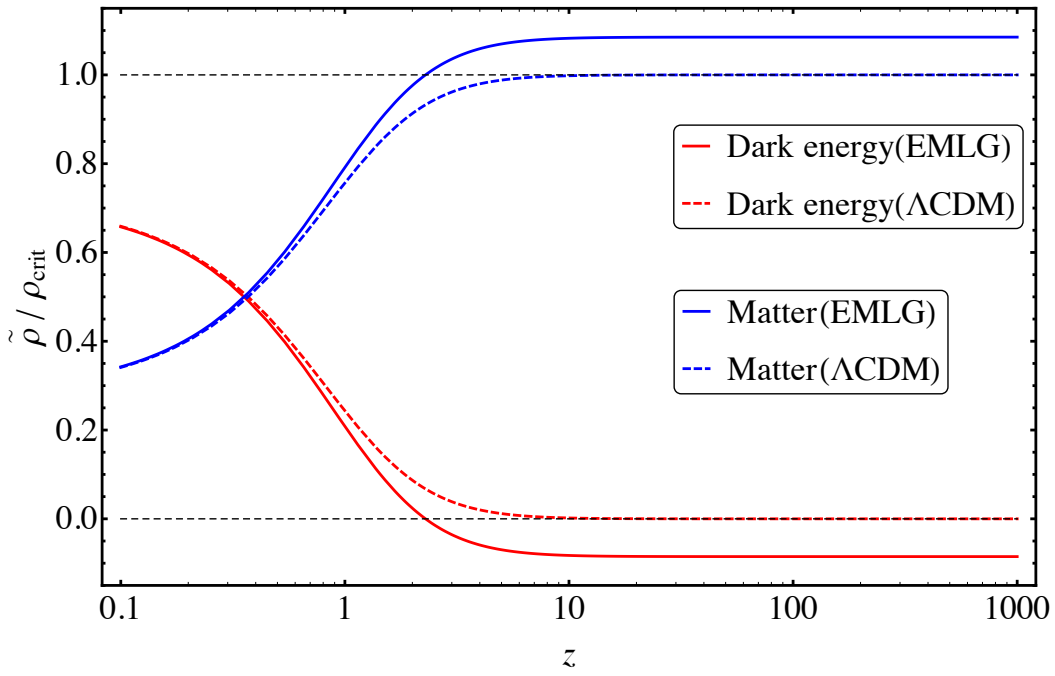

Fig. 4.5 Density parameters (shown as $\tilde{\rho}/\rho_{\rm crit}$) vs. z graphs of the EMLG and ΛCDM for dust and effective dark energy. Here $\tilde{\rho} = \rho_{\rm m,0}(1+z)^3$ for matter and $\tilde{\rho} = \rho_{\rm DE}$ for effective dark energy. Plotted by using $\Omega_{\rm m,0} = 0.28$ and $\alpha' = -0.04$.

both for the EMLG and ΛCDM models, the density parameters of dust, $\Omega_{\rm m} = \rho_{\rm m}/3H^2$, and the effective DE, $\Omega_{\rm DE} = \rho_{\rm DE}/3H^2$, ($\Omega_\Lambda = \rho_\Lambda/3H^2$ for the ΛCDM model) up to $z = 1100$ in Fig. 4.5. Note that the density parameters are the same for $z = 0$ and do not differ much for low redshifts. For large redshifts, in contrast, the unusual behavior of the EMLG model emerges, so that $\Omega_{\rm m}$ becomes equal to unity at $z = z_* = 2.29$ (at $z \to \infty$ for the ΛCDM model) and then settles in a plateau larger than unity for $z > z_* = 2.29$, which results from $\rho_{\rm DE}$ becoming negative at $z = z_* = 2.29$.

Next we calculate two important kinematical parameters that are of interest in cosmology in order to compare different models. Firstly, we calculate the deceleration parameter, $q = -1 - \frac{\dot{H}}{H^2}$, as

$$q = -1 + \frac{3}{2}\,\frac{\Omega_{\rm m,0}\left[(\rho_{\rm m}/\rho_{\rm m,0}) + \alpha'\right]}{1 - \Omega_{\rm m,0}\left[1 - (\rho_{\rm m}/\rho_{\rm m,0}) + \alpha' \ln(\rho_{\rm m}/\rho_{m,0})\right]}, \tag{4.56}$$

which can be written in terms of redshift, by using (4.38), as

$$\begin{aligned} q =& -1+\frac{3}{4}\Omega_{\mathrm{m},0}\Big[(1+\alpha')^2(1+z)^3 \\ &+\sqrt{-4\alpha'^2+\left[(1+\alpha')^2(1+z)^3-2\alpha'\right]^2}\Big]\Big/ \\ &\Big\{1-\Omega_{\mathrm{m},0}\Big\{1-\frac{1}{2}\Big[(1+\alpha')^2(1+z)^3-2\alpha' \\ &+\sqrt{-4\alpha'^2+\left[(1+\alpha')^2(1+z)^3-2\alpha'\right]^2}\Big]\Big\} \\ &+\alpha'\ln\Big\{\frac{1}{2}\Big[(1+\alpha')^2(1+z)^3-2\alpha' \\ &+\sqrt{-4\alpha'^2+\left[(1+\alpha')^2(1+z)^3-2\alpha'\right]^2}\Big]\Big\}\Big\}. \end{aligned} \tag{4.57}$$

Setting $\alpha'=0$ recovers the expression for these parameters in ΛCDM. We note that $q\to -1$ as $z\to -1$, implying that our model asymptotically approaches ΛCDM in the far future. For large redshifts, $z\gg 1$, in (4.56) the deceleration parameter of the dust dominated era in ΛCDM, $q=1/2$, is recovered. Calculating the current value of the deceleration parameter, we find $q_0=-1+\frac{3}{2}\Omega_{\mathrm{m},0}(1+\alpha')$. As can be seen in the top panel of Fig.4.6, the accelerated expansion begins at $z_{\mathrm{tr}}\approx 0.79$ and the present time value of the deceleration parameter is $q_0=-0.60$, whereas these are $z_{\mathrm{tr}}\approx 0.73$ and $q_0=-0.58$ for ΛCDM model. Secondly, we calculate the jerk parameter $j=\frac{\dddot{a}}{aH^3}$, which was discussed in Sec. 4.4 and, as mentioned, is simply equal to unity for ΛCDM (ommiting radiation). In contrast, for EMLG j is dynamical and is given by

$$\begin{aligned} j =& \Big\{\alpha'\rho_0\Omega_0(1+z)^2\rho_z^2-\alpha'\rho_0\Omega_0(1+z)\rho\Big[(1+z)\rho_{zz} \\ &-2\rho_z\Big]+\rho^2\Big[\Omega_0(1+z)\Big((1+z)\rho_{zz}-2\rho_z\Big) \\ &-2\rho_0\Big(\alpha'\Omega_0\ln\left(\rho/\rho_0\right)+\Omega_0-1\Big)\Big]+2\Omega_0\rho^3\Big\}\Big/ \\ &\Big\{2\rho^2\Big[\Omega_0\rho-\rho_0\Big(\alpha'\Omega_0\ln\left(\rho/\rho_0\right)+\Omega_0-1\Big)\Big]\Big\}, \end{aligned} \tag{4.58}$$

where we have written $\rho=\rho_{\mathrm{m}}(z)$, $\Omega_0=\Omega_{m,0}$, and a subscript of z denotes differentiation with respect to redshift. The explicit expression in terms of redshift can be obtained by substituting $\rho_{\mathrm{m}}(z)$ from (4.38), which we do not provide explicitly for reasons of brevity.

$j(z)$ is then depicted in the lower panel of Fig.4.6 which illustrates the dynamical nature of the jerk parameter in EMLG. It deviates from unity at $z \sim 0$ but we have $j \to 1$ in both limits as either $z \to \infty$ or $z \to -1$, hence EMLG recovers the kinematics of ΛCDM both at early times, and in the far future.

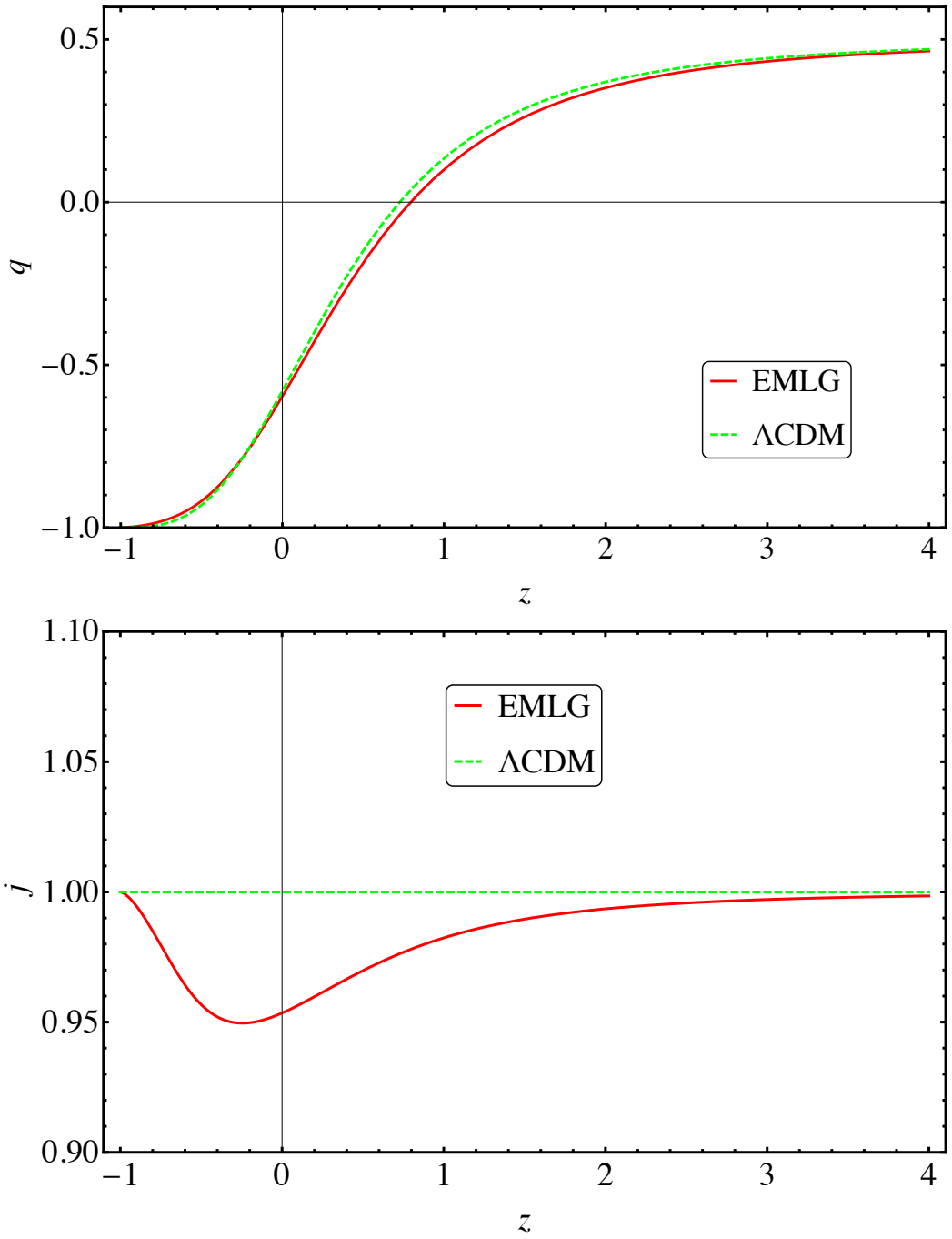

Fig. 4.6 $q(z)$ vs. z **(upper panel)** and $j(z)$ vs. z **(lower panel)** graphs of the EMLG and ΛCDM. Plotted by using $\Omega_{\mathrm{m},0} = 0.28$, $H_0 = 70\,\mathrm{km\,s^{-1}Mpc^{-1}}$ and $\alpha' = -0.04$.

4.4.4 Screening of Λ by the non-conservation of dust

In Section 4.4.3, we rearranged the original field equations of the EMLG model, (4.35) and (4.36), in order to compare with the model first described in [1]. For this comparison, we assumed that the energy density of the dust behaves as in GR, $\rho_{\rm m} \propto (1+z)^3$, and then compensated it as a part of the effective DE (4.47). In other words, we assume that all of the terms with α', including those coming from the true matter energy density (4.38) of EMLG, contribute to the energy density of the effective DE. Through this comparison, we have determined the parameter of our model, α', with which EMLG relaxes the issues of the ΛCDM model stated in [1].

We now examine the actual behavior of dust in EMLG. The energy density of dust in EMLG is given by (4.38) and includes terms with the EMLG modification parameter α'. Furthermore, we have new terms with α' in the original field equations, (4.35) and (4.36), arising due to the EMLG modification to GR. As a result, both the energy density of dust and the forms of the energy density and pressure equations of our model differ from those of GR. Consequently, we find it useful to depict, in Fig. 4.7, the redshift dependency of the density parameters corresponding to the components of the energy density equation (4.35). To do so, we define $\Omega_{\rm m} = \rho_{\rm m}/3H^2$ (red) for dust, $\Omega_\Lambda = \Lambda/3H^2$ (yellow) for Λ and $\Omega_{\rm X} = [\alpha'\rho_{\rm m,0} - \alpha'\rho_{\rm m,0}\ln(\rho_{\rm m}/\rho_{\rm m,0})]/3H^2$ (green) for the new terms which arise due to the EMLG modification. We use $\Omega_{\rm m,0} = 0.28$, $H_0 = 70\,{\rm km\,s^{-1}Mpc^{-1}}$ and $\alpha' = -0.04$, the same values used in previous sections. We note the small and non-monotonic contribution from $\Omega_{\rm X}$ in (4.35).

For a better view, we depict $\Omega_{\rm X}(z)$ separately in Fig. 4.8. This figure is of particular interest since it reveals an important point about the model under consideration; that the contribution from $\Omega_{\rm X}$ is negative at low redshifts, positive at $z \sim 1$ and then, whilst remaining positive, asymptotically approaches zero at larger redshifts. This means that $\Omega_{\rm X}$, due to the EMLG modification, screens Λ only at low redshifts in contrast to the arguments given in [1]. On the other hand, within the effective DE source interpretation of our model in line with [1, 106], we have already shown that $\rho_{\rm DE}$ is positive at low redshifts and passes below zero at $z = 2.29$ exactly as suggested in [1, 106]. This implies that the feature of screening Λ in the EMLG model does not arise from the new type of contributions of dust on the right-hand side of (4.35) which appear as an effective source with constant inertial mass density as $\rho' + p' = \alpha'\rho_{\rm m,0}$ (see 4.3.1), but

instead from the altered redshift dependency of ρ_{m} due to the non-conservation of the EMT in the EMLG model.

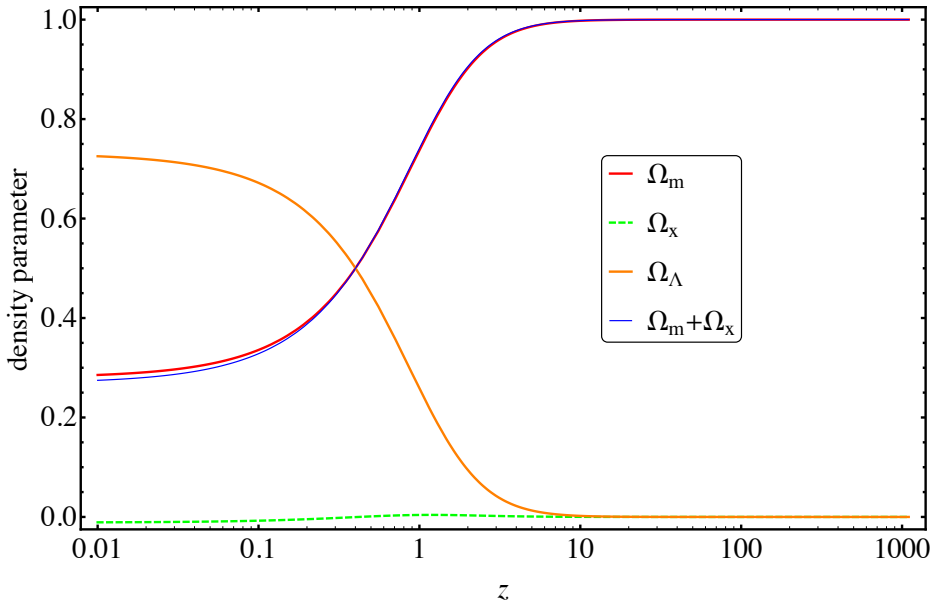

Fig. 4.7 Ω vs. z graphs of the EMLG for matter (Ω_{m}), modification terms (Ω_x), cosmological constant (Ω_Λ) and matter+modification ($\Omega_m + \Omega_x$). Plotted by using $\Omega_{\mathrm{m},0} = 0.28$, $H_0 = 70\,\mathrm{km\,s^{-1}Mpc^{-1}}$ and $\alpha' = -0.04$.

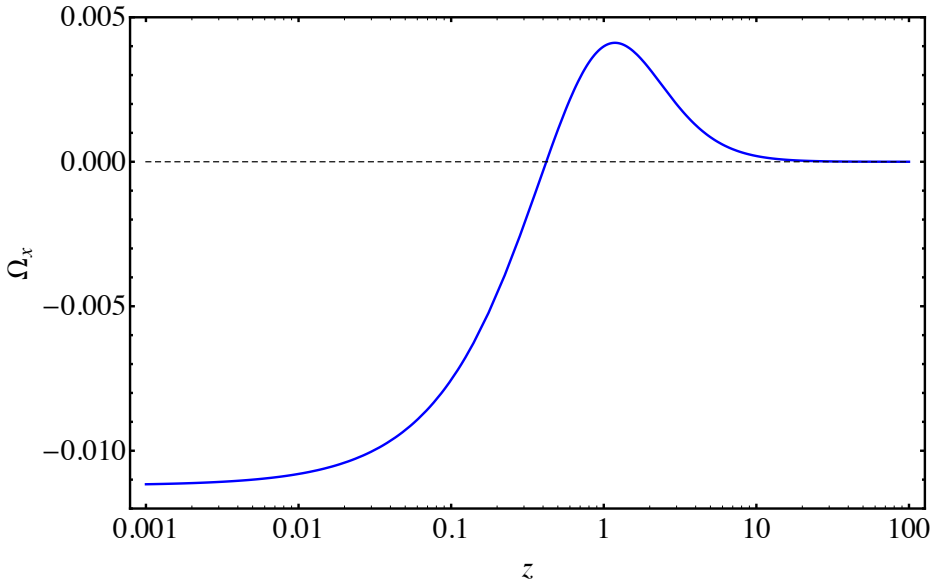

Fig. 4.8 The density parameter of modification terms (Ω_x) vs. z graph of the EMLG. Plotted by using $\Omega_{\mathrm{m},0} = 0.28$, $H_0 = 70\,\mathrm{km\,s^{-1}Mpc^{-1}}$ and $\alpha' = -0.04$.

4.4.5 Inclusion of radiation

In order to investigate the implications of our model for the early universe while preserving its agreement with the current data for the late universe, we need to look for solutions in the case that radiation is the second source besides dust. Including both fluids as sources in our model results in complicated field equations including the cross terms of $\rho_{\rm r}$ and $\rho_{\rm m}$ which make exact solutions impossible. On the other hand, if we use the same $\alpha' = -0.04$ value which corresponds to $\alpha = -0.02\rho_{m,0}$ for radiation, it remains outside today's viability interval (4.26) as we know from observations that $\rho_{m,0}/\rho_{r,0} \sim 10^3$. This arises from the fact that the interval (4.26) is valid only for a mono-fluid universe. We would need to decrease the absolute value $|\alpha|$ to find viable cosmological solutions when our model contains radiation as well. However, this would result in compromising the goodness of fit of our model with the latest data compared to that of ΛCDM for the late-time accelerated expansion of the universe. Thus, we conclude that it does not seem possible to expand our model by both adding radiation and preserving the features we have been discussing so far when there is only one α parameter involving in both sources.

A recent study [132] shows that different sources can couple to gravity in different ways for a particular example of $f(T_{\mu\nu}T^{\mu\nu})$ modification. One can follow the same idea in EMLG. Namely, the model can be constructed using different α parameters for different types of sources which means that different gravitational couplings occur for each source. To do so, one can start with a modification term as follows

$$f(T_{\mu\nu}T^{\mu\nu}) = \sum_i \alpha_i \ln(\lambda_i T^{(i)}_{\mu\nu} T^{\mu\nu}_{(i)}), \tag{4.59}$$

where α_i (the coupling parameter) and λ_i are the constants for i^{th} fluid. Note that the sum over i in (4.59) evades the issue of cross terms occurring in the case of more than one fluid. However, the number of free parameters is increased. To relax this issue, fluids can be separated as conventional sources, such as radiation (γ, ν) or baryons (b), and dark sector/unknown sources like cold dark matter. Then, one can assume that known sources couple to gravity according to GR, that is the corresponding α_i's are zero, whilst dark sector/unknown sources couple in accordance with the modified

theory [132]. With this idea, the field equations in EMLG read

$$\begin{aligned} 3H^2 =& \Lambda + \rho_\gamma + \rho_b + \rho_{\rm cdm} \\ &+ \alpha' \rho_{\rm cdm,0} \left[1 - \ln \left(\frac{\rho_{\rm cdm}}{\rho_{\rm cdm,0}} \right) \right], \end{aligned} \tag{4.60}$$

$$-2\dot{H} - 3H^2 = -\Lambda + \frac{\rho_\gamma}{3} + \alpha' \rho_{\rm cdm,0} \ln \left(\frac{\rho_{\rm cdm}}{\rho_{\rm cdm,0}} \right). \tag{4.61}$$

Here $\rho_\gamma \propto (1+z)^4$, $\rho_b \propto (1+z)^3$ as in GR and $\rho_{\rm cdm}$ obeys the modified continuity equation (4.24) when $w = 0$, which gives the energy density solution in (4.38). We reserve such an investigation to our future works.

4.5 Constraints from latest cosmological data

In the preceding sections we have investigated theoretically the EMLG model, particularly in comparison with the studies [1, 106]. For convenience, we assumed the values of the Hubble constant and dust density parameter as used in [1] and took a value of the coupling parameter of the EMLG modification so as to produce results similar to those discussed in [1]. In this section we analyse the constraints on the parameters of the EMLG model from the latest observational data and discuss the model further. In order to explore the parameter space, we make use of a modified version of a simple and fast Markov Chain Monte Carlo (MCMC) code, named SimpleMC [150, 106], that computes expansion rates and distances using the Friedmann equation. The code uses a compressed version of a recent reanalysis of Type Ia supernova (SN) data, and high-precision Baryon Acoustic Oscillation measurements (BAO) at different redshifts with $z < 2.36$ [106]. We also include a collection of currently available $H(z)$ measurements (CC), see [151] and references therein. For an extended review of cosmological parameter inference see [152]. Table 4.1 displays the parameters used throughout this chapter along with the corresponding flat priors. Note that we do not consider CMB data in our analysis, because the current EMLG model does not contain radiation (see Section 4.4.5 for the relevant discussion) and therefore we avoid radiation in the ΛCDM model in order to be able to compare these two models under the same conditions.

We use the dimensionless Hubble parameter $h = H/100\,\mathrm{km\,s^{-1}Mpc^{-1}}$ [153], the physical baryon density $\Omega_b h^2$ and the pressureless matter density (including CDM) $\Omega_{\rm m}$.

Table 4.1 Constraints on the EMLG parameters using the combined datasets BAO+SN+CC. For one-tailed distributions the upper limit 95% CL is given. For two-tailed the 68% is shown. Parameters and ranges of the uniform priors assumed in our analysis. Derived parameters are labeled with *.

Parameter	EMLG	ΛCDM	Priors
$\Omega_{\mathrm{m},0}$	0.2983 ± 0.0185	0.2861 ± 0.0102	[0.05,1.5]
$\Omega_{b,0}h_0^2$	0.02196 ± 0.00045	0.02205 ± 0.00045	[0.02, 0.025]
h_0	0.682 ± 0.021	0.668 ± 0.009	[0.4, 1.0]
α'	-0.032 ± 0.043	[0]	[-1, 1]
$^*w_{\mathrm{DE},0}$	-1.015 ± 0.019	[-1]	
$^*z_*$	2.23 ± 0.81	-	
$-\ln \mathcal{L}_{\max}$	34.22	34.49	–
AIC	76.44	74.98	–

Throughout the analysis we assume flat priors over our sampling parameters: $\Omega_{\mathrm{m},0} = [0.05, 1.5]$ for the pressureless matter density parameter today, $\Omega_{\mathrm{b},0}h_0^2 = [0.02, 0.025]$ for the baryon density parameter today and $h_0 = [0.4, 1.0]$ for the reduced Hubble constant. For the EMLG parameter we assume $\alpha' = [-1, 1]$, which is also the validity interval of our solution, see (4.38).

For simplicity, and noticing the near-gaussianity of the posterior distributions (Fig. 4.9), to perform a model selection we include the Akaike Information Criterion (AIC) [154], defined as:

$$\mathrm{AIC} = -2 \ln \mathcal{L}_{\max} + 2k, \tag{4.62}$$

where the first term incorporates the goodness-of-fit through the likelihood $\mathcal{L}$, and the second term is interpreted as the penalisation factor given by two times the number of parameters (k) of the model. The preferred model is then the one that minimises AIC. A rule of thumb used in the literature is that if the AIC value of a model relative to that of the preferred model $\Delta\mathrm{AIC} \leq 2$, it has substantial support; if $4 \leq \Delta\mathrm{AIC} \leq 7$, it has considerably less support, with respect to the preferred model. A Bayesian model selection applied to the dark-energy equation of state is performed by [100, 104, 103].

Table 4.1 summarizes the observational constraints on the free parameters (as well as the derived parameters, labelled by $*$) of the EMLG model using the combined dataset BAO+SN+CC. For comparison, we also include parameters describing the

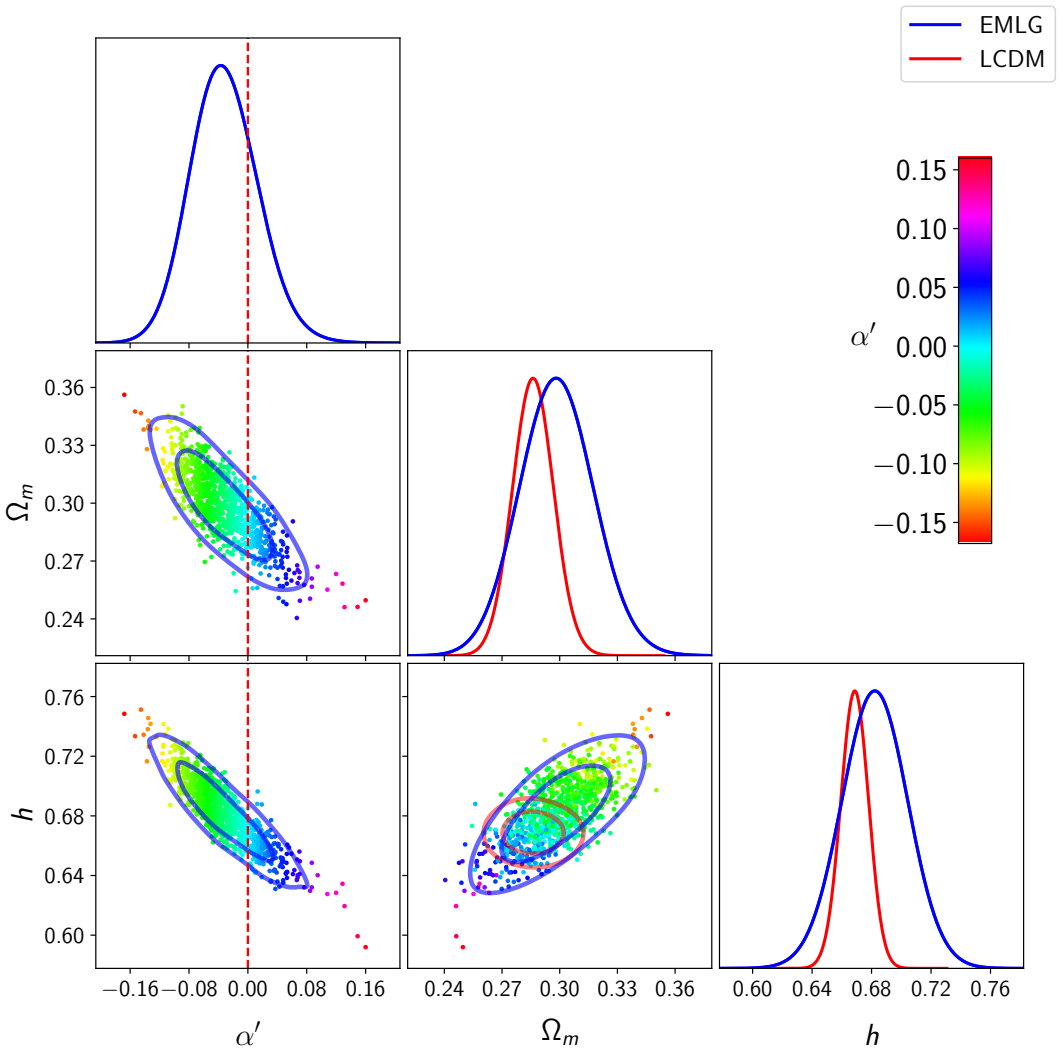

Fig. 4.9 1D and 2D marginalized posterior distributions of the parameters used to describe the EMLG model (blue) and the ΛCDM model (red). Scatter points indicate values of α' labelled by the colour bar, and the vertical line corresponds to the ΛCDM case ($\alpha' = 0$).

ΛCDM model. We notice the EMLG model fits the data slightly better, however EMLG is penalized by the inclusion of the extra parameter α, viz., with $\Delta\text{AIC} = 1.46$, and hence it has evidence to be a good model w.r.t. the ΛCDM model, but the ΛCDM model is slightly preferred over it. Figure 4.9 displays the 1D and 2D marginalized posterior distributions of the parameters used to describe the EMLG model (blue) and the ΛCDM model (red). The inner ellipses show the 68% confidence region, and the outer edges the 95% region. Scatter points indicate values of α' labelled by the colour bar, and the vertical line corresponds to the ΛCDM case ($\alpha' = 0$).

The data constrains the parameter of the EMLG model as $\alpha' = -0.032 \pm 0.043$ at 68 % C.L., which well covers $\alpha' = 0$ (ΛCDM), but prefers slightly negative values. In comparison with the ΛCDM model ($\alpha' = 0$), the preference of the EMLG model for slightly negative values of α' leads to a widening of the 1D posterior distributions of $\Omega_{\rm m,0}$ and h_0 towards larger values, which in turn shifts the peak values of both parameters to larger values as well. Indeed, we see in Table 4.1 that, in comparison with ΛCDM, the EMLG model predicts larger $\Omega_{\rm m,0}$ and h_0 values along with larger errors against the data. The strong anti-correlations on the parameters $\Omega_{\rm m,0}$ and α' and also on the h_0 and α' observed in 2D marginalised posterior distributions for the EMLG are an interesting point to note. These two anti-correlations lead to a correlation on the parameters $\Omega_{\rm m,0}$ and h_0, so that the larger negative values of α' lead to larger values of both of them. In contrast, in ΛCDM there is no noticeable correlation on the parameters $\Omega_{\rm m,0}$ and h_0. These can be observed directly in the $\{\Omega_{\rm m,0}, h_0\}$ panel of the 3D scatter colour Fig.4.9. For the EMLG model, 2D $\{\Omega_{\rm m,0}, h_0\}$ contours exhibit a tilt of about 45 degrees and the more reddish (implying larger negative values of α') corresponds to larger $\Omega_{\rm m,0}$ and h_0 values.

We study the constraints on the $Omh^2(z_i; z_j)$ diagnostic values of the EMLG model using (4.44) for $\{z_1, z_2, z_3\} = \{0, 0.57, 2.34\}$, where the latter two redshift values are chosen in accordance with the BOSS CMASS and Lyman-α forest measurements of $H(z)$, and obtain

$$\begin{aligned} Omh^2(z_1; z_2) &= 0.132 \pm 0.008, \\ Omh^2(z_1; z_3) &= 0.130 \pm 0.006, \quad \text{(EMLG)} \\ Omh^2(z_2; z_3) &= 0.130 \pm 0.006. \end{aligned} \tag{4.63}$$

Using the $\Omega_{\rm m,0}$ and h_0 obtained for the EMLG model in $Omh^2(z_i; z_j) = \Omega_{\rm m,0} h_0^2$ of the ΛCDM model (assuming $\alpha' = 0$) we find a larger value as $Omh^2(z_i; z_j) = 0.139 \pm 0.012$, which clearly shows the reducing effect of $\alpha' < 0$ on the $Omh^2(z_i; z_j)$. On the other hand, for the ΛCDM model, in our analysis the data predict a slightly lower value, with respect to those in the EMLG model, as

$$Omh^2(z_i; z_j) = 0.128 \pm 0.006, \quad \text{(ΛCDM)} \tag{4.64}$$

which results from $h_0 = 0.668 \pm 0.009$ and $\Omega_{\rm m,0} = 0.2861 \pm 0.0102$. Note that this low value for the ΛCDM model is very much consistent with $Omh^2 \approx 0.122 \pm 0.010$ from BOSS CMASS and Lyman-α forest measurements of $H(z)$, which is obtained since we

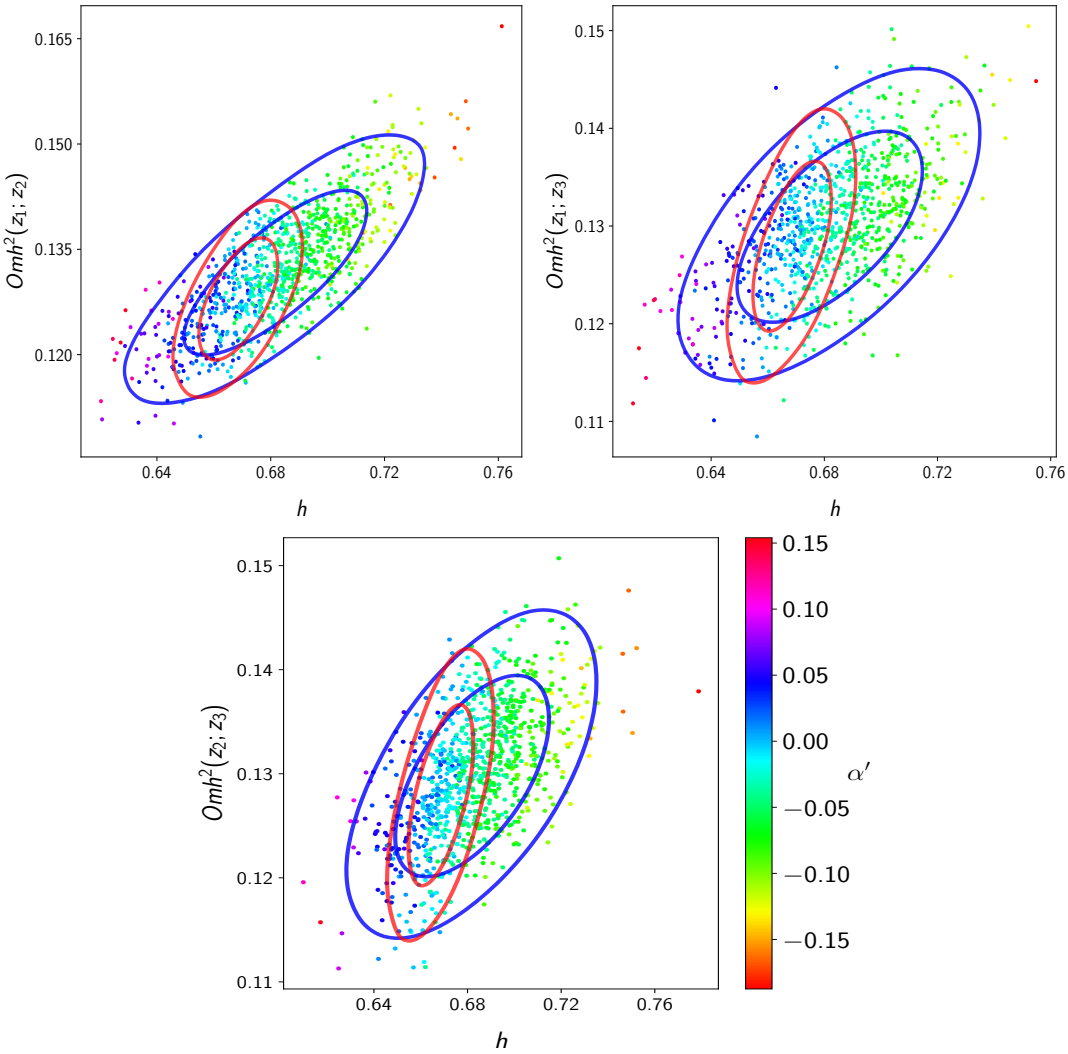

Fig. 4.10 Blue lines and 3D scatter colour plots described the EMLG model marginalised posterior distributions for EMLG parameter α' in the $\{\alpha', Omh^2(z_i; z_j), h_0\}$ subspace for $\{z_1, z_2\}$, $\{z_1, z_3\}$ and $\{z_2, z_3\}$. The colour code indicates the value of α' labeled by the colour bar. Red lines display 2D marginalised posterior distributions for the ΛCDM model.

do not consider CMB data in our analysis. Indeed, the Planck 2018 [96] release gives $\Omega_{\mathrm{m},0}h_0^2 = 0.1430 \pm 0.0011$ from $h_0 = 0.674 \pm 0.005$ and $\Omega_{\mathrm{m},0} = 0.315 \pm 0.007$. This shows that reducing the value of Omh^2 in ΛCDM comes at the cost of reducing $\Omega_{\mathrm{m},0}$ to values in tension with the Planck result, and also of reducing h_0 to values which, whilst consistent with Planck results, exacerbate the persistent tension in the measurement of H_0 between the Planck ΛCDM model and direct measurements from astrophysical data.

In Figure 4.10 we depict 3D scatter colour plots describing the EMLG model marginalised posterior distributions for the EMLG parameter, α', in the $\{\alpha', Omh^2(z_i; z_j), h_0\}$ subspace for $\{z_1, z_2\}$, $\{z_1, z_3\}$ and $\{z_2, z_3\}$. In this figure, we see that the 2D marginalised posterior distributions of $\{Omh^2(z_i; z_j), h_0\}$ for the EMLG model (blue contours) are more tilted than the ones for the ΛCDM model (red contours), implying that a certain increment in h_0 would lead to a lesser increment in $Omh^2(z_i; z_j)$ in the EMLG model compared to in the ΛCDM model, and that larger h_0 values are allowed for a given Omh^2 value provided that α' takes a correspondingly larger negative value, as can be seen from the colour gradient indicating α'. This implies that the EMLG model compensates for the larger values of h_0 by lowering the value of α' and keeps $Omh^2(z_i; z_j)$ at lower values. Whereas, in the ΛCDM model, lowering the value of Omh^2 would lead to low h_0 values (see Table 4.1) which would exacerbate the tension between the Planck ΛCDM model and direct H_0 measurements. Similarly, increasing the value of h_0 would lead to higher Omh^2 values but with the difference that a small increment in h_0 would lead to relatively larger increments in Omh^2 since the red contours for the ΛCDM model are almost vertical. Indeed, for the ΛCDM model, in this study we obtain $Omh^2 \approx 0.128$ along with $h_0 \approx 0.668$, whereas the recent Planck release gives $Omh^2 \approx 0.143$ along with $h_0 \approx 0.674$. Note that the about 1% larger value of h_0 is accompanied by a roughly 10% larger value of Omh^2.

The data predict the following constraints on the Hubble constant along with their errors at the 68% and 95% confidence levels for the EMLG and the ΛCDM models:

$$H_0 = 68.20 \pm 2.13 \pm 4.15 \text{ km s}^{-1} \text{ Mpc}^{-1}, \text{ (EMLG)} \tag{4.65}$$

$$H_0 = 66.86 \pm 0.90 \pm 1.74 \text{ km s}^{-1} \text{ Mpc}^{-1}. \text{ (ΛCDM)} \tag{4.66}$$

In comparison, the most recent distance-ladder estimates of H_0 from the SHOES (SN, H_0, for the equation of state of dark energy) project give $H_0 = 73.24 \pm 1.74 \text{km s}^{-1}\text{Mpc}^{-1}$ [110], $H_0 = 73.48 \pm 1.66 \text{km s}^{-1}\text{Mpc}^{-1}$ [155] and $H_0 = 73.52 \pm 1.62 \text{km s}^{-1}\text{Mpc}^{-1}$, using Gaia parallaxes [156]. We note that, at 68% C.L., H_0 values both from the EMLG model and the ΛCDM model are in tension with these, yet it is worse in the ΛCDM model. Indeed we see that, at 95% C.L., the H_0 of the EMLG model becomes consistent with these results, while the H_0 of the ΛCDM model remains in tension.

The upper panel of Figure 4.11 displays a subset of the BAO measurements (blue bars) from $z = 0$, $z = 0.57$ and $z = 2.34$ (see [106]) with scalings that illustrate their

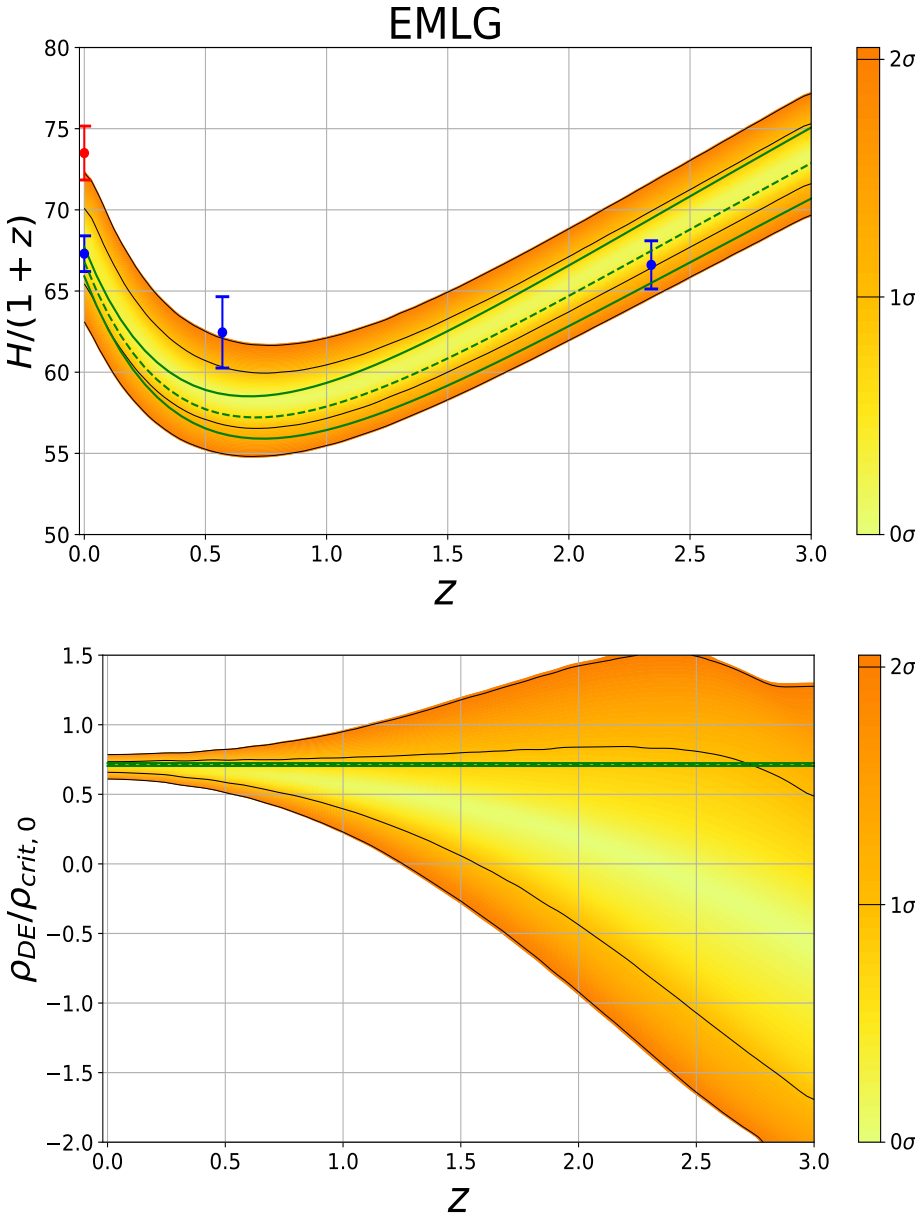

Fig. 4.11 **(Top panel)** $H(z)/(1+z)$ vs. z graph of the EMLG. **(Bottom panel)** $\rho_{\rm DE}/\rho_{\rm crit,0}$ vs. z graph of the EMLG. For both panels, these show the posterior probability $\Pr(g|z)$: the probability of g as normalised in each slice of constant z, with colour scale in confidence interval values. The 1σ and 2σ confidence intervals are plotted as black lines. Green lines display best-fit values (dotted line) and 1σ contour levels for the ΛCDM model.

physical content along with the distance-ladder estimate of H_0, the direct observational value (red bar) given in [155], and the plot of the posterior probability of $H(z)/(1+z)$, which is the proper velocity between two objects with a constant comoving separation of 1 Mpc, for the EMLG model. We note that the strip (yellow) of $H(z)/(1+z)$ for the EMLG model is consistent with all three BAO data at 1σ C.L. (though, marginally

with the data from $z = 0.57$), whereas it is in tension with the distance-ladder estimate of H_0 at 1σ but marginally consistent with it at 2σ C.L. These indeed are considerable improvement with respect to the ΛCDM model (green lines displaying the best-fit value (dotted line) and 1σ contour levels in the same figure) which is inconsistent with both the BAO data from $z = 0.57$ and the the distance-ladder estimate of H_0 even at 2σ C.L. [4]

The lower panel of Figure 4.11 shows the probability distribution (yellow tones) of the redshift dependency of the energy density of the effective DE scaled to the critical energy density of the present time Universe, viz., $\rho_{\rm DE}/\rho_{\rm crit,0}$, within 1σ and 2σ confidence levels for the EMLG model. Whereas the thin green strip in the panel is for the ΛCDM model at 1σ C.L.. We see that the effective DE achieves negative values after few redshifts, namely, we obtain $\rho_{\rm DE} = 0$ at $z_* = 2.23 \pm 0.81$ at 1σ C.L.. It is noteworthy that this value is in line with that in the BOSS collaboration paper [106] estimating DE with a negative energy density for $z > 1.6$ and paper [1] suggesting that cosmological models providing effective DE yielding signature change at $z \sim 2.4$ to obtain, from the model, Omh^2 values consistent with the model-independent estimations.

4.6 Conclusions

We have introduced a new model of Energy-Momentum Squared Gravity, which we call Energy-Momentum Log Gravity (EMLG). It is constructed by the addition of $f(T_{\mu\nu}T^{\mu\nu}) = \alpha \ln(\lambda\, T_{\mu\nu}T^{\mu\nu})$, envisaged as correction, to the standard Einstein-Hilbert action with cosmological constant Λ. We have studied the cosmological solutions of the Friedmann metric that arise from the field equations for this theory of gravitation. Using these solutions we then conducted an investigation into the ways in which the EMLG extension to ΛCDM addresses the tensions between existing data sets that beset the standard ΛCDM model. Among the tensions of various degrees of significance reported in the literature, we have focused on the ones discussed in [106, 1], which result from the Lyman-α forest measurement of BAO at $z \sim 2.3$ by the BOSS collaboration [111]. It has been argued that this tension can be alleviated in a physically motivated

[4]Note that in our case ΛCDM is in tension with the BAO data from $z = 0.57$ whereas it is consistent with the one from $z = 2.34$ in BOSS [106] and Planck [96]. The reason being that in our analysis we didn't consider the data from CMB since we omitted radiation in our models.

way through a modified gravity theory, rather than as a pure physical DE source within GR [1], since it requires a DE yielding negative energy density values at high redshifts [106, 1].

EMLG allows us to find an explicit exact solution for the dust density, $\rho_{\rm m}(z)$, and thus of $H(z)$ and $\rho_{\rm DE}(z)$ (effective DE), which has allowed us to conduct a detailed theoretical and observational investigation of the model without introducing further simplifications. Following this, upon setting $\Omega_{\rm m,0} = 0.28$ and $h_0 = 0.70$ for both models, we demonstrate analytically that EMLG with $\alpha' = -0.04$ produces effective DE behaving as suggested in [106, 1] and predicts Omh^2 diagnostic values consistent with the model-independent value from observations [1], whereas the value predicted by ΛCDM exhibits a significant tension with the model-independent value. We have constrained both models against the latest observational data from the combined dataset BAO+SN+CC and then discussed the improvements due to the EMLG modification. It emerges that the data does not rule out the ΛCDM limit of the model ($\alpha' = 0$), but prefers slightly negative values of the EMLG model parameter ($\alpha' = -0.032 \pm 0.043$), which leads to an effective DE indistinguishable from positive Λ at low redshifts but results in negative energy density values (i.e., screening of Λ) for redshift values larger than $z \sim 2.2$, in line with the arguments developed in [106, 1] for alleviating the tensions relevant to Lyman-α data. We concluded that this feature of the effective DE from the EMLG modification to ΛCDM arises from the altered redshift dependency of $\rho_{\rm m}$ due to its non-conservation in this model, not from the new type of contributions of it on the right-hand side of the Friedmann equation (4.35), which yields an effective EoS of a source with constant inertial mass density. We observe further that the EMLG model does this without lowering the values of $\Omega_{\rm m,0}$ and H_0 compared to the results from Planck [95, 96], and moreover relieves, at some level, the persistent tension with the measurements of H_0 within the standard ΛCDM model. In the case of ΛCDM, on the other hand, we observed that Omh^2 reduces to values consistent with the model independent value, since we did not consider CMB data in our observational analyses, but it happens at the cost of reducing $\Omega_{\rm m,0}$ to values in tension with the Planck result, and also of reducing H_0 to values which exacerbate the persistent tension in the measurement of H_0.

We see that although our findings are promising in favor of alleviating the tensions considered in this study, they are not yet conclusive. The reason for this is that we have studied only single fluid cosmology, that is we have considered only dust as the material

source and excluded the presence of radiation in our model, and equally in ΛCDM in order to conduct a fair comparison between the models. In order to confirm these initial results, the current study must be extended by the inclusion of radiation together with dust, and then can also be constrained by considering the CMB data along with the other data sets. We have discussed the difficulties of introducing radiation, either by itself or as the second source, in our model and noted a possible way of achieving this, which we reserve for our future works. Finally, we conclude that the current study demonstrates that, through our particular model, EMLG, Energy-Momentum Squared Gravity type extensions to ΛCDM model are capable of addressing some of the prominent tensions which beset ΛCDM and merit further investigation.

We would like to close the chapter with the following remarks. Our initial motivation for considering $f(T_{\mu\nu}T^{\mu\nu}) \propto \ln(\lambda\, T_{\mu\nu}T^{\mu\nu})$ was phenomenological, as gives rise to new contributions by dust on the right-hand side of the Einstein field equations which mimic a source with constant inertial mass density. The corresponding energy density could then change sign at high redshifts as has been suggested for addressing the tension relevant the Lyman-α measurements within the standard ΛCDM model, although it emerged that our model was able to do so because of the modified redshift dependency of dust due to the non-conservation of energy-momentum tensor. Our model is also expedient as it provides us with an explicit exact solution. On the other hand, one may question the microphysical motivation for such a term; in particular, whether there is a way of realising such a term in the action within a particular field theoretical model that leads to the energy-momentum tensor. For example, naively substituting $T_{\mu\nu}$ with the energy momentum tensor of a scalar field would lead to a quite non-standard (and probably non-analytic) action, which in turn would raise questions about a consistent quantization procedure, the consistency of the corresponding effective field theory, and so on. However, the current work's primary aim is to highlight the model's cosmological signatures, and in that sense, the work presented here can be understood as a phenomenological contribution to exploring the scope of possibilities. It would be interesting to look for a potential origin of this modification in a theory of fundamental physics and see whether some relationship as between the EMSG of the form $f(T^2) \propto T^2$ [47, 62, 131, 73] and loop quantum gravity [124, 125] as well as braneworld scenarios [75], all of which add quadratic contributions of the matter stresses' energy density to the Friedmann equation, could be found.

Chapter 5

Conclusions

In this thesis we have investigated various matter models in a Cosmological setting, which exhibit unusual behaviour compared to more standard models, in order to explore ways in which they might be able to resolve outstanding problems in the standard Cosmological model.

In Chapter 2 we considered a canonical scalar field acting in a potential, and investigated the characteristics of potentials that exhibit a particular kind of very weak singularity, known as a sudden singularity. Unlike stronger types of cosmological singularity, sudden singularities are not characterised by the divergence of the scale factor itself, but rather by the scale factor remaining finite whilst its second or higher derivative diverges. This type of singularity had previously been found to occur in the case of a canonical scalar field acting in the simple power-law potential $V(\phi) = \phi^n$ for n positive, but non-integer [58]. In this case the singularity arises because the first or higher derivative of the potential contains a singularity at $\phi = 0$, and it is possible to show that necessarily $\phi \to 0$ in finite time.

We extended the range of potentials known to exhibit this behaviour by considering which general properties are sufficient for the potential to manifest a sudden singularity. In particular, we found that if $V(\phi) > 0$ and $V'(\phi) > 0$ for $\phi > 0$, whilst $V'(\phi)$ also has at most finitely many stationary points, then $\dot{\phi}$ must become, and remain, negative after some finite time. If we place the further condition that $V'(\phi)$ must in fact be decreasing after some finite time, then this suffices to show that $\phi \to 0$ in finite time and hence a sudden singularity occurs. One example of potentials that satisfy these conditions are those of the form $V(\phi) = \tanh \phi^n$ for $0 < n < 1$, which is an increasing

function of ϕ with decreasing gradient. This is of relevance because this resembles potentials in the popular α-attractor family of observationally-favoured inflationary models. This provides models in this family with a potential mechanism for exiting inflation in a finite time, without the need for a necessarily highly physically destructive process. In future it would be of great interest to continue to investigate these models, in at least two directions. Firstly, to continue to expand the range of potentials known to feature sudden singularities - we have found some sufficient conditions, but these potentials by no means exhaust the possibilities. Secondly, continuing to investigate the physical behaviour encountered as the scalar field reaches the sudden singularity should provide further insight into their relevance for providing an exit from the inflationary regime.

In Chapter 3 we investigated a modification of General Relativity known as $F(R, T^{\mu\nu}T_{\mu\nu})$, or energy-momentum squared, gravity, in which the Ricci Scalar in the Einstein-Hilbert action is replaced by an arbitrary function of the Ricci Scalar and the square of the energy momentum tensor. This modification is part of a class of theories which modify general relativity by adding higher order matter contributions to the gravitational field equations. In particular, we investigated the cosmological phenomonology of a simple form of the modification $F(R, T^{\mu\nu}T_{\mu\nu}) = R + \eta(T^{\mu\nu}T_{\mu\nu})^n$, which in the cosmological setting results in the addition of terms of order $\rho^2 n$ to the right-hand side of the Friedmann equations.

We found a range of exact solutions for the cosmology in an isotropic universe, and in the $n = 1$ case, where the modifications become quadratic, we were able to find exact solutions in the physically relevant cases $w = -1$, dark energy, $w = -\frac{1}{3}$ curvature, $w = 0$ dust, and $w = \frac{1}{3}$ radiation. We also considered the case of constant density, de Sitter-like solutions with exponential expansion, and found that, as well as the standard $w = -1$ case, the modified theory exhibited another family of solutions, depending on the equation of state parameter w. We investigated the stability of these solutions under a homogeneous linear perturbation about the constant density solution, and found that for some values of the equation of state, these solutions were stable. By invetigating the high density behaviour of the $n = 1$ case we found that in some situations for non-negative curvature the modifications result in a maximum possible energy density depending on the values of η and w, meaning that the initial singularity of the big bang model is replaced by a 'bounce' at which only finite energy density is reached. Finally, we considered the anisotropic case of Bianchi I universes, and found

conditions for the initial singularity to be either isotropic or anisotropic. In future, the most important next steps in the study of Energy-Momentum Squared Gravity are to investigate which regions of the parameter space are permitted by observational considerations. The higher order matter terms will cause changes from the standard thermal history which would alter elemental abundances from big bang nucleosynthesis, as well as alterations to the CMB power spectrum. We'd also expect to see effects on the behaviour of astrophysical objects, such as the formation of galactic halos and the behaviour of compact objects such as stars. Using these observational tests it would be possible to determine whether EMSG can provide useful behaviour whilst evading the bounds set by observational tests. In this work we also restricted our investigation to single-fluid scenarios, but it will be important to extend this to multi-fluid models in order to perform numerical simulations of the universal evolution under the theory.

In Chapter 4 we continued to investigate $F(R, T^{\mu\nu}T_{\mu\nu})$ gravity, but this time in a model called Energy-Momentum Log Gravity, in which the modification takes the form $F(R, T^{\mu\nu}T_{\mu\nu}) = R + \alpha \ln(\lambda T^{\mu\nu}T_{\mu\nu})$. We envisaged the new term as a correction term to the Einstein-Hilbert action, and investigated the cosmological phenomonology of the model. We focussed particularly on whether it would be possible for the model to explain some of the existing tensions in the observational data for ΛCDM, particularly the ones resulting from the Lyman-α forest measurement of Baryon Acoustic Oscillations at $z \approx 2.3$ from the BOSS collaboration. In the EMLG theory we were able to find an explicit exact solution for the energy density of dust, $\rho_m(z)$, which was sufficient to allow us to investigate the behaviour of $H(z)$ and the effective dark energy $\rho_{DE}(z)$. By choosing an appropriate value of the parameter α', we were able to demonstrate that the model exhibits effective dark energy which acts as $\Lambda > 0$ at low redshifts, but which acts negatively, thus screening Λ at redshifts higher than $z \approx 2.2$, enabling the model to relieve the observational tension involving the Lyman-α forest, without lowering $\Omega_{m,0}$ and $H(z)$ compared to the Planck observations. However, by considering the Akaike Information Criterion for model comparison, we see that although EMLG fits the datasets we have considered better than ΛCDM, and has good support, the introduction of the new parameter α penalises the model, so from this perspective ΛCDM is still slightly preferred.

The future of work on EMLG must be to incorporate radiation into the model - the current work considered only a single fluid dust cosmology, and excluded radiation from the analysis of both EMLG and ΛCDM. By considering the dual-fluid cosmology

it would be possible to not only further reconstruct the history of the EMLG cosmology, but to constrain the model further using the CMB datasets. It would also be important to continue to develop the theoretical framework behind the model. Although we have conducted a phenomonological investigation to explore the effect of the modifications on the cosmology and to highlight the cosmological signatures, an explanation of the underlying microphysical behaviour is essential if the model is to have continued application beyond providing a demonstration of mechanisms that can resolve tensions in the observational data.

References

[1] V. Sahni, A. Shafieloo and A. A. Starobinsky, *Model independent evidence for dark energy evolution from Baryon Acoustic Oscillations*, *Astrophys. J.* **793** (2014) L40 [1406.2209].

[2] Archimedes, *THE SAND-RECKONER*, Cambridge Library Collection - Mathematics. Cambridge University Press, 2009, 10.1017/CBO9780511695124.017.

[3] I. Newton, *Philosophiae naturalis principia mathematica*. J. Societatis Regiae ac Typis J. Streater, 1687.

[4] E. Harrison, *Newton and the infinite universe*, *Physics Today* **39** (1986) 24.

[5] A. Friedmann, *Über die Krümmung des Raumes*, *Zeitschrift fur Physik* **10** (1922) 377.

[6] A. Friedmann, *Über die Möglichkeit einer Welt mit konstanter negativer Krümmung des Raumes*, *Zeitschrift fur Physik* **21** (1924) 326.

[7] G. Lemaître, *Un Univers homogène de masse constante et de rayon croissant rendant compte de la vitesse radiale des nébuleuses extra-galactiques*, *Annales de la Société Scientifique de Bruxelles* **47** (1927) 49.

[8] H. Bondi and T. Gold, *The Steady-State Theory of the Expanding Universe*, *Mon. Not. R. Astron. Soc.* **108** (1948) 252.

[9] F. Hoyle, *A New Model for the Expanding Universe*, *Mon. Not. R. Astron. Soc.* **108** (1948) 372.

[10] G. Lemaitre, *Republication of: The beginning of the world from the point of view of quantum theory*, *Nature* **127** (1931) 706.

[11] A. A. Penzias and R. W. Wilson, *A Measurement of Excess Antenna Temperature at 4080 Mc/s.*, *Astrophys. J.* **142** (1965) 419.

[12] Planck collaboration, *Planck 2018 results. VI. Cosmological parameters*, 1807.06209.

[13] A. D. Linde, *A New Inflationary Universe Scenario: A Possible Solution of the Horizon, Flatness, Homogeneity, Isotropy and Primordial Monopole Problems*, *Phys. Lett.* **108B** (1982) 389.

[14] R. M. Wald, *General relativity*. Chicago Univ. Press, Chicago, IL, 1984.

[15] C. W. Misner, K. S. Thorne and J. A. Wheeler, *Gravitation*. W H Freeman and Company, 2 ed., 1973.

[16] S. M. Carroll, *Spacetime and geometry: An introduction to general relativity*. Cambridge University Press, 2019.

[17] S. Weinberg, *Gravitation and Cosmology*. John Wiley and Sons, New York, 1972.

[18] P. Peter and J.-P. Uzan, *Primordial cosmology*, Oxford Graduate Texts. Oxford Univ. Press, Oxford, 2009, 019966515X.

[19] S. Dodelson, *Modern cosmology*. Academic Press, San Diego, CA, 2003.

[20] S. Weinberg, *Cosmology*, Cosmology. OUP Oxford, 2008.

[21] E. W. Kolb and M. S. Turner, *The Early Universe*, *Front. Phys.* **69** (1990) 1.

[22] P. Collaboration et al., *Planck 2018 results. VII. Isotropy and Statistics of the CMB*, June, 2019.

[23] W. L. Freedman et al., *The Carnegie-Chicago Hubble Program. VIII. An Independent Determination of the Hubble Constant Based on the Tip of the Red Giant Branch*, 1907.05922.

[24] A. G. Riess, S. Casertano, W. Yuan, L. M. Macri and D. Scolnic, *Large Magellanic Cloud Cepheid Standards Provide a 1% Foundation for the Determination of the Hubble Constant and Stronger Evidence for Physics beyond ΛCDM*, *Astrophys. J.* **876** (2019) 85 [1903.07603].

[25] A. Einstein, *Kosmologische Betrachtungen zur allgemeinen Relativitätstheorie, Sitzungsberichte der Königlich Preußischen Akademie der Wissenschaften (Berlin), Seite 142-152.* (1917) .

[26] R. M. Wald, *Asymptotic behavior of homogeneous cosmological models in the presence of a positive cosmological constant*, *Phys. Rev.* **D28** (1983) 2118.

[27] P. Szekeres, *A class of inhomogeneous cosmological models*, *Communications in Mathematical Physics* **41** (1975) 55–64.

[28] A. H. Guth, *Inflationary universe: A possible solution to the horizon and flatness problems*, *Phys. Rev. D* **23** (1981) 347.

[29] V. F. Mukhanov and G. V. Chibisov, *Quantum Fluctuations and a Nonsingular Universe*, *JETP Lett.* **33** (1981) 532.

[30] A. D. Linde, *Inflationary Cosmology*, *Lect. Notes Phys.* **738** (2008) 1 [0705.0164].

[31] L. Kofman, A. D. Linde and A. A. Starobinsky, *Reheating after inflation*, *Phys. Rev. Lett.* **73** (1994) 3195 [hep-th/9405187].

[32] A. D. Linde, *Chaotic Inflation*, *Phys. Lett.* **129B** (1983) 177.

[33] J. J. M. Carrasco, R. Kallosh and A. Linde, *α-Attractors: Planck, LHC and Dark Energy*, *JHEP* **10** (2015) 147 [1506.01708].

[34] R. Kallosh and A. Linde, *Universality Class in Conformal Inflation*, *JCAP* **1307** (2013) 002 [1306.5220].

[35] G. Hinshaw, D. Larson, E. Komatsu, D. N. Spergel, C. L. Bennett, J. Dunkley et al., *Nine-year wilkinson microwave anisotropy probe (wmap) observations: Cosmological parameter results*, *The Astrophysical Journal Supplement Series* **208** (2013) 19.

[36] C. Brans and R. H. Dicke, *Mach's principle and a relativistic theory of gravitation*, *Phys. Rev.* **124** (1961) 925.

[37] LIGO Scientific, Virgo collaboration, *GW170817: Observation of Gravitational Waves from a Binary Neutron Star Inspiral*, *Phys. Rev. Lett.* **119** (2017) 161101 [1710.05832].

[38] A. Goldstein, P. Veres, E. Burns, M. S. Briggs, R. Hamburg, D. Kocevski et al., *An ordinary short gamma-ray burst with extraordinary implications: Fermi -gbm detection of grb 170817a*, *The Astrophysical Journal* **848** (2017) L14.

[39] T. Baker, E. Bellini, P. Ferreira, M. Lagos, J. Noller and I. Sawicki, *Strong constraints on cosmological gravity from GW170817 and GRB 170817A*, *Phys. Rev. Lett.* **119** (2017) 251301 [1710.06394].

[40] A. De Felice and S. Tsujikawa, *f(R) theories*, *Living Rev. Rel.* **13** (2010) 3 [1002.4928].

[41] T. Clifton, P. G. Ferreira, A. Padilla and C. Skordis, *Modified Gravity and Cosmology*, *Phys. Rept.* **513** (2012) 1 [1106.2476].

[42] A. A. Starobinsky, *A New Type of Isotropic Cosmological Models Without Singularity*, *Phys. Lett.* **91B** (1980) 99.

[43] Planck collaboration, *Planck 2018 results. X. Constraints on inflation*, 1807.06211.

[44] J. Middleton, *On The Existence Of Anisotropic Cosmological Models In Higher-Order Theories Of Gravity*, *Class. Quant. Grav.* **27** (2010) 225013 [1007.4669].

[45] J. Middleton and J. D. Barrow, *The Stability of an Isotropic Cosmological Singularity in Higher-Order Gravity*, *Phys. Rev.* **D77** (2008) 103523 [0801.4090].

[46] T. Harko, F. S. N. Lobo, S. Nojiri and S. D. Odintsov, $f(R,T)$ *gravity*, *Phys. Rev.* **D84** (2011) 024020 [1104.2669].

[47] M. Roshan and F. Shojai, *Energy-Momentum Squared Gravity*, *Phys. Rev.* **D94** (2016) 044002 [1607.06049].

[48] N. Katırcı and M. Kavuk, $f(R,T_{\mu\nu}T^{\mu\nu})$ *gravity and Cardassian-like expansion as one of its consequences*, *Eur. Phys. J. Plus* **129** (2014) 163 [1302.4300].

[49] X. Liu, T. Harko and S.-D. Liang, *Cosmological implications of modified gravity induced by quantum metric fluctuations*, *The European Physical Journal C, 76(8), 1-20 (2016)* (2016) [1607.04874v1].

[50] R. R. Caldwell, M. Kamionkowski and N. N. Weinberg, *Phantom energy and cosmic doomsday*, *Phys. Rev. Lett.* **91** (2003) 071301 [astro-ph/0302506].

[51] J. D. Barrow, *Sudden future singularities*, *Classical and Quantum Gravity* **21** (2004) L79 [gr-qc/0403084].

[52] J. D. Barrow, *Sudden future singularities*, *Class. Quant. Grav.* **21** (2004) L79 [gr-qc/0403084].

[53] J. D. Barrow, *More general sudden singularities*, *Class. Quant. Grav.* **21** (2004) 5619 [gr-qc/0409062].

[54] L. Fernandez-Jambrina and R. Lazkoz, *Geodesic behaviour of sudden future singularities*, *Phys. Rev.* **D70** (2004) 121503 [gr-qc/0410124].

[55] K. Lake, *Sudden future singularities in FLRW cosmologies*, *Class. Quant. Grav.* **21** (2004) L129 [gr-qc/0407107].

[56] S. Nojiri, S. D. Odintsov and S. Tsujikawa, *Properties of singularities in (phantom) dark energy universe*, *Phys. Rev.* **D71** (2005) 063004 [hep-th/0501025].

[57] M. Bouhmadi-Lopez, P. F. Gonzalez-Diaz and P. Martin-Moruno, *Worse than a big rip?*, *Phys. Lett.* **B659** (2008) 1 [gr-qc/0612135].

[58] J. D. Barrow and A. A. H. Graham, *Singular Inflation*, *Phys. Rev. D 91, 083513 (2015)* (2015) [1501.04090v2].

[59] K. Harigaya, M. Ibe, K. Schmitz and T. T. Yanagida, *Chaotic Inflation with a Fractional Power-Law Potential in Strongly Coupled Gauge Theories*, *Phys. Lett.* **B720** (2013) 125 [1211.6241].

[60] J. J. M. Carrasco, R. Kallosh and A. Linde, *Cosmological Attractors and Initial Conditions for Inflation*, *Phys. Rev. D 92, 063519 (2015)* (2015) [1506.00936v2].

[61] L. Perivolaropoulos, *Fate of bound systems through sudden future singularities*, *Phys. Rev. D* **94** (2016) 124018 [1609.08528].

[62] C. V. R. Board and J. D. Barrow, *Cosmological Models in Energy-Momentum-Squared Gravity*, *Phys. Rev.* **D96** (2017) 123517 [1709.09501].

[63] J. D. Barrow and D. J. Shaw, *A New Solution of The Cosmological Constant Problems*, *Phys.Rev.Lett.106:101302,2011* (2011) [1007.3086v3].

[64] E. J. Copeland, M. Sami and S. Tsujikawa, *Dynamics of dark energy*, *Int. J. Mod. Phys.* **D15** (2006) 1753 [hep-th/0603057].

[65] A. De Felice and S. Tsujikawa, *f(R) theories*, *Living Rev. Rel.* **13** (2010) 3 [1002.4928].

[66] A. Paliathanasis, J. D. Barrow and P. G. L. Leach, *Cosmological Solutions of $f(T)$ Gravity*, *Phys. Rev. D 94, 023525 (2016)* (2016) [1606.00659v2].

[67] J. D. Barrow, *Graduated inflationary universes.*, *Physics Letters B* **235** (1990) 40.

[68] S. Nojiri and S. D. Odintsov, *Inhomogeneous equation of state of the universe: Phantom era, future singularity, and crossing the phantom barrier*, *Phys. Rev. D* **72** (2005) 023003.

[69] J. D. Barrow, *String-Driven Inflationary and Deflationary Cosmological Models*, *Nucl. Phys.* **B310** (1988) 743.

[70] A. Liddle, A. Mazumdar and J. Barrow, *Radiation matter transition in Jordan-Brans-Dicke theory*, *Physical Review D* **58** (1998) .

[71] X. Chen and M. Kamionkowski, *Cosmic microwave background temperature and polarization anisotropy in Brans-Dicke cosmology*, *Phys. Rev. D* **60** (1999) 104036 [astro-ph/9905368].

[72] B. Li and J. D. Barrow, *Does bulk viscosity create a viable unified dark matter model?*, *Phys. Rev. D* **79** (2009) 103521.

[73] N. Nari and M. Roshan, *Compact stars in Energy-Momentum Squared Gravity*, *Phys. Rev.* **D98** (2018) 024031 [1802.02399].

[74] M. Bojowald, *Loop Quantum Cosmology*, *Living Reviews in Relativity* **8** (2005) 11 [gr-qc/0601085].

[75] P. Brax and C. van de Bruck, *Cosmology and brane worlds: A Review*, *Class. Quant. Grav.* **20** (2003) R201 [hep-th/0303095].

[76] P. Singh and E. Wilson-Ewing, *Quantization ambiguities and bounds on geometric scalars in anisotropic loop quantum cosmology*, *Class. Quant. Grav.* **31** (2014) 035010 [1310.6728].

[77] B. Gupt and P. Singh, *Contrasting features of anisotropic loop quantum cosmologies: The Role of spatial curvature*, *Phys. Rev.* **D85** (2012) 044011 [1109.6636].

[78] T. Harko and F. S. N. Lobo, *f(R,L_m) gravity*, *Eur. Phys. J.* **C70** (2010) 373 [1008.4193].

[79] O. Akarsu, N. Katirci and S. Kumar, *Cosmic acceleration in dust only Universe via energy-momentum powered gravity*, *Phys. Rev. D 97, 024011 (2018)* (2018) [1709.02367v3].

[80] M. Roshan and F. Shojai, *Energy-Momentum Squared Gravity*, *Physical Review D 94, 044002 (2016)* (2016) [1607.06049v2].

[81] N. Katirci and M. Kavuk, *$f(R, T_{\mu\nu}T^{\mu\nu})$ gravity and Cardassian-like expansion as one of its consequences*, *Eur. Phys. J. Plus (2014) 129: 163* (2014) [1302.4300v3].

[82] J. D. Barrow, G. J. Galloway and F. J. Tipler, *The closed-universe recollapse conjecture*, *Mon. Not. R. Astron. Soc.* **223** (1986) 835.

[83] J. D. Barrow, *More general sudden singularities*, *Classical and Quantum Gravity* **21** (2004) 5619.

[84] J. D. Barrow and S. Hervik, *Magnetic brane-worlds*, *Classical and Quantum Gravity* **19** (2001) 155.

[85] J. D. Barrow and R. Maartens, *Kaluza-Klein anisotropy in the CMB*, *Physics Letters B* **532** (2002) 153 [gr-qc/0108073].

[86] A. Coley, *Isotropic singularity in brane cosmological models*, *arXiv e-prints* (2003) gr [gr-qc/0312073].

[87] A. A. Coley, Y. He and W. C. Lim, *Isotropic singularity in inhomogeneous brane cosmological models*, *Classical and Quantum Gravity* **21** (2004) 1311.

[88] R. R. Caldwell, M. Kamionkowski and N. N. Weinberg, *Phantom Energy: Dark Energy with $w < -1$ Causes a Cosmic Doomsday*, *Phys. Rev. Lett.* **91** (2003) 071301.

[89] L. D. Landau and E. M. Lifshitz, *The Classical Theory of Fields*. Butterworth-Heinemann, 4 ed., Jan., 1980.

[90] J. D. Barrow and J. Middleton, *Stable isotropic cosmological singularities in quadratic gravity*, *Phys. Rev. D* **75** (2007) 123515.

[91] J. Middleton and J. D. Barrow, *Stability of an isotropic cosmological singularity in higher-order gravity*, *Phys. Rev. D* **77** (2008) 103523.

[92] J. D. Barrow, *Cosmological limits on slightly skew stresses*, *Phys. Rev. D* **55** (1997) 7451.

[93] O. Akarsu, J. D. Barrow, C. V. R. Board, N. M. Uzun and J. A. Vazquez, *Screening Λ in a new modified gravity model*, *Eur. Phys. J.* **C79** (2019) 846 [1903.11519].

[94] D. Larson, J. Dunkley, G. Hinshaw, E. Komatsu, M. R. Nolta, C. L. Bennett et al., *Seven-Year Wilkinson Microwave Anisotropy Probe (WMAP) Observations: Power Spectra and WMAP-Derived Parameters*, *Astrophys.J.Suppl.192:16,2011* (2010) [1001.4635v2].

[95] Planck collaboration, *Planck 2015 results. XIII. Cosmological parameters*, *Astron. Astrophys.* **594** (2016) A13 [1502.01589].

[96] Planck collaboration, *Planck 2018 results. VI. Cosmological parameters*, 1807.06209.

[97] S. Weinberg, *The Cosmological Constant Problem*, *Rev. Mod. Phys.* **61** (1989) 1.

[98] P. J. E. Peebles and B. Ratra, *The Cosmological constant and dark energy*, *Rev. Mod. Phys.* **75** (2003) 559 [astro-ph/0207347].

[99] T. Padmanabhan, *Cosmological constant: The Weight of the vacuum*, *Phys. Rept.* **380** (2003) 235 [hep-th/0212290].

[100] J. Alberto Vazquez, M. Bridges, M. P. Hobson and A. N. Lasenby, *Reconstruction of the Dark Energy equation of state*, *JCAP* **1209** (2012) 020 [1205.0847].

[101] A. Bhattacharyya, U. Alam, K. L. Pandey, S. Das and S. Pal, *Are H_0 and σ_8 tensions generic to present cosmological data?*, *Astrophys. J.* **876** (2019) 143 [1805.04716].

[102] M. Raveri and W. Hu, *Concordance and discordance in cosmology*, *Phys. Rev. D* **99** (2019) 043506.

[103] D. Tamayo and J. A. Vazquez, *Fourier-series expansion of the dark-energy equation of state*, *Mon. Not. Roy. Astron. Soc.* **487** (2019) 729 [1901.08679].

[104] S. Hee, J. A. Vázquez, W. J. Handley, M. P. Hobson and A. N. Lasenby, *Constraining the dark energy equation of state using Bayes theorem and the Kullback–Leibler divergence*, *Mon. Not. Roy. Astron. Soc.* **466** (2017) 369 [1607.00270].

[105] E. Di Valentino, *Crack in the cosmological paradigm*, *Nat. Astron.* **1** (2017) 569 [1709.04046].

[106] E. Aubourg et al., *Cosmological implications of baryon acoustic oscillation measurements*, *Phys. Rev.* **D92** (2015) 123516 [1411.1074].

[107] G.-B. Zhao et al., *Dynamical dark energy in light of the latest observations*, *Nat. Astron.* **1** (2017) 627 [1701.08165].

[108] J. S. Bullock and M. Boylan-Kolchin, *Small-Scale Challenges to the ΛCDM Paradigm*, *Ann. Rev. Astron. Astrophys.* **55** (2017) 343 [1707.04256].

[109] W. L. Freedman, *Cosmology at a Crossroads*, *Nat. Astron.* **1** (2017) 0121 [1706.02739].

[110] A. G. Riess et al., *A 2.4% Determination of the Local Value of the Hubble Constant*, *Astrophys. J.* **826** (2016) 56 [1604.01424].

[111] BOSS collaboration, *Baryon acoustic oscillations in the Lyα forest of BOSS DR11 quasars*, *Astron. Astrophys.* **574** (2015) A59 [1404.1801].

[112] R. R. Caldwell and M. Kamionkowski, *The Physics of Cosmic Acceleration*, *Ann. Rev. Nucl. Part. Sci.* **59** (2009) 397 [0903.0866].

[113] S. Capozziello and M. De Laurentis, *Extended Theories of Gravity*, *Phys. Rept.* **509** (2011) 167 [1108.6266].

[114] S. Nojiri, S. D. Odintsov and V. K. Oikonomou, *Modified Gravity Theories on a Nutshell: Inflation, Bounce and Late-time Evolution*, *Phys. Rept.* **692** (2017) 1 [1705.11098].

[115] S. Nojiri and S. D. Odintsov, *Unified cosmic history in modified gravity: from F(R) theory to Lorentz non-invariant models*, *Phys. Rept.* **505** (2011) 59 [1011.0544].

[116] V. Faraoni, E. Gunzig and P. Nardone, *Conformal transformations in classical gravitational theories and in cosmology*, *Fund. Cosmic Phys.* **20** (1999) 121 [gr-qc/9811047].

[117] B. Boisseau, G. Esposito-Farese, D. Polarski and A. A. Starobinsky, *Reconstruction of a scalar tensor theory of gravity in an accelerating universe*, *Phys. Rev. Lett.* **85** (2000) 2236 [gr-qc/0001066].

[118] V. Sahni and A. Starobinsky, *Reconstructing Dark Energy*, *Int. J. Mod. Phys.* **D15** (2006) 2105 [astro-ph/0610026].

[119] O. Akarsu, N. Katirci, N. Ozdemir and J. A. Vazquez, *Anisotropic massive Brans-Dicke gravity extension of standard ΛCDM model*, 1903.06679.

[120] A. D. Dolgov, *Field model with a dynamic cancellation of the cosmological constant*, *JETP Lett.* **41** (1985) 345.

[121] F. Bauer, J. Sola and H. Stefancic, *Dynamically avoiding fine-tuning the cosmological constant: The 'Relaxed Universe'*, *JCAP* **1012** (2010) 029 [1006.3944].

[122] S.-Y. Zhou, E. J. Copeland and P. M. Saffin, *Cosmological Constraints on $f(G)$ Dark Energy Models*, *JCAP* **0907** (2009) 009 [0903.4610].

[123] V. Sahni and Y. Shtanov, *Brane world models of dark energy*, *JCAP* **0311** (2003) 014 [astro-ph/0202346].

[124] A. Ashtekar, T. Pawlowski and P. Singh, *Quantum Nature of the Big Bang: Improved dynamics*, *Phys. Rev.* **D74** (2006) 084003 [gr-qc/0607039].

[125] A. Ashtekar and P. Singh, *Loop Quantum Cosmology: A Status Report*, *Class. Quant. Grav.* **28** (2011) 213001 [1108.0893].

[126] A. Chodos and S. Detweiler, *Where has the fifth dimension gone?*, *Phys. Rev. D* **21** (1980) 2167.

[127] T. Dereli and R. Tucker, *Dynamical reduction of internal dimensions in the early universe*, *Physics Letters B* **125** (1983) 133–135.

[128] O. Akarsu and T. Dereli, *The Dynamical Evolution of 3-Space in a Higher Dimensional Steady State Universe*, *Gen. Rel. Grav.* **45** (2013) 959 [1210.1155].

[129] O. Akarsu and T. Dereli, *Late Time Acceleration of the 3-Space in a Higher Dimensional Steady State Universe in Dilaton Gravity*, *JCAP* **1302** (2013) 050 [1210.8106].

[130] J. G. Russo and P. K. Townsend, *Late-time Cosmic Acceleration from Compactification*, *Class. Quant. Grav.* **36** (2019) 095008 [1811.03660].

[131] O. Akarsu, J. D. Barrow, S. Çıkıntoğlu, K. Y. Ekşi and N. Katırcı, *Constraint on energy-momentum squared gravity from neutron stars and its cosmological implications*, *Phys. Rev.* **D97** (2018) 124017 [1802.02093].

[132] O. Akarsu, N. Katirci, S. Kumar, R. C. Nunes and M. Sami, *Cosmological implications of scale-independent energy-momentum squared gravity: Pseudo nonminimal interactions in dark matter and relativistic relics*, *Phys. Rev.* **D98** (2018) 063522 [1807.01588].

[133] M. C. F. Faria, C. J. A. P. Martins, F. Chiti and B. S. A. Silva, *Low redshift constraints on energy-momentum-powered gravity models*, *Astron. Astrophys.* **625** (2019) A127 [1905.02792].

[134] S. Bahamonde, M. Marciu and P. Rudra, *Dynamical system analysis of generalized energy-momentum-squared gravity*, 1906.00027.

[135] E. Elizalde, N. Godani and G. C. Samanta, *Cosmological dynamics in R^2 gravity with logarithmic trace term*, 1907.05223.

[136] D. Lovelock, *The Einstein tensor and its generalizations*, *J. Math. Phys.* **12** (1971) 498.

[137] D. Lovelock, *The four-dimensionality of space and the einstein tensor*, *J. Math. Phys.* **13** (1972) 874.

[138] P. Bull et al., *Beyond ΛCDM: Problems, solutions, and the road ahead*, *Phys. Dark Univ.* **12** (2016) 56 [1512.05356].

[139] N. Straumann, *General relativity with applications to astrophysics*. 2004.

[140] J.-P. Uzan, *Varying Constants, Gravitation and Cosmology*, *Living Rev. Rel.* **14** (2011) 2 [1009.5514].

[141] H. B. Sandvik, J. D. Barrow and J. Magueijo, *A simple cosmology with a varying fine structure constant*, *Phys. Rev. Lett.* **88** (2002) 031302 [astro-ph/0107512].

[142] J. Magueijo, J. D. Barrow and H. B. Sandvik, *Is it e or is it c? Experimental tests of varying alpha*, *Phys. Lett.* **B549** (2002) 284 [astro-ph/0202374].

[143] J. D. Barrow and J. Magueijo, *Cosmological constraints on a dynamical electron mass*, *Phys. Rev.* **D72** (2005) 043521 [astro-ph/0503222].

[144] Harrison E. R., *Observational tests in cosmology*, *Nature* **260** (1976) 591–592.

[145] V. Sahni, T. D. Saini, A. A. Starobinsky and U. Alam, *Statefinder: A New geometrical diagnostic of dark energy*, *JETP Lett.* **77** (2003) 201 [astro-ph/0201498].

[146] M. Visser, *Jerk and the cosmological equation of state*, *Class. Quant. Grav.* **21** (2004) 2603 [gr-qc/0309109].

[147] M. Dunajski and G. Gibbons, *Cosmic Jerk, Snap and Beyond*, *Class. Quant. Grav.* **25** (2008) 235012 [0807.0207].

[148] G. Efstathiou, *H0 Revisited*, *Mon. Not. Roy. Astron. Soc.* **440** (2014) 1138 [1311.3461].

[149] B. A. Reid, L. Samushia, M. White, W. J. Percival, M. Manera, N. Padmanabhan et al., *The clustering of galaxies in the SDSS-III Baryon Oscillation Spectroscopic Survey: measurements of the growth of structure and*

expansion rate at $z = 0.57$ from anisotropic clustering, *Mon. Not. Roy. Astron. Soc.* **426** (2012) 2719 [1203.6641].

[150] A. Slosar and J. Vazquez, *April*, *GitHub repository https://github.com/slosar/april/* (2014) .

[151] A. Gomez-Valent and L. Amendola, *H_0 from cosmic chronometers and Type Ia supernovae, with Gaussian Processes and the novel Weighted Polynomial Regression method*, *JCAP* **1804** (2018) 051 [1802.01505].

[152] L. E. Padilla, L. O. Tellez, L. A. Escamilla and J. A. Vazquez, *Cosmological parameter inference with Bayesian statistics*, 1903.11127.

[153] E. Komatsu, K. M. Smith, J. Dunkley, C. L. Bennett, B. Gold, G. Hinshaw et al., *Seven-year Wilkinson Microwave Anisotropy Probe (WMAP) Observations: Cosmological Interpretation*, *Astrophys. J. Suppl.* **192** (2011) 18 [1001.4538].

[154] H. Akaike, *A new look at the statistical model identification*, *IEEE Transactions on Automatic Control* **19** (1974) 716.

[155] A. G. Riess, S. Casertano, W. Yuan, L. Macri, J. Anderson, J. W. MacKenty et al., *New Parallaxes of Galactic Cepheids from Spatially Scanning the Hubble Space Telescope: Implications for the Hubble Constant*, *Astrophys. J.* **855** (2018) 136 [1801.01120].

[156] A. G. Riess et al., *Milky Way Cepheid Standards for Measuring Cosmic Distances and Application to Gaia DR2: Implications for the Hubble Constant*, *Astrophys. J.* **861** (2018) 126 [1804.10655].